




Universitetet
i Stavanger

FACULTY OF SCIENCE AND TECHNOLOGY

MASTER'S THESIS

Study programme/specialisation: Constructions and Materials/Offshore Constructions	Spring semester, 2017 Open/ Confidential
Author: Kristian Ydstebø	 (signature of author)
<u>Faculty supervisors:</u> Sudath C. Siriwardane, Hirpa G. Lemu and Ove Mikkelsen <u>External supervisors:</u> Ole Gabrielsen and Kjetil Dahl	
Title of master's thesis: Capacity of Bolted T-stub Connections Between Different Materials Subjected to Tension and Thermal Load	
Credits (ECTS): 30	
Keywords: Bolted Connection T-Stub Tension and thermal load Stiffness	Number of pages: 95 + Enclosure: 8 Stavanger, 14/06-2016

PREFACE

This is the final project of my master's degree in Civil and Structural Engineering at the University of Stavanger. It was written during the spring semester of 2017. Parts of the thesis was written at DNV-GL. All laboratory work performed for this thesis has been carried out at the University of Stavanger.

I would like to express my gratitude for the help and guidance I have received from my faculty supervisors Sudath C. Siriwardane, Hirpa G. Lemu, Ove Mikkelsen and external supervisors Ole Gabrielsen and Kjetil Dahl. Their help has been of vital importance for the progress of my thesis. Special thanks to Johan Thorikaas for the valuable help and guidance with the laboratory work both preparations and the tensile tests.

Gratitude to Marine Aluminium for their willingness to supply the materials needed.

Stavanger, Thursday 14th June, 2017

Kristian Ydstebø

ABSTRACT

The purpose of this thesis is to study the behaviour of bolted T-stub connections of different materials subjected to tension and thermal load. In the Eurocode, NS-EN 1993-1-8 [1], there are given rules and guidelines for determining the stiffness and capacity of a T-stub connection.

In this thesis, the theoretical capacity from the Eurocode is compared to both an experimental and numerical investigation. It is emphasised to study the connections real behaviour and thoroughly investigate how well a T-stub connection can be estimated with the Eurocode and a finite element (FE) model.

In the experimental investigation, a total of six tensile tests of the T-stub connections connected by two bolts has been performed. The tests were divided into two configurations, a steel – steel connection and an aluminium – steel connection. It has also been performed numerical analysis of the same geometries in the finite element software, Abaqus. The numerical analysis is, together with the theoretical calculations from the Eurocode, compared with the experimental results. It was found that the result from the Eurocode is conservative and do not identify the failure mode achieved in the tensile tests for both configurations. The stiffness was also overestimated. The FE model was a good approximation to the real behaviour and capacity of the tensile tests.

It was also established an FE model of the connections subjected to thermal load, where temperature increased from the range of -20 – 200 °C. The connections were preloaded before adding the thermal load. It was found that with all the components of steel, preload force maintained the same throughout the load. The connection with both aluminium and steel components, the preload force increased due to the different rate of expansion of the materials.

TABLE OF CONTENTS

Preface	i
Abstract	ii
Table of Contents	iii
List of Figures	v
List of Tables	vi
Nomenclature	vi
1 Introduction	1
1.1 Background.....	1
1.2 Aim of the thesis	2
1.3 Scope of work	2
1.4 Limitations	3
2 Literature review	4
2.1 Stiffness.....	4
2.1.1 General stiffness relation	4
2.1.2 Bolt stiffness.....	6
2.1.3 Member stiffness	8
2.2 Joint Design.....	10
2.2.1 Mechanical properties/Material mechanics	10
2.2.2 Joint Diagram.....	12
2.2.3 Preload force	14
2.3 Temperature Effects.....	16
2.4 Technical description of a helideck.....	18
2.4.1 Materials in the support structure.....	18
2.4.2 Support structure of a helideck	18
3 Regulations and guidelines.....	21
3.1 Bolts	21
3.2 Categories of bolted connections	22
3.3 Design resistance	23
3.3.1 Shear resistance	23
3.3.2 Bearing resistance	25
3.3.3 Tension resistance.....	26
3.3.4 Design slip resistance	26
3.4 Equivalent T-stub	27
3.4.1 Prying force	30
3.4.2 Stiffness of T-stub connection	33
3.4.3 Determination of the stiffness coefficients	34
4 Considered bolted connection	37
4.1 Geometry	38
5 Capacity of the bolted connection: experimental investigation	41
5.1 Preparations	42
5.2 Test setup.....	46
5.3 Test results	46

5.3.1	Steel – steel connection	47
5.3.2	Aluminium – steel Connection	48
6	Capacity of the bolted connection: theoretical investegation	51
6.1	Effective length - l_{eff}	51
6.2	Design resistance	52
6.2.1	Bolts	52
6.2.2	Steel T-stub	53
6.2.3	Aluminium T-stub	53
6.3	Stiffness	54
7	Capacity of the bolted connection: Numerical investegation	58
7.1	Calibration of the material parameters	58
7.1.1	True stress and true strain	58
7.1.2	Bolts	60
7.1.3	Tensile tests	61
7.2	Initial Model	64
7.2.1	Simplified bolt.....	65
7.3	Element characteristics	66
7.4	Step- and increment size	67
7.5	Boundary conditions	67
7.6	Interactions	68
7.7	Load	69
7.8	Results	70
7.8.1	Tension load.....	71
7.8.2	Thermal load	76
8	Discussion of results.....	83
8.1	Tension capacity	83
8.2	Stiffness	87
8.3	Thermal load	89
9	Conclusion	92
9.1	Further work.....	93
	Bibliography	94
	Appendices	96
	Appendix A	96
	Appendix B	97
	Appendix C	98
	Appendix D	99
	Appendix E	101
	Appendix F	102
	F.1 Tensile tests: Steel – steel.....	102
	F.2 Tensile tests: Aluminium – steel	103

LIST OF FIGURES

Figure 1.1: Fracture near a bolted connection [3]	1
Figure 2.1: Installed bolt [7]	4
Figure 2.2: Rod with various cross sections exposed to axial forces [5]	5
Figure 2.3: Dimensions of a bolt with nut [8]	7
Figure 2.4: Clamping force [10]	9
Figure 2.5: Tensile Stress-Strain Diagram	10
Figure 2.6: Distribution of elastic and plastic strain [12]	11
Figure 2.7: Joint diagram [10]	12
Figure 2.8: Joint fully unloaded [6]	13
Figure 2.9: Low preload force	15
Figure 2.10: High preload force	15
Figure 2.11: Helideck on Gudrun	19
Figure 3.1: Tearing in front of an between fasteners	25
Figure 3.2: Dimensions of an equivalent T-stub flange	27
Figure 3.3: Yield patterns	29
Figure 3.4: Failure modes of tension loaded T-stubs	29
Figure 3.5: Model for determining the prying force, Q [20]	31
Figure 3.6: Static system and moment diagram due to external load	31
Figure 3.7: Static system and moment diagram due to virtual load	31
Figure 3.8: Prying force on a T-stub	32
Figure 3.9: static models	34
Figure 3.10: Bolt in tension	36
Figure 4.1: Steel – Aluminium connection on a helideck [3]	39
Figure 4.2: T-stub connection	40
Figure 5.1: Tensile test of T-stub connection	41
Figure 5.2: Cutting and abrading profiles	42
Figure 5.3: Drilling holes in the aluminium flange	42
Figure 5.4: Steel – Steel (left) and Aluminium – Steel (right) configurations	43
Figure 5.5: Steel – steel connection	44
Figure 5.6: Aluminium – Steel connection	45
Figure 5.7: Clamping of the webs (left) and extensometer (right)	46
Figure 5.8: Force – displacement curves for steel – steel connection	47
Figure 5.9: Specimen 1 (SS1) before and after test	48
Figure 5.10: Force – displacement curves for aluminium – steel connection	49
Figure 5.11: Specimen 1 (AS1) before and after test	50
Figure 5.12: Failure at nut (left) and failure at bolt (right)	50
Figure 7.1: Material data for bolt	60
Figure 7.2: Geometry of specimen	61
Figure 7.3: Specimens before and after tensile test	62
Figure 7.4: Stress – strain of steel	63
Figure 7.5: Stress – strain of aluminium	64
Figure 7.6: Subcomponents used in the analyse	64
Figure 7.7: Simple bolt model	65
Figure 7.8: Force-displacement curve for simplified M16 bolt [28]	66
Figure 7.9: Hexahedral element, C3D8R	66
Figure 7.10: Boundary conditions	68
Figure 7.11: Interactions	69
Figure 7.12: Load application and nodes on top web	69
Figure 7.13: Initial conditions, step 1 and step 2	70
Figure 7.14: Reference points for measuring displacement in steel – steel connection	70
Figure 7.15: Force – displacement curves at two different reference points	71
Figure 7.16: Original model (left) mirrored in YZ-plane (right)	71
Figure 7.17: Force – displacement curves for steel – steel connection	72
Figure 7.18: Steel – steel connection at 166.3 kN	73
Figure 7.19: Force – displacement curves for aluminium – steel connection	74
Figure 7.20: Aluminium – steel connection at 171.9 kN	75
Figure 7.21: Simplified preloaded connection before and after thermal load	76
Figure 7.22: Percent preload stress – Temperature	77
Figure 7.23: Expansion in Y-direction	78
Figure 7.24: Preloaded bolt before and after thermal load	79
Figure 7.25: Preloaded bolt on flanges before and after thermal load	79

Figure 7.26: Percent preload stress – Temperature	80
Figure 7.27: Expansion in Y-direction	81
Figure 7.28: Preloaded bolt before and after thermal load	81
Figure 7.29: Preloaded bolt on flanges before and after thermal load.....	82
Figure 8.1: Comparison of the deformation from SS1	83
Figure 8.2: Comparison of capacity for steel – steel connection	84
Figure 8.3: Comparison of the deformation from AS1	84
Figure 8.4: Comparison of capacity for aluminium – steel connection	85
Figure 8.5: Comparison of stiffness for steel – steel connection	87
Figure 8.6: Comparison of stiffness for aluminium – steel connection	88
Figure 8.7: Preload stress of both configurations	90
Figure 8.8: Expansion of bolt and flanges of both configurations.	91

LIST OF TABLES

Table 2.1: Preload force for metric threaded fasteners	14
Table 3.1: Nominal values of yield strength f_{yb} and ultimate tensile strength f_{ub}	21
Table 3.2: Elongation of different bolt classes [6]	21
Table 3.3: Effective lengths for an unstiffened column flange	28
Table 3.4: Design resistance $F_{T,1,Rd}$ of a T-stub flange	30
Table 4.1: Material properties	37
Table 4.2: Dimensions and materials.....	38
Table 4.3: T-stubs with dimensions (mm)	39
Table 5.1: Test results	47
Table 5.2: Test results	48
Table 6.1: Dimensions of a T-stub flange	51
Table 6.2: Calculations of effective length	52
Table 6.3: Design loads of T-stubs	54
Table 6.4: Summary of total elastic stiffness and stiffness coefficients.....	57
Table 7.1: Material data for 8.8 bolt	60
Table 8.1: Comparison of tension capacities	86
Table 8.2: Summary of stiffness's	88

NOMENCLATURE

A	Is the area
A_d	Is the major diameter area of fastener
A_s	Is the tensile stress area
A_t	Is the tensile-stress area
$B_{p,Rd}$	Is the design punching shear resistance of the bolt head and the nut
E	Is the Young's modulus
E_b	Is the bolt Young's modulus
E_m	Is the member Young's modulus
F_0	Is the preload force
F	Is the Force
F_A	Is the change of force in material
F_b	Is the force of bolt
F_m	Is the force of member
F_T	Is the change of force in bolt
$F_{t,Ed}$	Is the design tensile force per bolt for the ultimate limit state
$F_{t,Rd}$	Is the design tension resistance per bolt
$F_{v,Rd}$	Is the design shear resistance per bolt
$F_{b,Rd}$	Is the design bearing resistance per bolt
$F_{s,Rd}$	Is the design slip resistance per bolt at the ultimate limit state
$F_{v,Ed}$	Is the design shear force per bolt for ultimate limit state
I	Is the moment of inertia
K	Is the total stiffness
L	Is the length

L_g	Is the grip length
M_T	Is the torque
$M_{j,Rd}$	Is the design moment resistance of a joint
$N_{net,Rd}$	Is the plastic resistance of the net cross-section at bolt holes
Q	Is the prying force
T_0	Is the initial temperature
T_1	Is the final temperature
d	Is the bolt diameter
d_h	Is the hole diameter
d_s	Is the nominal diameter
e_{min}	Is the distance from centre of bolt hole to the edge of flange
f_u	Is the ultimate tensile strength
f_y	Is the yield strength
k	Is a factor where it occurs
k_b	Is the total stiffness of bolt
k_i	Is the stiffness of different parts of a rod or a connection
k_m	Is the total stiffness of member
k_5	Is a stiffness coefficient of plate in bending
k_{10}	Is a stiffness coefficient of bolt in tension
l_{eff}	Is the effective length
l_d	Is the length of unthreaded portion of grip
l_t	Is the length of threaded portion of grip
m	Is the distance from the centre of bolt hole to the end of web
n_f	Is the nut factor
t_f	Is the thickness of flange
t_w	Is the thickness of web
u	Is the displacement
w	Is the distance between the bolts
α	Is the thermal expansion coefficient or a factor where it occurs
σ	Is the stress
σ_{true}	Is the true stress
σ_{eng}	Is the engineering stress
ε	Is the strain
ε_{eng}	Is the engineering strain
ε_{true}	Is the true strain
δ	Is the elongation
δ_T	Is the deflection of bolt
δ_A	Is the deflection of material
γ_M	Is the partial safety factor
β_p	Is the reduction factor
μ	Is the slip factor

1 INTRODUCTION

1.1 Background

Bolted connections have been used for decades and are widely used in mechanical design. Connections, where flanges are subjected to tension, are very common in offshore structures, i.e. bolted end-plates, beam-to-column connections, flange cleat in bending and base plate in bending under tension/compression. In the recent years, there were some incidents where bolted connections have not performed as expected. Some of them are related to offshore structures, [2] and [3]. On 9th March 2015, there was an unusual sound and movement in the helicopter deck when a helicopter took-off from Gudrun [4]. An inspection revealed a fracture in an aluminium profile (T-shaped element) in the outer part of the structure under the helideck. Among other things, missing and loose nuts in bolted joints were discovered. The supporting structure for a helideck is normally welded construction using steel. The top deck and underlying structure are welded and bolted aluminium and the beams connecting the helideck and living quarter is in steel.

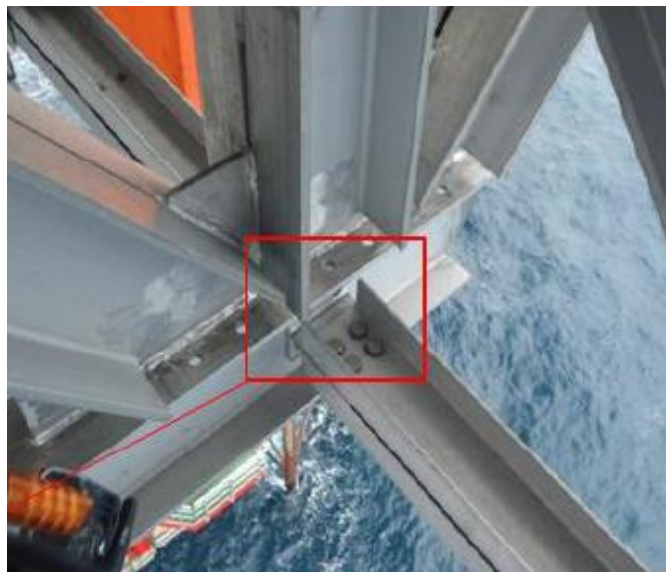


Figure 1.1: Fracture near a bolted connection [3]

The contractor for the kit solution on Gudrun was Aluminium Offshore in Singapore. They offered a structure that was bolted together with several thousand bolts that could be transported in smaller parts to Norway. When structures are transported from warm climates, such as mentioned earlier, from Singapore to Norway where it is colder climate, the construction is exposed to a temperature change. The change of temperature must be taken into consideration, due to thermal expansion of the different parts in the connection. A change in temperature will affect the thickness of the joint and the length of the bolts [5]. Bolted connections represent a weakness in a

system where temperature applications can lead to decreased product performance due to increase or decrease of joint clamping force. If the joint material expands at a higher rate than the bolt, the tension on the bolt could damage the joint or even break the bolt [6]. Selecting the appropriate materials, dimensions and design approach can at times be challenging in particular when the connections are between different materials and subjected to load reversals.

Bolted connections should be able to withstand the elongation of the bolts in addition to deformations of the end plate and/or flange. The tension zone from the flange and bolt may be modelled by using a T-stub. According to the standard NS-EN 1993 1-8 [1], an equivalent T-stub may be used for examination the behaviour of common structural components.

1.2 Aim of the thesis

The aim of the thesis is to explore the behaviour of a T-stub connection between aluminium and steel subjected to tension and thermal load. It is emphasised to study the design method which is given in NS-EN 1993-1-8, guidelines and literature, create finite element models, and perform tests of the connection in a laboratory. The experimental results should be compared with the capacity due to Eurocode 3 as well as the response from finite element analysis.

1.3 Scope of work

There is no fastener material which is unique for every environment. Careful consideration must be given to variables such as strength, temperature, vibration and fatigue. However, with some basic knowledge and understanding, a critical analysis can be made. The main objectives are as follows:

- Perform a literature study on current knowledge of bolted connections.
- Select an actual design case related to offshore structures.
- Perform laboratory tests of the design case - T-stub connection.
- Develop local finite element models of the bolted connections between two different materials that can be compared to estimates from Eurocode 3. Both tensile load and thermal load will be applied in the finite element model.
- Extract bolt tensions from the FE model.
- Validate the T-stub connection from the FE model and Eurocode 3 to the behavior observed in the laboratory
- Reporting

1.4 Limitations

This thesis is limited by the following considerations:

- For laboratory work, the bolted connection have to be scaled down for achieving fracture and yielding.
- Maximum tension load of the test facility is 250 kN.
- Test facility area can adapt a bolted connection within a range of 200x200x500 (mm)
- Due to lack of time and resources, planned tests of the bolted connection exposed to thermal load was not executed.

2 LITERATURE REVIEW

Steel constructions are mainly composed of various structural components (beams, columns, etc.), and it is therefore necessary to join the components together using fasteners. The fasteners that are mainly used in steel constructions are welded connections and connections made with bolts, rivets and pins. A very common fastener in offshore structures is the welded connection. In some cases, welding can be difficult and unfortunate, and in those cases bolted connections is more applicable. Bolts as fasteners can be arranged to take shear loads, tensile loads or both. The official European standard for dimensioning bolted connections is the Eurocode 3, part 1-8, design of joints (NS-EN 1993-1-8) [1], which is discussed in Chapter 3.

To gain a deeper understanding of bolts, bolted connections and their behaviour, as well as the factors affecting their capacity, background theory from literature is introduced. Figure 2.1 shows a typical bolt connection.

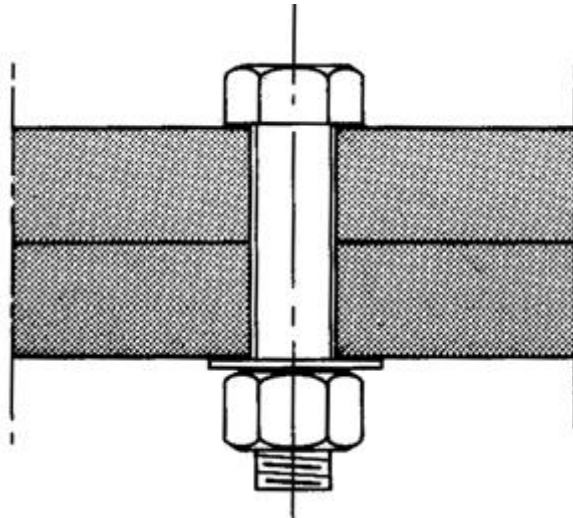


Figure 2.1: Installed bolt [7]

2.1 Stiffness

2.1.1 General stiffness relation

Bolted connections act as stiff springs exposed to tensile loading. The stiffness for a bolted connection is an important parameter and closely related to the strain of the bolt and member.

Hooke's law can be used for an accurate approximation for calculating deformation with a known stiffness factor. A rod with a uniform cross section exposed to axial force, Hooke's law is used, as long as it is within the linear area in the stress-strain diagram (elastic area). A rod assembled by different parts with various cross sections,

as in Figure 2.2, shall be considered. There may be established a corresponding spring model for such a rod since Hooke's law also applies in the case of non-uniform cross-section. It is desirable to determine the expression of the rod stiffness. To determine the total change of length or the total stiffness of the assemblies, the superposition principle can be used.

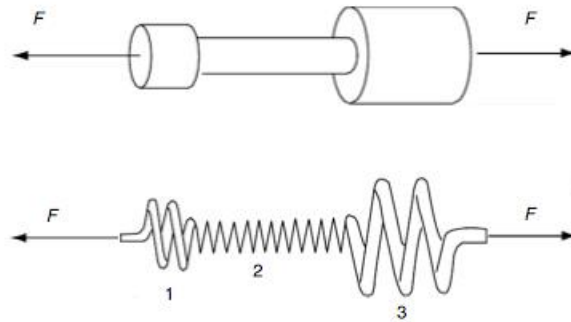


Figure 2.2: Rod with various cross sections exposed to axial forces [5]

The total change of the rod length is equal to the sum of changes of length for in each part of the rod.

$$\Delta L_c = \Delta L_1 + \Delta L_2 + \Delta L_3 \quad 2.1$$

where ΔL_1 , ΔL_2 and ΔL_3 is the extension of respectively part 1, 2 and 3.

By implementing Hooke's law, the change of length in each part of the rod can be expressed as

$$\Delta L_i = \frac{FL_i}{EA_i} \quad i = 1,2,3, \quad 2.2$$

where ΔL_i is the change of length and A_i is the cross-section area for the part i of the rod, L_i is the original length of the part, E is the Young's modulus, and F is the applied force.

Since the different rod members are connected in series with the same Young's modulus and subjected to the same axial force, the force can be factorised. By inserting Equation 2.1 in Equation 2.2. the following relation is given

$$\Delta L_c = F \left(\frac{L_1}{EA_1} + \frac{L_2}{EA_2} + \frac{L_3}{EA_3} \right) \quad 2.3$$

The general definition for spring stiffness is

$$K = \frac{F}{\Delta L} \quad 2.4$$

The spring stiffness of the assembled rod in Figure 2.2, where the different part of the rod is connected in series is

$$\frac{1}{K_T} = \frac{1}{K_1} + \frac{1}{K_2} + \frac{1}{K_3} \quad 2.5$$

where K_T is the total stiffness of the system and K_1 , K_2 and K_3 are the stiffness for the different parts of the rod.

The Equation 2.4 can be rearranged as

$$\Delta L = \frac{F}{K} \quad 2.6$$

By combining Equation 2.3 and Equation 2.6 results in the following relation

$$\frac{1}{K_T} = \frac{L_1}{EA_1} + \frac{L_2}{EA_2} + \frac{L_3}{EA_3} \quad 2.7$$

From Equation 2.7 the total stiffness is described as the relation between the length and the cross section for each part of the rod.

2.1.2 Bolt stiffness

The equations developed for a rod in the previous Chapter 2.1.1 can be used for bolts, but the axial force will not be applied over the entire length of the bolt. For a bolt with a nut, the part of the unthreaded and threaded portions of the bolt in the clamped zone are, l_t and l_d shown in Figure 2.3. The grip l of the connection is the total thickness of the clamped material. In Figure 2.3 the grip is the sum of the thickness of washer and both members.

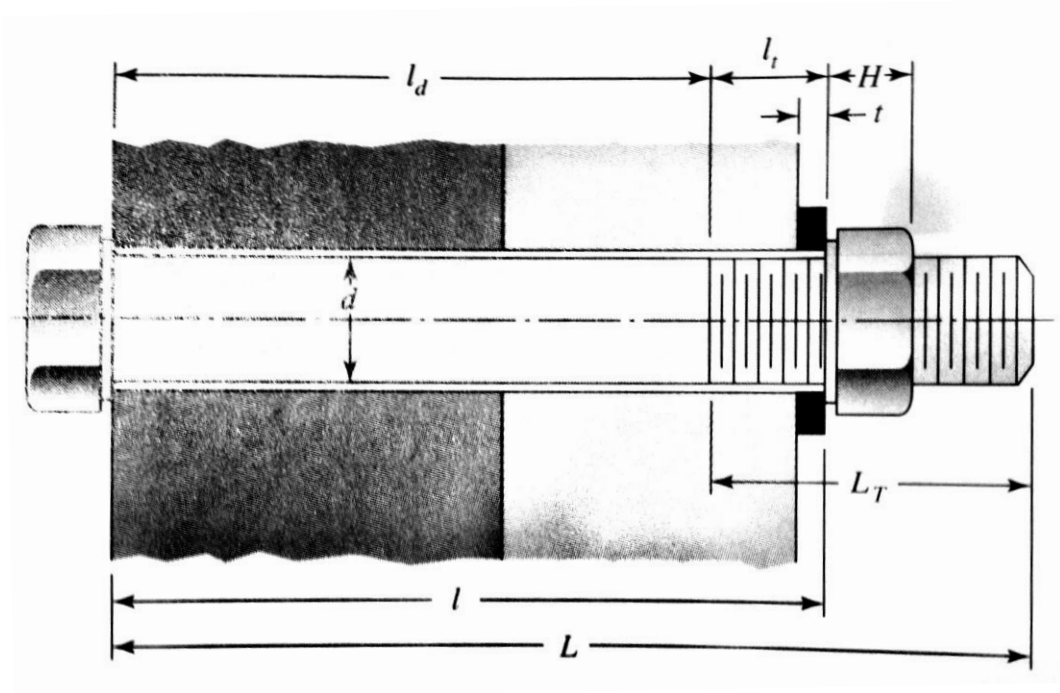


Figure 2.3: Dimensions of a bolt with nut [8]

The stiffness in the threaded and the unthreaded portion of the clamped zone can, as expressed in Equation 2.8 and 2.9, be treated a series of springs, respectively,

$$k_t = \frac{A_t E}{l_t} \quad 2.8$$

$$k_d = \frac{A_d E}{l_d} \quad 2.9$$

where

A_t = tensile-stress area

l_t = length of threaded portion of grip

A_d = major diameter area of fastener

l_d = length of unthreaded portion of grip

By substituting these stiffness's the total effective stiffness of the bolt is found to be:

$$k_b = \frac{A_t A_d E}{A_d l_t + A_t l_d} \quad 2.10$$

For short fasteners where the unthreaded area is small, Equation 2.8 can be used to find a good estimate for k_b . For long fasteners, where the threaded area is relatively small, the Equation 2.9 can be used to find a good estimate for k_b [8].

2.1.3 Member stiffness

In the previous chapter, the stiffness of the bolt in the clamped zone was determined. In this chapter, the stiffness of the members in the clamped zone is studied. The stiffness of the bolt and member must be known in order to learn what will happen when the assembled connection is subjected to an external tensile loading. In a bolted joint there may be more than two members, and all together they act like a series of compressive springs. The total spring rate of the members would then be

$$\frac{1}{k_m} = \frac{1}{k_1} + \frac{1}{k_2} + \frac{1}{k_3} \dots + \frac{1}{k_i} \quad 2.11$$

where k_m is the total stiffness of the member. If one of the connected members is a soft gasket, the stiffness of the other members can be neglected since the stiffness in the gasket is usually so small in comparison. For practical purposes, the gasket stiffness is the only one used. If there is no gasket, the compression spreads out between the bolt head and the nut. The area of the pressure distributed is not uniform, so the stiffness of the members is more difficult to obtain.

By experimentation, the stiffness can be determined as Ito [9] did. Ito used ultrasonic techniques to determine the pressure distribution at the interface of the members. The effective area of the connecting force and the measured interface pressure distribution shows that the pressure exceeds out to 1.5 bolt radii. Further away from the bolt, the pressure reduces. Ito suggested the use of pressure-cone method developed by Rotcher [10] for stiffness calculation with variable cone angles, shown in Figure 2.4 (horizontal hatched lines).

Recent surveys show that the method by Rotcher gives higher stiffness of the member causing small values for the external force. To be on the safe side, one should calculate the member stiffness by considering the member clamping zone as a cylinder with the outer diameter equal to the diameter of the nut (vertical hatched lines). The latter method gives smaller values for the member stiffness.

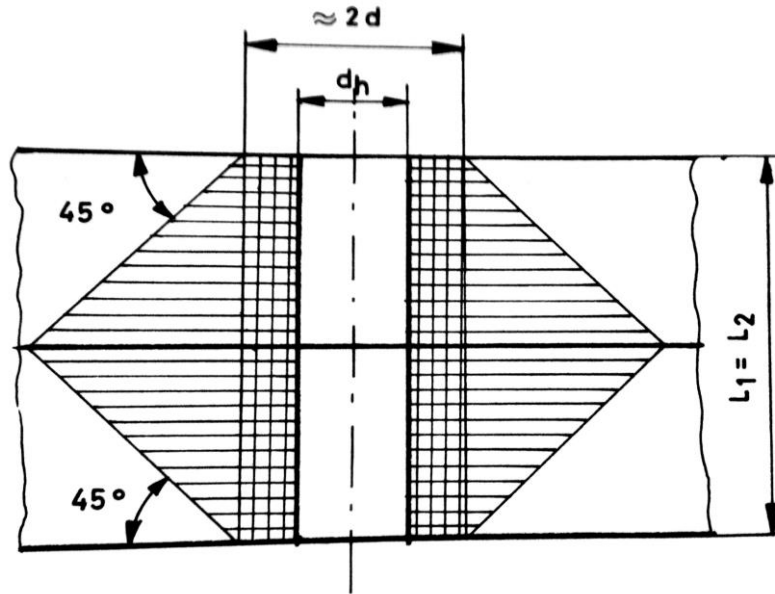


Figure 2.4: Clamping force [10]

where

bolt diameter = d

hole diameter, $d_h \approx 1,1 \cdot d$

diameter of nut contact face, $D \approx 2 \cdot d$

bolt Young's modulus = E_b

member Young's modulus = E_m

The member stiffness becomes the following

$$k_m = \frac{\pi(D^2 - d_h^2) E_m}{4 L_m} = \frac{\pi((2d)^2 - (1,1d)^2) E_m}{4 L_m} \approx 2,2d^2 \frac{E_m}{L_m} \quad 2.12$$

By assuming,

- Each part of member has equal length, $L_1 = L_2$ and total length of member, L_m
- Each part of member has the same elastic modulus, $E_{m1} = E_{m2}$
- The effective length of the bolt is unthreaded

the following ratio of force between the bolt and member is deduced.

$$\frac{F_b}{F_m} = \frac{k_b \delta}{k_m \delta} = \frac{\frac{\pi d^2 E_b}{4 L}}{2,2d^2 \frac{E_m}{L}} \approx \frac{0,79E_b}{2,2E_m} = 0,36 \frac{E_b}{E_m} \quad 2.13$$

If both the member and bolt is made of steel, $E_s = E_m$, the ratio of external force and force of bolt

$$\frac{F_b}{F} = \frac{k_b \delta}{(k_b + k_m) \delta} = \frac{0,36}{1,36} = 0,26 \quad 2.14$$

In this case, it shows that the force increased in the bolt is approximately a quarter of the external force [8] [10].

2.2 Joint Design

2.2.1 Mechanical properties/Material mechanics

A main challenge is to determine a proper material model, which gives the correct material behaviour when applying external load. To be able to predict and understand the response of the material, an examination of the material is necessary. A tensile stress-strain relation gives important information about the material, and it is a common tool for characterise the properties of the material. A typical tensile stress-strain diagram is illustrated in Figure 2.5. If a fastener approaches its maximum strength, it will be permanently deformed. To avoid permanent deformation, alloy or carbon steel bolts have a defined *proof load*. The proof load represents the usable strength range for each particular fastener, 85-95% of yield. It is by definition the applied tensile load the fastener must sustain without permanent deformation.

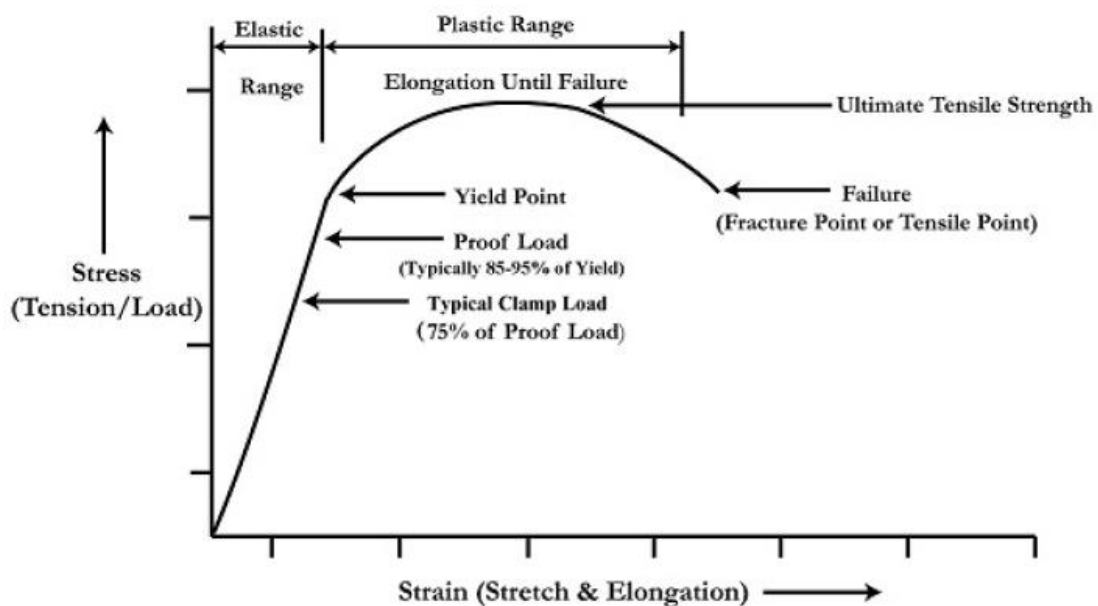


Figure 2.5: Tensile Stress-Strain Diagram

2.2.1.1 Elasticity

Before reaching the yield point, displayed in Figure 2.5, it is characterized as the elastic domain. In the elastic area the deformations are infinite small and the stress-strain relation is linear. For isotropic materials as steel, the linear elastic stress-strain relation is described by Hooke's Law and simplified to

$$\sigma = E\varepsilon \quad 2.15$$

where ε refers to the elastic strain and σ to the stress. For steel NS-EN 1993-1-1 [11] the Young's Modulus, E , is defined as 210 GPa. There is certain amount of elasticity in a steel material as it is stretched. A bolt that is tensioned within the proof load is functioning in the elastic range. If the load is removed (within the elastic range) the fastener will always recover to its original configuration.

2.2.1.2 Plasticity

From recoverable deformation in the elastic range, the deformation starts to deform the material permanently (exceeding its yield point) when increasing the applied load. At this point the steel is not able to recover to its original shape when the load is removed. It has entered the plastic range. The total strain, ε_t , consists by both elastic strain, ε^e , and plastic strain, ε^p , see Figure 2.6.

$$\varepsilon_t = \varepsilon^e + \varepsilon^p \quad 2.16$$

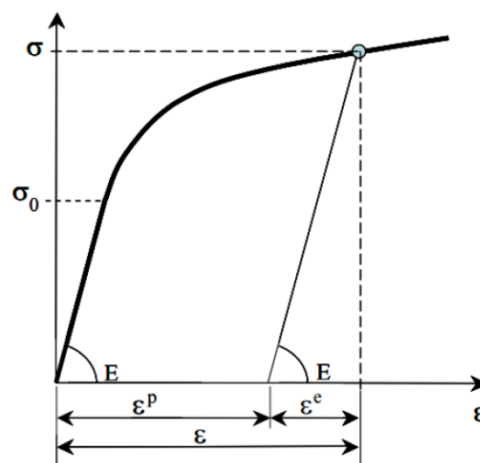


Figure 2.6: Distribution of elastic and plastic strain [12]

If the fastener is applied more load, it would eventually reach a point of maximum

stress known as ultimate tensile strength. Beyond this point the fastener continues to “neck down” and elongate further while the stress is reducing until it breaks.

2.2.2 Joint Diagram

When tightening a bolt and nut, a tensile stress is produced, which is approximately equal to the compressive stress in the joint material. The behaviour and life of the joint depends on how long they can maintain their preload. A proper amount of preload force in the bolts is vital. When tightening a bolt with too much clamping force, one may exceed the proof load of the bolt. Even if the bolt does not break during assembly, it might break later when exposed to external loads. The members in the joint may also be damaged if the clamping force is too high. By tightening the bolt too loose, the joint may loosen, and a bolted connection subjected to cyclical loads with a too small clamping force, fatigue on the bolt will occur [6].

As mentioned earlier, bolts acts like a spring when exposed to axial force. When joining materials, the same analogy can be made. During assembly, the bolts are compressed like a spring, and they gain a clamping force as long as the bolts are stretched. Applying external load which reduces the clamping force (“relaxes” the bolt), will release some of the energy in the spring. This can result in bolt failure or loosening of the joint.

A joint diagram is a good tool for visualise the behaviour of a bolted connection subjected to tension. The joint diagram is displaying the load deflection characteristics of a bolt and the material the bolt is connecting. It illustrates how a bolted joint sustains the external load. Based on the joint diagram shown in Figure 2.7, equations for dimensioning a bolted connection due to axial forces are developed.

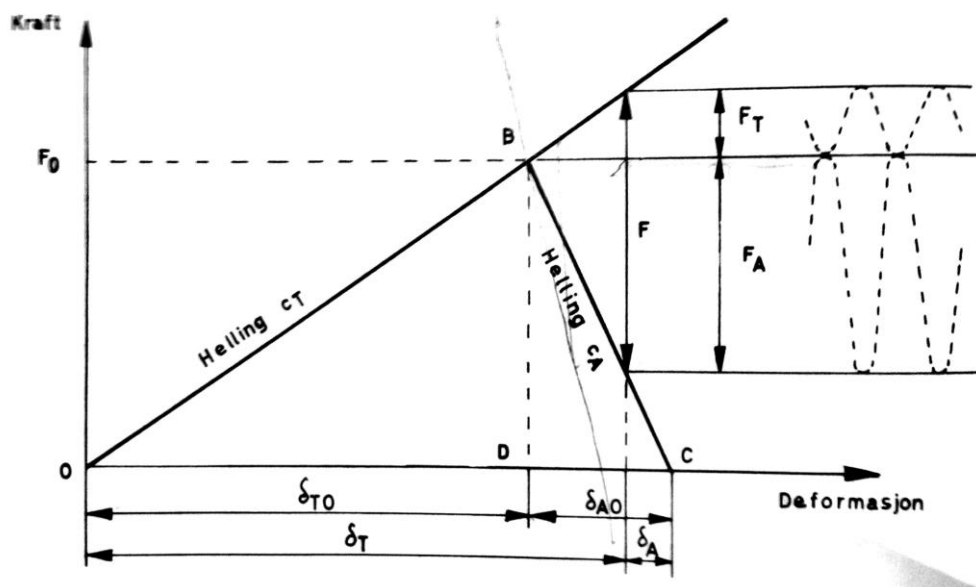


Figure 2.7: Joint diagram [10]

- δ_{T0} = Deflection of bolt with preload force
- δ_T = Deflection of bolt with added external force
- δ_{A0} = Deflection of material with preload force
- δ_A = Deflection of material with added external force
- F_0 = Preload force
- F = External load
- F_A = Change of force in material
- F_T = Change of force in bolt

As the bolt is tightened, the internal forces are resisting the elongation (δ_{T0}) of the bolt, creating the preload force F_0 . The straight line from 0 to B is the relationship between the force and elongation. The curve will be straight until the fastener begins to yield. On the right side of B is the reaction force, compressing of the joint. The angle of the deformation in the bolt and member corresponds to the stiffness for each of the components. The elongation of the compression is represented by δ_{A0} . At this point, the compression force on the joint is equal the tension force on the bolt.

If an external force (F) is been applied to the joint, the clamping force is reduced (F_A), and additional force (F_T) is applied on the bolt. F_A and F_T are different since the bolt and the joint have different stiffness. By adding the external force, the bolt will continue to elongate δ_T and the joint compression will be reduced to δ_A (the increase of elongation is equal to the increase in thickness of the joint).

If the external load increases, the clamp force will eventually decrease until the joint is fully unloaded, and any further increase will result in a gap between the plates. The bolt then sustains all of the additional force, see Figure 2.8.

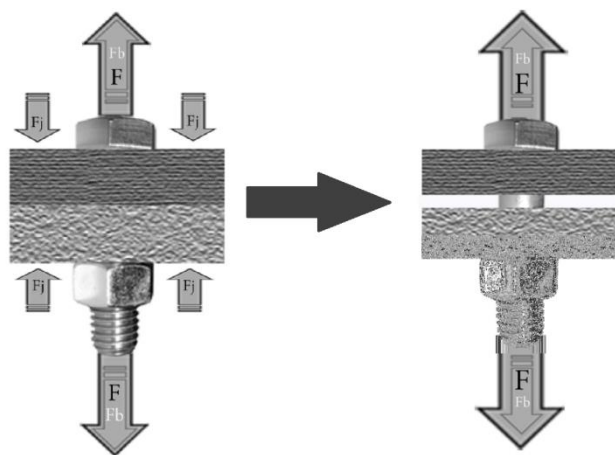


Figure 2.8: Joint fully unloaded [6]

The reliance on bolt tension or preload is a concern regarding tension joints. If the clamping force is not correct, the joint can fail in several ways. It may fail by vibration loosening, bolt fatigue, stress corrosion cracking or hydrogen embrittlement.

2.2.3 Preload force

If the head of the bolt and the nut are seated against a non-compressible material, a tightening on the assembly has the effect that it will stretch the bolt, thereby creating tension in the bolt. To make a fastening in a connection, it is in most cases required with preload. For some bolted connections, it is important to preload the bolts with a given force. This is especially important for connections subjected to tension and dynamic load. The preload shall adapt the strength of the bolt, and that should be approximately 90 % of the yield strength. In bolted connections that require preload should be connected by high strength bolts. The preload forces required are determined by tensile tests, and it is defined as the load which provides a durable deformation of 0.0125 mm of the bolt [13]. The two most common bolt classes is

$$\text{Bolt class: 8.8} \quad F_0 = 0.89f_y A_s = 0.72f_u A_s \quad 2.17$$

$$\text{Bolt class: 10.9} \quad F_0 = 0.86f_y A_s = 0.78f_u A_s \quad 2.18$$

Table 2.1 specifies the preload force for metric threaded fasteners

Table 2.1: Preload force for metric threaded fasteners

		M16	M18	M20	M22	M24	M27	M30	M33	M36
A_s (mm ²)		157	192	245	303	353	459	561	694	817
F_0 (kN)	8.8	89.3	109.9	140.3	172.7	201.1	261.9	319.8	396.3	466.0
	10.9	121.5	149.1	190.3	235.4	274.7	357.1	435.6	539.6	634.7

If a bolted connection is not tightened with the maximum required preload force the bolts are fairly more exposed for failure when subjected to tension. In Figure 2.9 it is illustrated a connection with a low preload force. The force reduction in the material, F_A , can never be greater than the preload force, F_0 . This causes the force increase, F_T , in the bolt to become too large compared to the material, and the risk of fatigue of the bolts increases. Thus it is very disadvantageous with a too low pre-load force [12].

In Figure 2.10 a joint diagram for the same connection is shown, but with a large preload force. When the external load, F_T , is applied the first time, the bolt may deform somewhat plastically, but it will return elastically along the dash-dotted. The preload

force is reduced from F_0 to F'_0 . By subsequent loads, there is no further plastically yielding in the bolt.

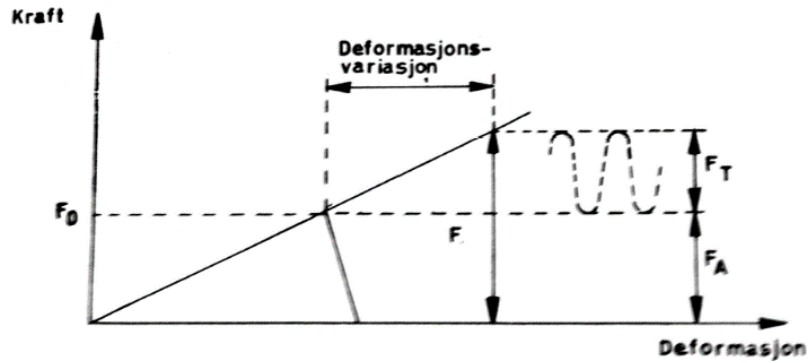


Figure 2.9: Low preload force

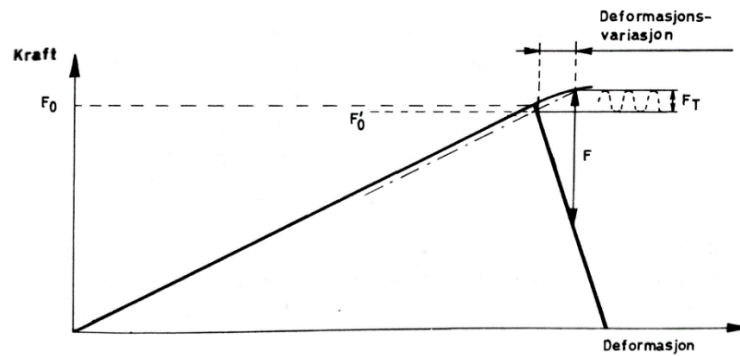


Figure 2.10: High preload force

Experience shows that preload with time can have a certain tendency to reduce due to plastically deformations. The main rule is therefore simple; one should always achieve as high preload force as possible [10].

In most cases of preloading one cannot be sure of obtaining exactly the desired preload. Due to varying friction, conditions, etc. significant deviations should be expected. The higher preload force one wish to achieve, the greater the risk is that the bolt will break during tightening. In literature [10], there is specified a theoretical equation for torque when tightening.

$$M_T = n_f \cdot F_0 \cdot d_s \quad 2.19$$

where

M_T	is the torque
$n_f \approx 0.2$	is a torque variable (Nut factor)
F_0	is the preload force
$d_s = \sqrt{\frac{4A_s}{\pi}}$	is the nominal diameter

The two variables F_0 and d_s are well defined, but the problem with the equation is the nut factor, n_f . The nut factor is dependent on what increases or decreases the friction within the threads of the nut and is a combination of three sub-factors [6]:

- K1 – Shape of the threads
- K2 – Thread friction between the threads of the bolt and threads of the nut
- K3 – Friction between the nut and the member it rotates on

2.3 Temperature Effects

In bolted connections, the materials are temperature sensitive i.e. their properties are influenced by the change in temperature. As the temperature increases, the strength of the metal fasteners declines and effects such as stress relaxation or creep may occur [14]. The definition of creep is continued extension of a material when subjected to constant stress. The creep rate depends on the material, and when the material is subjected to temperature, the creep rate increases. When a bolt starts to creep, the extension of the bolt increases without any increase in the bolt load. As a result, the bolt stress reduces and ultimately, reduces the clamping force. The definition of creep applies for constant stress, so when the stress reduces due to temperature effects, the phenomenon is known by other term such as temperature stress relaxation, but the cause is the same.

Thermal expansion is one of the most problematic effects due to the temperature effects [6]. At significant temperatures, differential thermal expansion rates between the joint and the fastener may cause failure. It is mainly a problem when dealing with dissimilar materials having different thermal expansion coefficients [5]. As temperature rises, the heat will cause the joint and bolt materials to expand, but at different rates if the coefficient differs. Consider using aluminium in conjunction with carbon steel fasteners as an example. Then the aluminium will expand approximately twice as much as some of the carbon steel fasteners. Using a grade 8 bolt as the fastener for connecting an aluminium joint, it would be expected to see a significant increase in the bolt tension as the temperature increases, which would lead to an increase of clamping force. The joint or gasket material could be damaged by this reaction, or in worst case, even break the bolt. In the other way around, with a bolt material expanding more than the joint, the clamping force would be reduced. If the material of the joint and bolt are of the same material, the differential expansion problems could occur, by heating up the bolt and joint in different rates. Different thermal expansion would also cause the joint and the bolt to expand at different rates.

Regarding the expansion of a bolt and joint exposed to a temperature increase, the length of the bolt and thickness can be calculated with the following equations [5].

$$L_G \cdot \alpha_1 \cdot (T_1 - T_0) = \Delta L_B \quad 2.20$$

$$L_G \cdot \alpha_2 \cdot (T_1 - T_0) = \Delta L_J \quad 2.21$$

where L_G (mm) is the grip length of the joint, α is the thermal expansion coefficient (mm/mm⁰C) and (T_1-T_0) (⁰C) is the difference between the initial temperature and the final temperature. ΔL_B and ΔL_J are the change in thickness of the joint and length of the bolt.

In a non-preloaded bolted connection which is assembled, the additional tension (or reduced tension) created in the bolt between the joint and bolt (F_T) can be approximated by

$$\frac{A_s \cdot E_b}{L_E} (\Delta L_J - \Delta L_B) = F_T \quad 2.22$$

where L_E is the effective length of bolt (mm) and F_T (N) is the additional or reduces tension created by thermal expansion.

2.4 Technical description of a helideck

2.4.1 Materials in the support structure

Low weight is the outstanding and best known characteristic property of aluminium. Aluminium has an atomic weight of 26.98 and a specific weight of 2.7, approximately a third of the weight of other ordinary used metals. Aluminium alloys in the 6000- and 7000 series is widely used in lightweight- or alloy structures. The mechanical properties of aluminium, such as yield strength, young's modulus and fatigue limit, is substantially lower compared to carbon steel. The driving force for the use of aluminium in structures is the low density and weight compared to carbon steel. Characteristics of aluminium are equivalent to one-third of the characteristics of steel.

The stiffness is defined as the product of the moment of inertia (I) and Young's modulus (E). This determines the deflection when subjected to bending load. When extruding aluminium profiles, it is possible to create numerous of complex structural shapes. The key is to optimize the strength by improve the design of an aluminium profile. The extrusion process gives the opportunity for achieve maximum efficiency in the shape of a section. Aluminium is mostly used in an extruded shape, and extruding is considered as modern technology. Aluminium in the 6000- and 7000 series get its high strength by precipitation hardening (heat treatment technique). Even though aluminium is a resistant metal, it is needed special treatment when connecting it with other metals where moisture may occur. The risk in those dissimilar connections is getting galvanic corrosion. In a maritime environment, the use of high strength carbon bolts is deprecated. Instead it is recommended to use stainless bolts [4].

2.4.2 Support structure of a helideck

In terms of helideck, the supportive structure is normally welded steel, while the top deck is in aluminium. On Gudrun [4] the connection between the top deck and supportive structure is connected by bolts. The support structure is mounted on foundations on the living quarters.

In most years the helideck used on the Norwegian shelf has been built in Europe, which has led to short distances for transportation. Regarding the helideck on Gudrun, the aluminium deck top was built in China. The structure was built in small sections so that it could be transported in containers. As a result, it was decided that the sections should be connected by bolts.



Figure 2.11: Helideck on Gudrun

Originally it was not defined that the bolted connections should be preloaded non-slip connection, but so-called "snug tight" shear connection. Snug tight i.e. no defined torque, but the bolts were tightened to the point where the mechanics decided it was ok. The bolted connections consisted of M20 and M24 bolts. In addition to snug tight connection, there are several possible methods to bolt the structural component. The choice of method depends on the load (tension, shear, bending moment) and whether it is dynamic or static.

The different methods are

- Pass bolts
- Preloaded non-slip connection
- Snug tight

Pass bolts are bolts where the holes are adapted bolts with a high degree of accuracy. The hole diameter should be no more than 0.3 mm larger than the hole through which the bolt is going through. Therefore, there are great demands for precision in fabrication. This type of connection may be used in static shear connections and preloaded/non-preloaded tension connections. Pass bolts are also intended for shear connections subjected to dynamic load.

In a preloaded non-slip connection is the bolt tightened so hard so that the clamping force establishes a frictional force between the connected parts. If the frictional force is large enough, it will resist the external loads. It is important that the surfaces are straight, parallel, not greasy and has the right roughness. According to NS-EN 1999-1-1:2007/NA:2009 paragraph NA 3.3.2.2 [15] bolts of class 8.8 and 10.9 may be used as preloaded bolts. Stainless bolts have a tendency to elongate over time. This requires the bolts to have controlled tightening, provided they conform to the requirements for preloaded bolts in existing ENs, prENs.

Spring washers must not be used because of they, due to the opening, increase the risk of galvanic corrosion. They should not be used where there are preloaded non-slip connections.

Dynamic structures should be bolted together by preloaded non-slip connections or pass bolts. The non-slip connection shall resist the dynamic loads in the bolted connections that may lead to loosening of bolts or damaged connections.

The inaccurate and inconsistent tightening of the bolt preload force is compensated by the engineers by over-designing the joints. The designers specify more or larger bolts to ensure that the joints are sufficiently clamped together. When tightening the bolts, the torque wrench according to BS EN ISO 6789 [16] used is required to have an accuracy of $\pm 4\%$. Weekly, each wrench should be checked for accuracy.

3 REGULATIONS AND GUIDELINES

In this chapter the regulations for design of joints will be presented and how bolted connections are dimensioned according to Eurocode NS-EN 1993-1-8 [1].

3.1 Bolts

On the market, there are many different types of bolts and nuts. Bolts and nuts that should be used in design of steel structures according to the standard are:

- Hexagon head bolts – EN ISO 4014
- Hexagon nuts – EN ISO 4032

The rules in the standard is valid the bolt classes listed in the table below.

Table 3.1: Nominal values of yield strength f_{yb} and ultimate tensile strength f_{ub}

Bolt class	4.6	4.8	5.6	5.8	6.8	8.8	10.9
f_{yb} (N/mm ²)	240	320	300	40	480	640	900
f_{ub} (N/mm ²)	400	400	500	500	600	800	1000

The first digit in the bolt class number represents the tensile strength (f_{ub}) and the digit represents the yield strength (f_{yb}). The first digit is obtained by dividing the tensile strength by 100 (N/mm²) and the second digit is specified by $(f_{yb}/f_{ub}) \cdot 10$. For an 8.8 bolt, the ultimate tensile strength is $f_{ub} = 8 \cdot 100 = 800$, and the yield strength is $f_{yb} = 8 \cdot 8 \cdot 10 = 640$.

There are also requirements regarding elongation, δ_5 , of bolts in different bolt classes, see Table 3.2. For steel structure bolts of class 4.6, 8.8 and 10.9 are most common. Bolts of 8.8 and 10.9 have considerably higher tensile strength than bolt of 4.6, because of higher content of carbon. With higher carbon content, the elongation reduces. Steel with increasing carbon increases the strength but reduces the ductility.

Table 3.2: Elongation of different bolt classes [6]

Bolt class	4.6	8.8	10.9
δ_5 (%)	25	12	9

Clearance in holes

Requirements for clearance in holes is given in EN-NS 1090-2 [17].

For regular holes;

M12-M14: $d_0 \leq d + 1 \text{ mm}$

M16-M24: $d_0 \leq d + 2 \text{ mm}$

M27 - : $d_0 \leq d + 3 \text{ mm}$

3.2 Categories of bolted connections

According to NS-EN 1993-1-8 [1] bolted connections are divided into two different categories, shear connections and tension connections. For bolted connections exposed to shear loads, they should be designed as one of the following:

- **Category A: Bearing type**

In this category bolts from class 4.6 up to and including class 10.9 should be used. No preloading and special provisions for contact surfaces are required. The design ultimate shear load should not exceed the design shear resistance, obtained from 3.3.1, nor the design bearing resistance, obtained from 3.3.2.

$$F_{v,Ed} \leq F_{v,Rd}, \quad F_{v,Ed} \leq F_{b,Rd}$$

- **Category B: Slip resistant at serviceability limit state**

In this category preloaded bolts of class 8.8 and 10.9 should be used. Slip should not occur at the serviceability limit state. The design serviceability shear load should not exceed the design slip resistance, obtained from 3.3.4. The design ultimate shear load should not exceed the design shear resistance, nor the design bearing resistance.

$$F_{v,Ed} \leq F_{s,Rd}, \quad F_{v,Ed} \leq F_{v,Rd}, \quad F_{v,Ed} \leq F_{b,Rd}$$

- **Category C: Slip-resistant at ultimate limit state**

In this category preloaded bolts of class 8.8 and 10.9 should be used. Slip should not occur at the ultimate limit state. The design ultimate shear load should not exceed the design slip resistance, nor the design bearing resistance. In addition for a connection in tension, the design plastic resistance of the net cross-section at bolt holes $N_{net,Rd}$ [11] should be checked, at the ultimate limit state.

$$F_{v,Ed} \leq F_{s,Rd}, \quad F_{v,Ed} \leq F_{b,Rd}, \quad F_{v,Ed} \leq N_{net,Rd}$$

Bolted connections loaded in tension should be designed as one of the following:

- **Category D: non-preloaded**

In this category bolts from class 4.6 up to and including class 10.9 should be used. No preloading is required. This category should not be used where the connections are frequently subjected to variations of tensile loading. However, they may be used in connections designed to resist normal wind loads. $F_{t,Rd}$ and $B_{p,Rd}$ is obtained from 3.3.3.

$$F_{t,Ed} \leq F_{t,Rd}, \quad F_{t,Ed} \leq B_{p,Rd}$$

- **Category E: preloaded**

In this category preloaded 8.8 and 10.9 bolts with controlled tightening in conformity with EN 1090-2 [17].

$$F_{t,Ed} \leq F_{t,Rd}, \quad F_{t,Ed} \leq B_{p,Rd}$$

3.3 Design resistance

In this chapter the design, resistance for individual fasteners will be discussed. Each bolt in a bolted connection shall meet the capacity requirements given in Eurocode 3 Part 1-8.

3.3.1 Shear resistance

For bolts in classes 4.6, 5.6 or 8.8, where the shear plane passes through the threaded portion of the bolt the shear resistance (per shear plane) is

$$F_{v,Rd} = \frac{0.6f_{ub}A_s}{\gamma_{M2}} \quad 3.1$$

where f_{ub} is the ultimate tensile strength, A_s is the tensile stress area and γ_{M2} is the partial safety factor. According to the Standard $\gamma_{M2} = 1.25$

As for a bolt in class 10.9, the shear resistance is

$$F_{v,Rd} = \frac{0.5f_{ub}A_s}{\gamma_{M2}} \quad 3.2$$

The reason for a smaller value of the factor 0.5 given in Equation 3.2 is due to the ductility that is smaller in bolts in class 10.9.

If the shear plane passes through the unthreaded portion of the bolt, the shear resistance is equal for bolts in 4.6, 8.8 and 10.9

$$F_{v,Rd} = \frac{0.6f_{ub}A}{\gamma_{M2}} \quad 3.3$$

where A is the area of the unthreaded portion of the bolt. When designing with shear connections, it is always more safe by assuming that the shear plane passes through a threaded portion of a bolt giving extra capacity reserve.

These design resistances should only be used if the bolts are manufactured in conformity with 1.2.4 Reference Standard: Group 4, i.e. rolled threads.

For bolts with cut threads, the design shear resistance reduces and should be multiplied by a factor of 0.85.

If there is a packing in between the members of total thickness t_p greater than one-third of the nominal diameter d of the bolts, the capacity should be multiplied by a reduction factor β_p given by:

$$\beta_p = \frac{9d}{8d + 3t_p} \quad 3.4$$

The reason for the reduction of capacity when increasing the total thickness of the plate-connection, is when the grip length in the bolt increases the bolt is exposed to a bigger moment due to the shear forces that moves further apart.

3.3.2 Bearing resistance

If the bolted connection is subjected to shear forces, the bolt shaft may interact with the connecting material. It is important to control the stresses induced on the material by calculating the bearing resistance for the bolted connection. For simplification, the stress is assumed to be uniformly distributed on the shaft diameter d and the thickness of the material t , see Figure 3.1. If the distance e_1 is too small, the edge of the material will be torn out. If p_1 is too small, the fracture between the bolts will occur. If the distances e_1 and p_1 is too large, plastic deformations will occur on the material in front of the bolts, which then leads to a deformed (oval), enlarged hole.

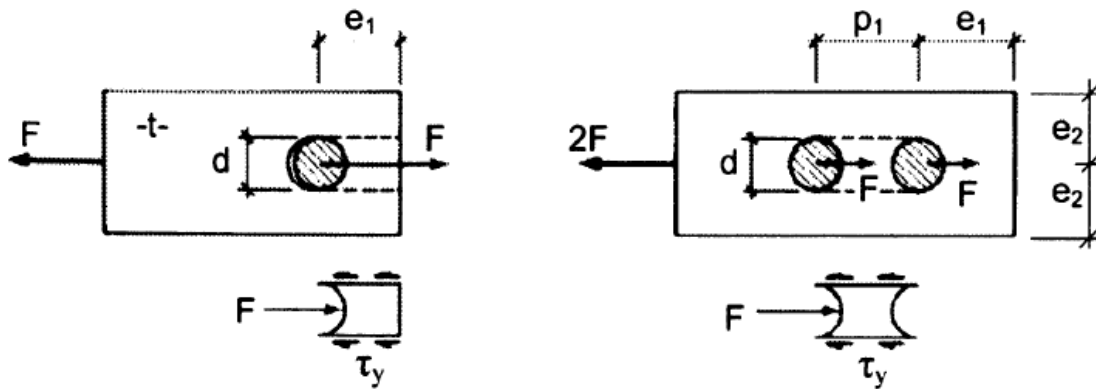


Figure 3.1: Tearing in front of an between fasteners

The bearing resistance is

$$F_{b,Rd} = \frac{k_1 a_b f_u d t}{\gamma_{M2}} \quad 3.5$$

where a_b is the smallest of

$$a_b = \min \left\{ a_d; \frac{f_{ub}}{f_u}; 1 \right\} \quad 3.6$$

In the same direction as the load, the factor a_d is

$$a_d = \begin{cases} \frac{e_1}{3d_0} & \text{for end bolts} \\ \frac{p_1}{3d_0} - \frac{1}{4} & \text{for inner bolts} \end{cases} \quad 3.7$$

Perpendicular to the direction of the load, the factor k_1 is

$$k_1 = \min \left\{ 2.8 \frac{e_2}{d_0} - 1.7; 2.5 \right\} \quad \text{for end bolts} \quad 3.8$$

$$k_1 = \min \left\{ 1.4 \frac{p_2}{d_0} - 1.7; 2.5 \right\} \quad \text{for inner bolts} \quad 3.9$$

3.3.3 Tension resistance

Tension resistance applies for bolted connections in category D (non-preloaded) and E (preloaded). Failure in a bolt due to tension load will occur at the smallest area, which is the cross-section in the minor diameter on the thread.

The tension resistance is

$$F_{t,Rd} = \frac{k_2 f_{ub} A_s}{\gamma_{M2}} \quad 3.10$$

where $k_2 = 0.63$ for countersunk bolt, otherwise $k_2 = 0.9$. With respect to punching through the material, $F_{t,Ed} \leq B_{p,Rd}$ as mentioned earlier

$$B_{p,Rd} = \frac{0,6\pi d_m t_p f_u}{\gamma_{M2}} \quad 3.11$$

where d_m is the mean of the across points and across flats dimensions of the bolt head or the nut, whichever is smaller and t_p is the thickness of plate under the bolt or the nut.

3.3.4 Design slip resistance

High strength bolts of class 8.8 or 10.9 can be preloaded and then have a design slip resistance. The capacity of the connection is then obtained from the friction between the surfaces. The design slip resistance should be taken as

$$F_{s,Rd} = \frac{k_s n \mu}{\gamma_{M3}} F_0 \quad 3.12$$

where k_s is the reduction factor that takes into account the bolt hole dimension. For bolts in normal holes, $k_s = 1$. n is the number of friction surfaces, μ is the slip factor and F_0 is the preload force shown in Equation 2.17.

3.4 Equivalent T-stub

According to the design standard NS-EN 1993-1-8 [1] it is possible to use an equivalent T-stub in bolted connections for modelling the design resistance of the following basic components:

- Column flange in bending
- End-plate in bending
- Flange cleat in bending
- Base plate in bending under tension

When using the equivalent T-stub model, an effective length $\sum l_{eff}$ must be determined. The effective length is a notational length and does not necessarily correspond to the physical length of the joint component that it may represent. According to the standard, the effective length should be such that the design resistance of the flange is equivalent to the joint component that it represents. Dimensions of an equivalent T-stub flange is shown in Figure 3.2.

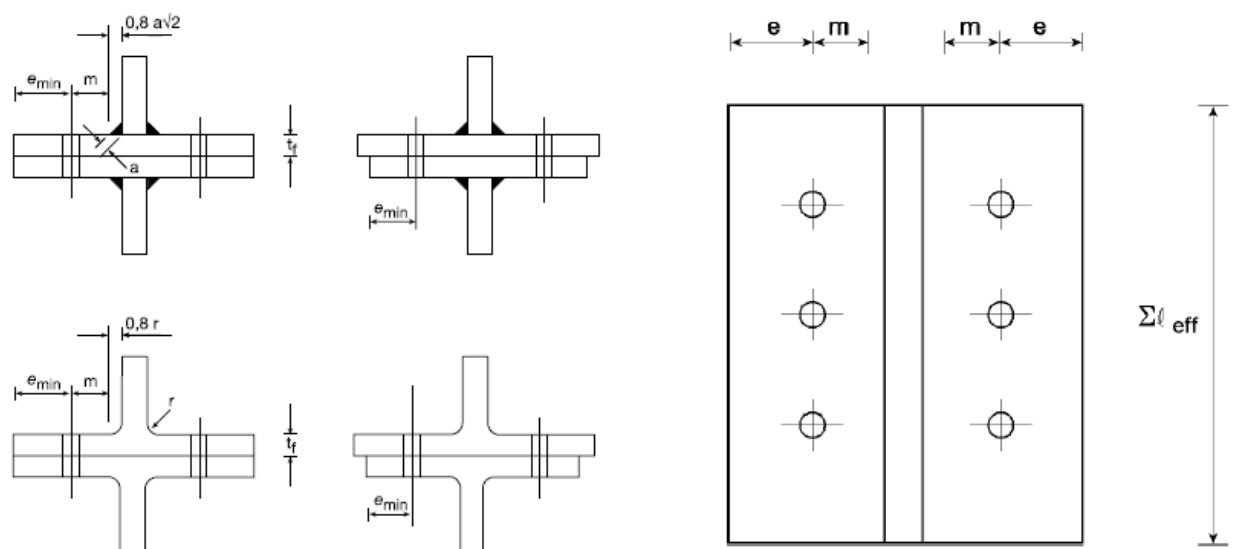


Figure 3.2: Dimensions of an equivalent T-stub flange

When determine the design resistance of a T-stub flange one of the three different failure modes will be the dominant failure mode. For failure mode 1 and 2, the plastic moment must be known. The effective length is then necessary to know when calculating the plastic moment, see Equation 3.13 and 3.14.

Plastic moment - Failure mode 1

$$M_{pl.1.Rd} = 0.25 \sum \frac{l_{eff} \cdot t_f^2 f_y}{\gamma_{M0}} \quad 3.13$$

Plastic moment - Failure mode 2

$$M_{pl.2.Rd} = 0.25 \sum \frac{l_{eff,2} t_f^2 f_y}{\gamma_{M0}} \quad 3.14$$

The effective length l_{eff} depends on the positioning of the bolts and whether the column flange is stiffened, unstiffened or if it is an end-plate. The Table 3.3 which is obtained by NS-EN 1993-1-8 [1] is the effective lengths of an unstiffened column flange. The standard divides the pattern into circular and non-circular patterns as well as individually bolt-rows, and part of a group of bolt-rows.

Table 3.3: Effective lengths for an unstiffened column flange

Bolt-row Location	Bolt-row considered individually		Bolt-row considered as part of a group of bolt-rows	
	Circular patterns $l_{eff,cp}$	Non-circular patterns $l_{eff,nc}$	Circular patterns $l_{eff,cp}$	Non-circular patterns $l_{eff,nc}$
Inner bolt-row	$2\pi m$	$4m + 1,25e$	$2p$	p
End bolt-row	The smaller of: $2\pi m$ $\pi m + 2e_1$	The smaller of: $4m + 1,25e$ $2m + 0,625e + e_1$	The smaller of: $\pi m + p$ $2e_1 + p$	The smaller of: $2m + 0,625e + 0,5p$ $e_1 + 0,5p$
Mode 1:	$l_{eff,1} = l_{eff,nc}$ but $l_{eff,1} \leq l_{eff,cp}$		$\sum l_{eff,1} = \sum l_{eff,nc}$ but $\sum l_{eff,1} \leq \sum l_{eff,cp}$	
Mode 2:	$l_{eff,2} = l_{eff,nc}$		$\sum l_{eff,2} = \sum l_{eff,nc}$	

For a separate T-stub, $p = L$. In Figure 3.3, it is illustrated four examples of yields patterns that can appear for an unstiffened column flange. Yield pattern number 1 and 2, are circular patterns and yield pattern number 3 and 4 are non-circular pattern. Number 1, 2 and 3 are gathered from the column "Bolt-row considered individually and number 4 is gathered from the column "Bolt-row considered as part of a group of bolt-rows," in Table 3.3 [18].

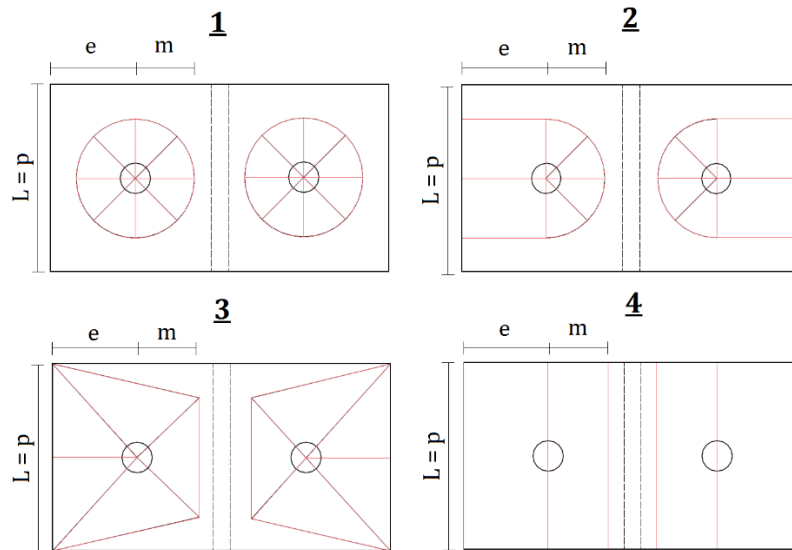


Figure 3.3: Yield patterns

As mentioned there are three possible failure modes of a tension loaded T-stub. The three different failure modes are described below.

- Mode 1 – When the bolts are strong compared to the flange, complete yielding of the flange occurs.
- Mode 2 – With adapted capacity of bolt and flange, the connection is yielding in the middle end of the flange (middle part in Figure 3.3) simultaneous as bolt failure. It is often desirable to achieve this failure mode because it implies that neither the flange nor the bolt is over-dimensioned, and the connection gets ductile in the flange before failure in the bolt.
- Mode 3 – When the bolts are weak compared to the flange, failure in the bolts occurs. For this failure mode, the prying forces can be ignored.

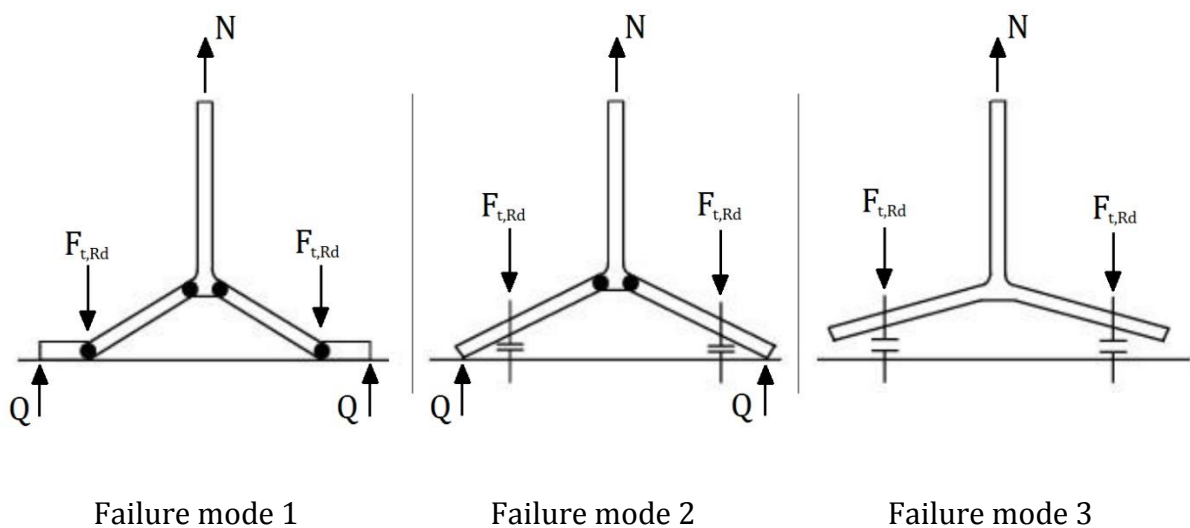


Figure 3.4: Failure modes of tension loaded T-stubs

The three modes differs with the amount of yield lines, and if the bolt will break or not. The force Q is the prying force (derived in Chapter 3.4.1) appearing at failure mode 1 and 2. $F_{T,Rd}$ is the design resistance for each of the failure modes, equally divided on each bolt. For every failure mode, Table 6.2 in the Eurocode displayed in Table 3.4, can be used for calculating the design resistance of the joint component. The lowest value of the three modes determines the resistance of the T-stub.

Table 3.4: Design resistance $F_{T,1,Rd}$ of a T-stub flange

	Prying forces may develop, i.e. $L_b \leq L_b^*$		No prying forces
Mode 1	Method 1	Method 2 (alternative method)	$F_{T,1-2,Rd} = \frac{2M_{pl,1,Rd}}{m}$
without backing plates	$F_{T,1,Rd} = \frac{4M_{pl,1,Rd}}{m}$	$F_{T,1,Rd} = \frac{(8n - 2e_w)M_{pl,1,Rd}}{2mn - e_w(m+n)}$	
with backing plates	$F_{T,1,Rd} = \frac{4M_{pl,1,Rd} + 2M_{bp,Rd}}{m}$	$F_{T,1,Rd} = \frac{(8n - 2e_w)M_{pl,1,Rd} + 4nM_{bp,Rd}}{2mn - e_w(m+n)}$	
Mode 2	$F_{T,2,Rd} = \frac{2M_{pl,2,Rd} + n\Sigma F_{t,Rd}}{m+n}$		
Mode 3	$F_{T,3,Rd} = \Sigma F_{t,Rd}$		

3.4.1 Prying force

When a T-stub is subjected to a tension force F , a contact pressure between the flange and the substrate is established. The contact pressure is modelled as a concentrated force Q , which acts as an additional force on the bolts. The bolts are therefore dimensioned for both the external and the prying force.

The prying force can be determined by modelling the T-stub shown in Figure 3.5, where the bolt and the prying force is modelled as roller support. According to NS-EN 1993-1-8 [1], the maximum distance n is $1.25m$. The fixed support in point C is at a distance $0.8r$ from the web. Now that the system is statically indeterminate, the unit load method [19] may be used for determining the prying force, Q .

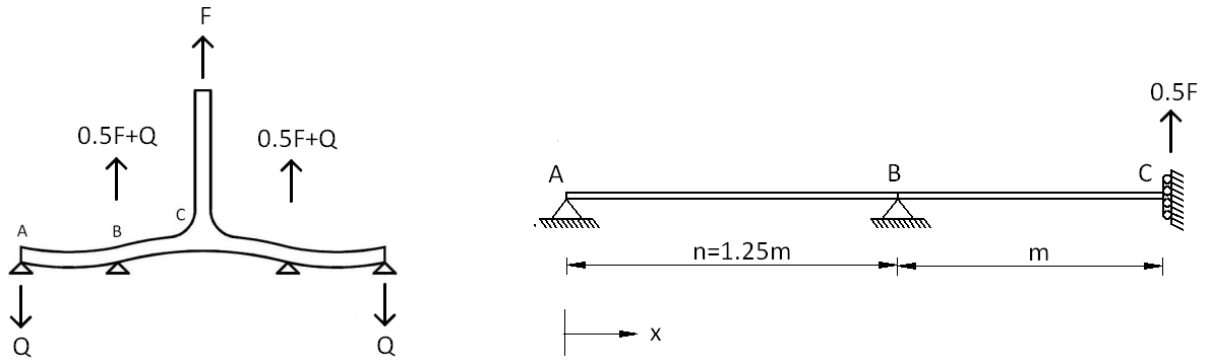


Figure 3.5: Model for determining the prying force, Q [20]

If the support at B is removed, the system becomes statically determinate, and the new system with external force and corresponding moment diagram is shown in Figure 3.6.

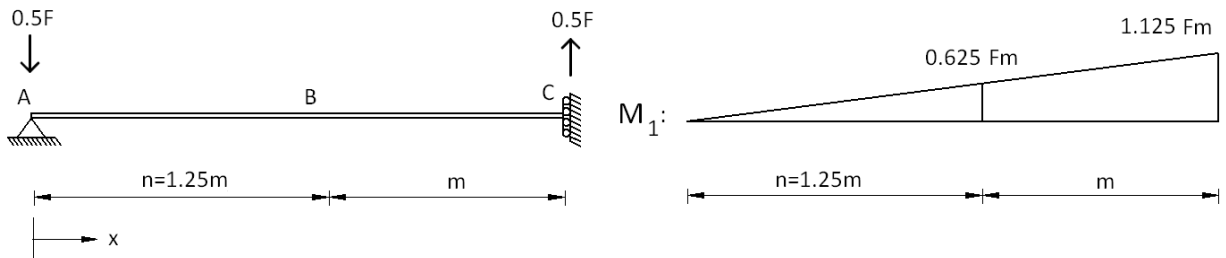


Figure 3.6: Static system and moment diagram due to external load

$$M_1(x) = 0.5Fx \quad 3.15$$

Then the outer load is removed and a unit load is applied at point B, Figure 3.7.

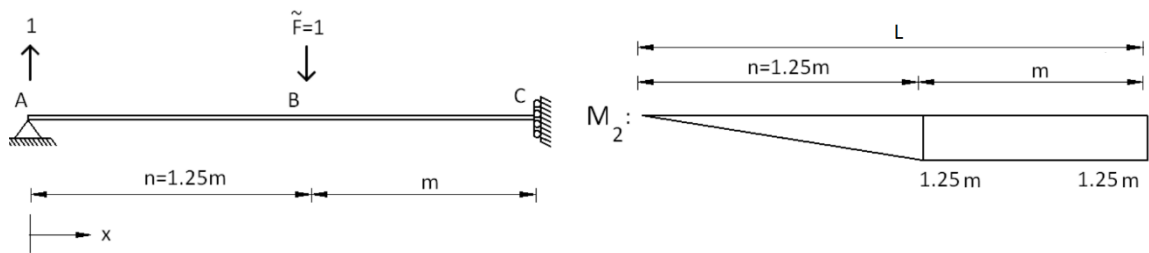


Figure 3.7: Static system and moment diagram due to virtual load

$$M_2(x) = -x \quad \text{if } x \leq n \quad 3.16$$

$$M_2(x) = -1.25m \quad \text{if } n \leq x \leq 2.25m \quad 3.17$$

Now that these two moment diagrams are known, the vertical displacement of the bolt due to the external load (Δ_1) and unit load (Δ_2) can be determined. The moment

diagrams are combined are integrated from 0 to 2.25m. Detailed calculations are attached in Appendix A.

$$\Delta_1 = \int_0^L \frac{M_1 M_2}{EI} dx = -\frac{545 F m^3}{384 EI} \quad 3.18$$

$$\Delta_2 = \int_0^L \frac{M_2 M_2}{EI} dx = \frac{425 m^3}{192 EI} \quad 3.19$$

The force of the bolt is determined by assuming zero displacement in support B, shown in 3.20, where the unknown bolt force is X.

$$\Delta_1 - X \Delta_2 = 0 \rightarrow X = \frac{\Delta_1}{\Delta_2} = -\frac{545 F m^3}{384 EI} \cdot \frac{192 EI}{425 m^3} = 0.64 F \quad 3.20$$

The bolt force is 0.64F, and then the prying force must be 0.14F.

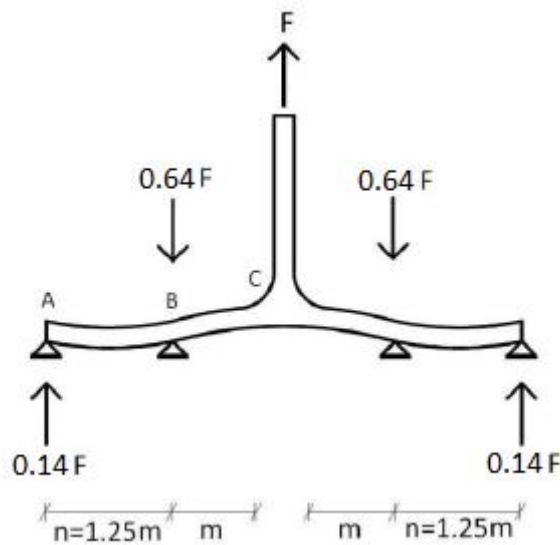


Figure 3.8: Prying force on a T-stub

3.4.2 Stiffness of T-stub connection

Spring in a serial connection can be compared to the total stiffness of the T-stub connection, where each basic component contributes to the total stiffness. The relation between the displacement, u , the force, F , and the stiffness, k_{tot} , is given as

$$F = k_{tot} \cdot u \quad 3.21$$

where

$$k_{tot} = \frac{1}{2} \frac{1}{\sum \frac{1}{k_i}} \quad 3.22$$

k_i represents the stiffness from component i . For T-stub connection subjected to tension, only the bolts and flange will contribute. As the calculations are based on one T-stub, the total stiffness of the system, which contains two T-stubs, will be reduced by a factor of 1/2.

The stiffness coefficients, k_j , which contribute to the stiffness in a T-stub, are described in NS-EN 1993-1-8 [1] as

$$\begin{array}{l} \text{Plate in} \\ \text{bending:} \end{array} \quad k_5 = \frac{0.9 \cdot l_{eff} \cdot t_p^3}{m^2} \quad 3.23$$

$$\begin{array}{l} \text{Bolt in} \\ \text{tension:} \end{array} \quad k_{10} = \frac{1.6 \cdot A_s}{L_b} \quad 3.24$$

where l_{eff} is the smallest of the effective lengths given in Table 3.3 and m is as defined in Figure 3.2. A_s is the tensile stress area, and L_b is the bolt elongation length, which is equal to the grip length (total thickness of material and washers), in addition to half the height of the bolt head and the height of the nut.

The stiffness coefficients are given in the unit millimetre. To achieve the correct unit of the stiffness, the following relation is defined as

$$k_i = E \cdot k_j \quad 3.25$$

where Young's Modulus, E , is taken into account.

3.4.3 Determination of the stiffness coefficients

In this chapter, the expressions for the stiffness coefficients, k_5 and k_{10} given in the Eurocode, will be derived. The derivation of the stiffness coefficients will be based on the prying force of $0.14F$ and the bolt force of $0.64F$ obtained in Chapter 3.4.1.

3.4.3.1 Stiffness coefficient for flange in bending, k_5

The stiffness coefficient for a flange in bending is based on calculations of the equivalent T-stub connection, where one flange is taken into consideration. The distance n , defined in Figure 3.8, is set to the maximum length used in NS-EN 1993-1-8 [1], which is $1.25m$.

The static models that are used in the determination of the coefficient are shown in Figure 3.9. The prying force and the bolt are modelled as roller supports with no possibility for movement in vertical direction.

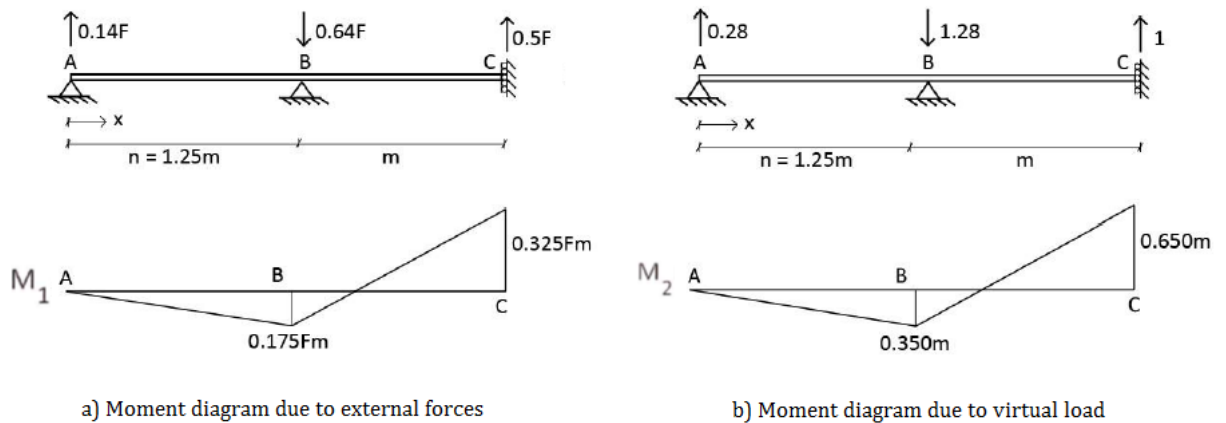


Figure 3.9: static models

The unit load method is used to determine the stiffness of the flange, where the displacement is given as

$$u = \int_0^L M_1 \frac{M_2}{EI} dx = 0.079 \frac{Fm^3}{EI} \quad 3.26$$

where M_1 and M_2 is the corresponding moment diagram for the virtual and external load shown in the figure over. In the expression for the plate's area moment of inertia the width to the T-stub is replaced by an initial effective length, $l_{eff,ini}$, shown in the equation below.

$$I = \frac{l_{eff.ini} \cdot t_f^3}{12} \quad 3.27$$

which leads to

$$F = 12.66 \frac{EIu}{m^3} = 1.055 \frac{l_{eff.ini} \cdot t_f^3 \cdot E \cdot u}{m^3} \quad 3.28$$

For a rectangular beam with $W_{pl} = 1.5W_{el}$ [21], the relation between plastic and elastic load capacity is defined as

$$F_{Rd.pl} = \frac{3}{2} F_{Rd.el} \quad 3.29$$

According to Weynand, Jaspart and Steenhuis [22] the elastic load capacity is expressed as.

$$F_{Rd.el} = \frac{M_{max}}{0.332m} \quad 3.30$$

And the plastic load capacity according to NS-EN 1993-1-8 [1] corresponds to failure mode 1

$$F_{Rd.pl} = F_{T.1.Rd} = \frac{4M_{pl.Rd}}{m} = \frac{l_{eff} \cdot t_f^2 \cdot f_y}{m \cdot \gamma_{M0}} \quad 3.31$$

By inserting Equation 3.30 and 3.31 in Equation 3.29 the relation between the initial and plastic effective lengths is determined as

$$l_{eff.ini} = 0.859l_{eff} \quad 3.32$$

Inserting Equation 3.32 in 3.28

$$F = \frac{0.906l_{eff} \cdot t_f^3 \cdot E \cdot u}{m^3} \quad 3.33$$

The stiffness coefficient of the flange is then utilized by combining the Equation 3.21 with 3.33 and 3.25

$$k_{flange} = \frac{0.906l_{eff} \cdot t_f^3}{m^3} \approx k_5 \quad 3.34$$

3.4.3.2 Stiffness coefficient for bolt in tension, k_{10}

The stiffness coefficient for the bolt is based on calculations of the stress- strain relation for a rod in tension (Hooke's law, see Chapter 2.1.1), and can be expressed by the Equation 3.35.

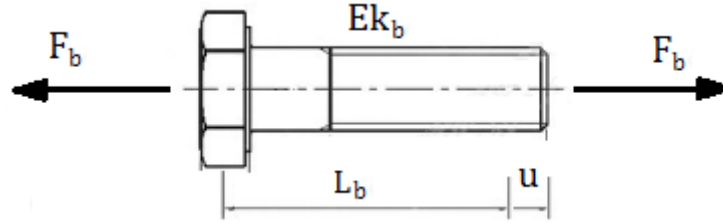


Figure 3.10: Bolt in tension

$$\sigma = E\varepsilon \Rightarrow \frac{F_b}{A_b} = E \frac{u}{L_b} \Rightarrow F_b = \frac{EA_b u}{L_b} \quad 3.35$$

The bolt load distribution obtained in Chapter 3.4.1 is inserted in Equation 3.35 and the force of the T-stub is

$$F_b = 0.64F = \frac{EA_b u}{L_b} \Rightarrow F = \frac{1.56EA_b u}{L_b} \quad 3.36$$

Where A_b is the cross section of the bolt, and F_b is the force contributed on the bolt. With known force, the stiffness coefficient for the bolt can be calculated by

$$k_b = \frac{1.587A_b}{L_b} \approx k_{10} \quad 3.37$$

4 CONSIDERED BOLTED CONNECTION

In the following chapters, it shall be carried out load capacity evaluation by theoretical approach following the guidelines in NS-EN 1993-1-8 [1], a finite element (FE) analysis and laboratory experiments on a bolted connection. Included in the FE analysis, the effect of thermal load will be studied. In this chapter details relevant to the considered T-stub bolted connection will be presented. Regarding the bolts properties and behaviour, it is important to know the chosen materials nominal values for yield and ultimate tensile strength and the thermal expansion coefficient. In this thesis it is preferred to use the following materials in Table 4.1 with properties according to NS-EN 1999-1-1 [15] and NS-EN 1993-1-1 [23]. In NS-EN 1993-1-1/NA 2015 the ultimate tensile strength, f_u , has been modified from 510 to 490 MPa.

Table 4.1: Material properties

Material:	Steel	Aluminium
	S355	6082 T6
f_u (MPa)	490	310
f_y (MPa)	355	260
E (MPa)	210 000	70 000
ν	0.3	0.3
Thermal expansion coefficient	$11.1 \times 10^{-6} \text{ C}^{-1}$	$23 \times 10^{-6} \text{ C}^{-1}$

The T-stub considered shall be connected by bolts between different materials, aluminium against steel and steel against steel for comparison. Galvanic corrosion is a form of corrosion when two dissimilar metals are joined, such as aluminium and steel. The corrosivity of the offshore environment is, in particular, the operation condition that has significant influence on the fatigue strength [13]. In this thesis, the fatigue strength of the bolted connection will not be considered, so galvanic corrosion between the materials will be ignored.

The motivation for exploring the behaviour for bolted connection is the incident on the helideck at the Gudrun platform [3] where there was a fracture in an aluminium profile (T-shape element) in the outer part of the helicopter deck connected to steel beams from the underlying structure. In addition, as regard of an aluminium – steel connection, it is also interesting to discover the behaviour of the connection exposed

to different temperature ranges. Offshore structures, as for the helideck on Gudrun, was constructed in Singapore and shipped to Norway. Temperature differences applied on a structure during shipping may differ from 30~40 °C in Asia to -15~20 °C in Norway (Barents Sea) [24], which results in a temperature difference of 50~60 °C. The temperature differences on a bolted steel – aluminium connection compared to a steel – steel connection are therefore important to investigate regarding the behaviour of the T-stub connection.

4.1 Geometry

According to the standard NS-EN 1993 1-8 [1], an equivalent T-stub may be used for examination of the behaviour of common structural components. As the thesis implies, it shall be examined a T-stub with one bolt-row (total of two bolts). It would be useful to study whether there is compliance among the standards, the finite element analysis and the laboratory experiments.

The dimensions of the considered T-stub for the theoretical approach, finite element analysis and the laboratory experiments are scaled down from the bolted connections used on a helideck. On a helideck on an offshore installation [25], the bolted connections with the materials and dimensions for the beams and bolts are listed as follows.

Table 4.2: Dimensions and materials

	Dimension	Material/Quality
Helideck [25]	250·250·15·25 (h·b·t _w ·t _f)	Aluminium alloy 6082 T6
	Steel plate (Figure 4.1)	Steel - S420
	M24 bolt (EN ISO 4104)	8.8
	M24 nut (EN ISO 4032)	8.8
Materials used in this study	300·200·10·16 (h·b·t _w ·t _f)	Aluminium alloy 6082 T6
	HEA 200	Steel – S355
	M16 bolt (EN ISO 4014)	8.8
	M16 Nut (EN ISO 4032)	8.8

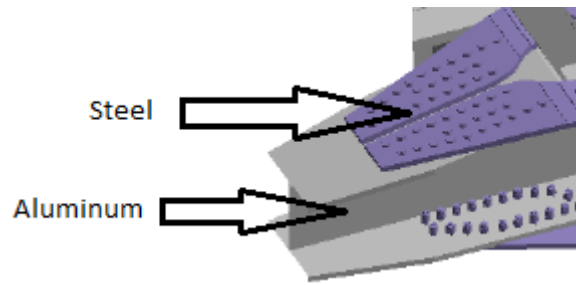


Figure 4.1: Steel – Aluminium connection on a helideck [3]

The bolts connecting the T-stubs are related to bolts used on a helideck [25], M24 of quality 8.8. For the experimental procedure, the bolts and the T-stubs are scaled down in order to get the acquired behaviour within the limitations of the test facilities. The design resistance of tension load is decided by whether of the three failure modes, described in Chapter 3.4, which will appear. In order to get a ductile behaviour on the flange combined with bolt failure, the T-stubs have been connected by fully threaded M16 bolts of quality 8.8. The dimensions of the T-stubs are measured from the parts used in the laboratory work. The laboratory experiments have been conducted on two configurations, steel against steel and steel against aluminium. The length (L) of the T-stubs were dimensioned to have similar behaviour in both tension load capacity and initial elastic stiffness among the two configurations.

The dimensions for the steel and aluminium T-stubs are based on the given profiles where one of the flanges is removed. The dimensions and the bolted T-stub connection are shown in Table 4.3 and Figure 4.2. All dimensions are in millimetre.

Table 4.3: T-stubs with dimensions (mm)

		Steel T-stub	Aluminium T-stub
Thickness of web	t_w	6.5	10
Thickness of flange	t_f	10	16
Width	b	200	200
Radius	r	18	18
Length	L	110	110
Bolt hole clearance	$d + 2\text{mm}$	18	18

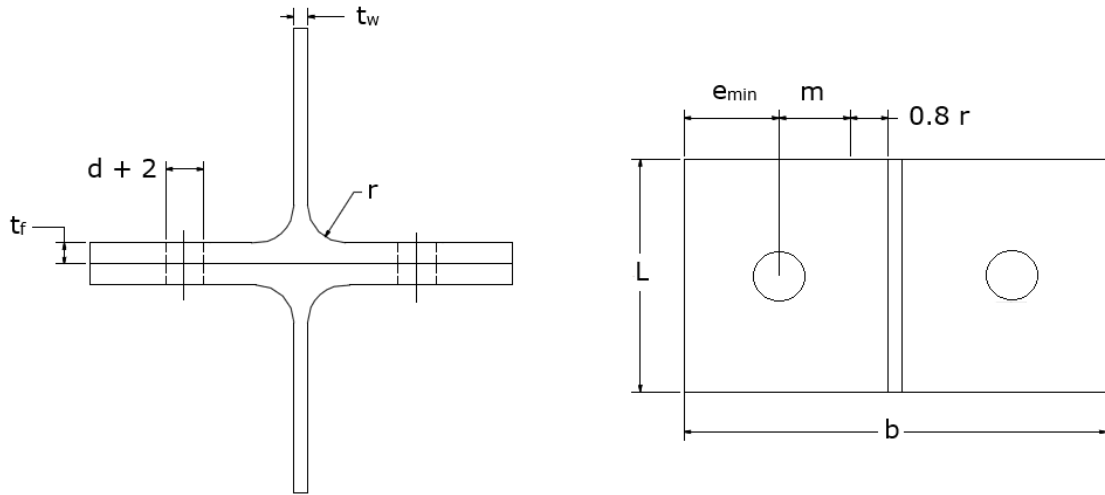


Figure 4.2: T-stub connection

The clearance in the holes is 18 mm, which is the maximum clearance in holes for an M16 – M24 bolt, $d+2\text{mm}$ [17]. The effective length l_{eff} of the connection is the length in the plane. The distance between the centre of bolt hole to the end of web, m , and the distance from centre of bolt hole to the edge of the flange, e_{min} , is determined in Chapter 6.1, and based on these dimensions the effective length is calculated (Appendix B).

5 CAPACITY OF THE BOLTED CONNECTION: EXPERIMENTAL INVESTIGATION

This chapter describes the experimental work conducted on bolted T-stub connections. Six tests subjected to tension have been performed on a variation of T-stub connections, steel against steel and steel against aluminium. Each connection consisted of two T-stubs, two bolts and nuts. The nuts were preloaded with the limit of a moment of 50 Nm, due to the tools accessible in the laboratory. Most importantly, each bolt was consistently tightened with the same preload force. Washers were ignored at the tension test.

By subjecting the bolted connection to pure tension, the goal was to investigate the failure modes and the maximum resistance load. The bolted connection subjected to thermal load it was of interest to investigate how and if the temperature difference in the joint would have any significant effect on the clamping force of the connection.

Through the laboratory experiments, the load capacity of the bolted connection was obtained.



Figure 5.1: Tensile test of T-stub connection

5.1 Preparations

When the T-stubs were made, the extruded aluminium beam and the HEA 200 steel beam were rough cut in ~ 110 mm long H-profiles. Then they were cut in the middle into T-stubs. In order to obtain an accurate length of 110 mm, the flanges were abraded. It was cut a total of nine steel and three aluminium T-stubs.

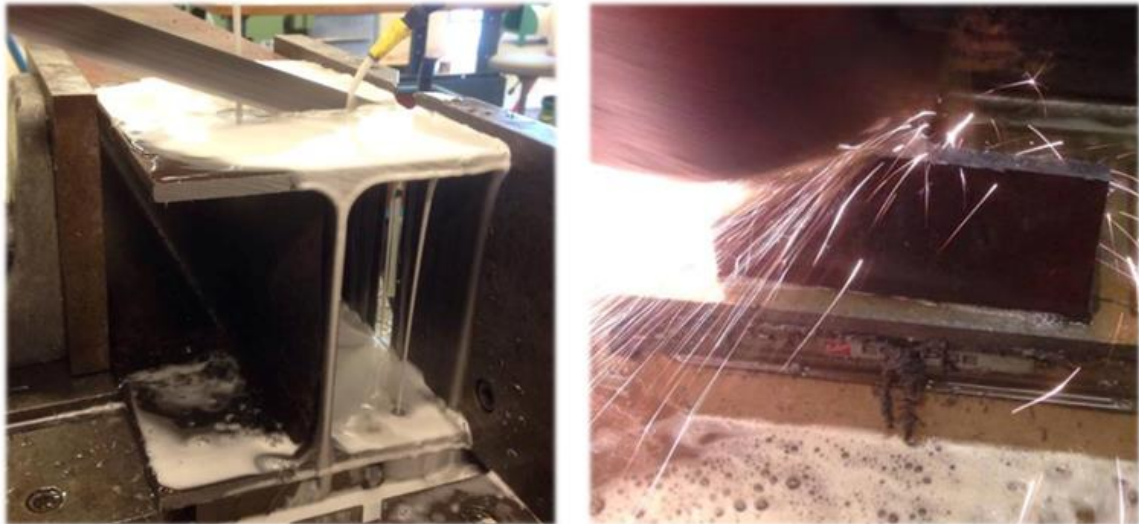


Figure 5.2: Cutting and abrading profiles

After the T-stubs had been cut, there were drilled holes for the bolts. For each test and configuration M16 bolts were used, so the diameter of the holes for the bolt was 18 mm, which is the biggest hole diameter allowable according to EN-NS 1090-2.

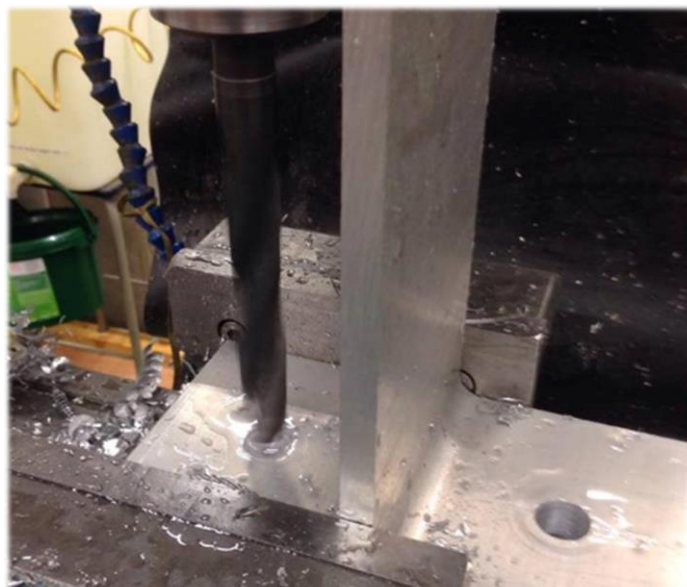


Figure 5.3: Drilling holes in the aluminium flange

Figure 5.5 and Figure 5.6 displays the geometry and Figure 5.4 shows one of each of the assembled configurations, which was used in the tensile tests.

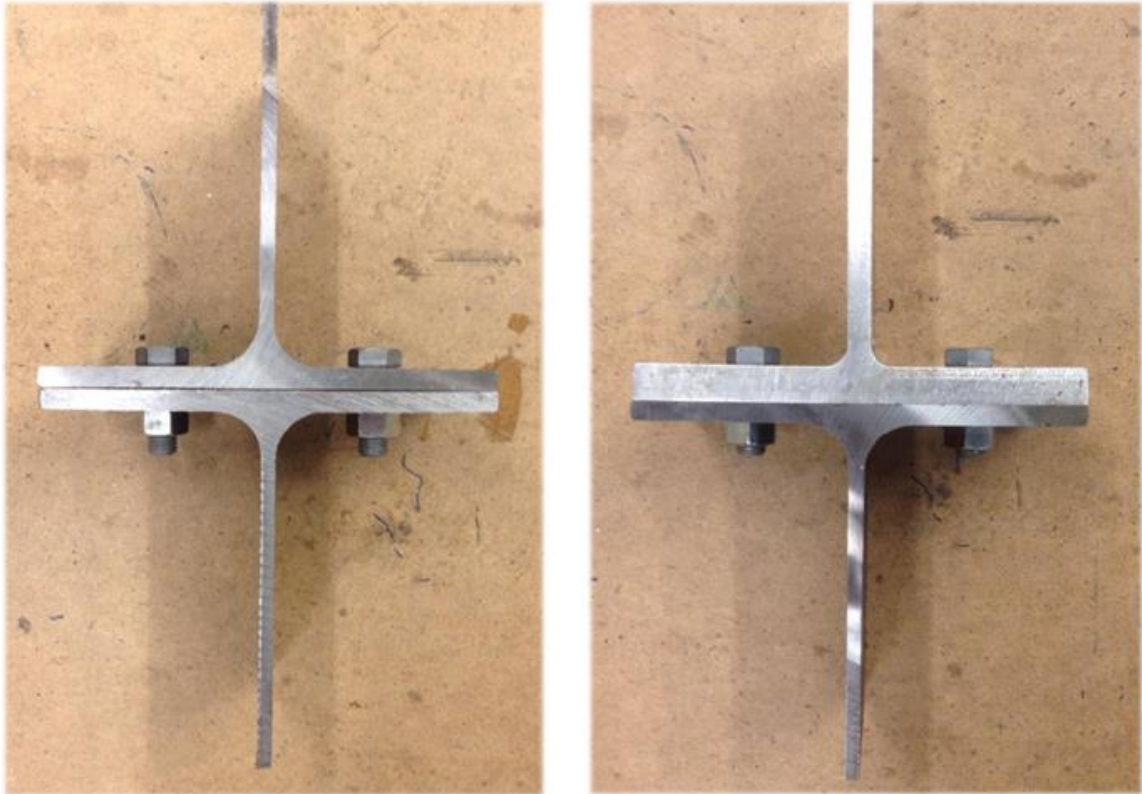


Figure 5.4: Steel - Steel (left) and Aluminium - Steel (right) configurations

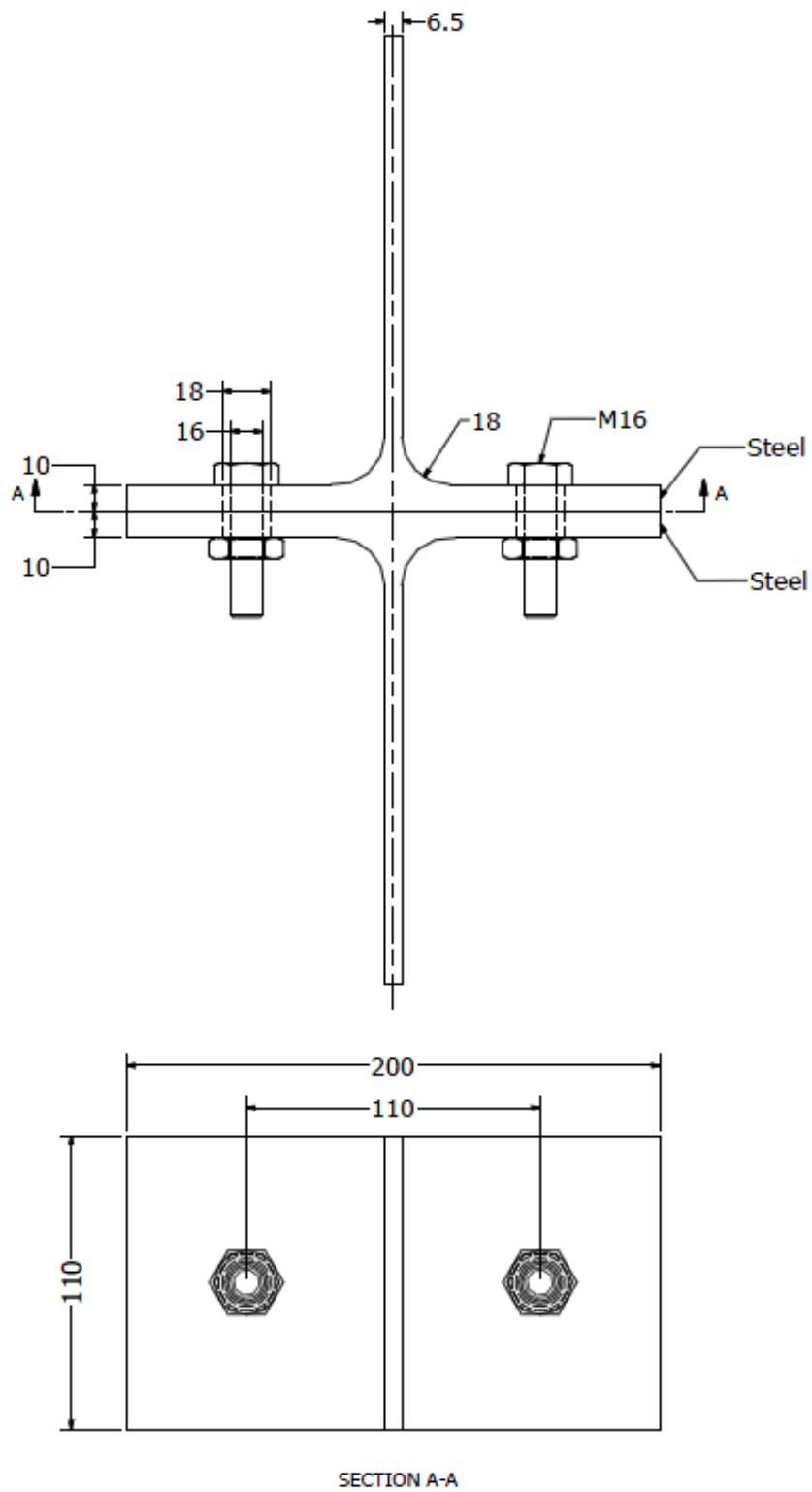


Figure 5.5: Steel - steel connection

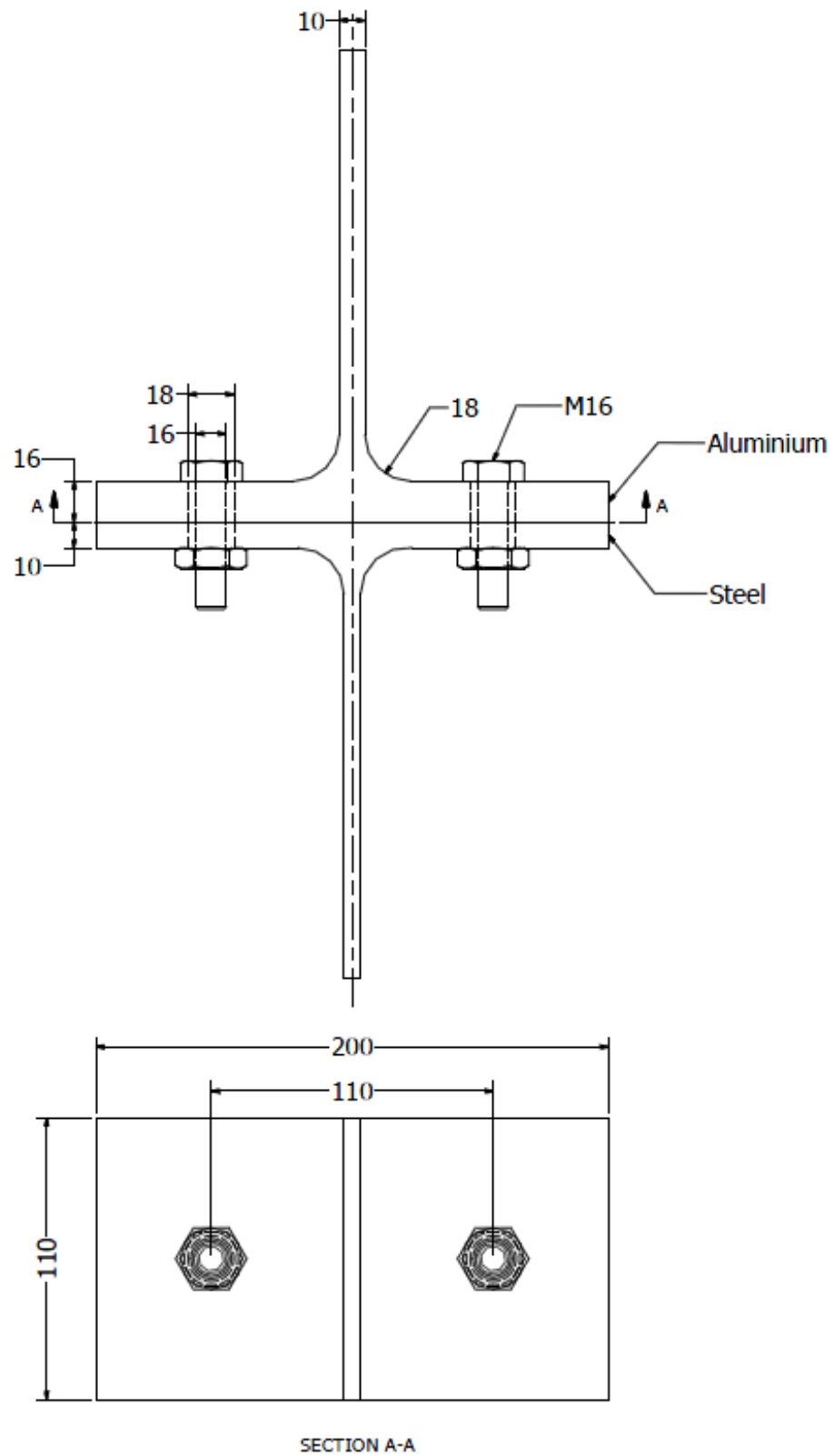


Figure 5.6: Aluminium - Steel connection

5.2 Test setup

All tension loaded tests were performed in the test machine Instron 5985 that has a maximum tension capacity of 250 kN. The test specimen were fastened by clamping of the webs as indicated in Figure 5.7. The web at the lowest t-stub was withheld from translation in all directions, and the web of the upper t-stub was pulled with a constant velocity. The load were applied with a constant velocity of $0.00025 \frac{mm}{mm} \cdot \frac{1}{s}$ for all the tests in the elastic zone and increased to a constant velocity of $0.00067 \frac{mm}{mm} \cdot \frac{1}{s}$ in the plastic zone, recommended from NS-EN ISO 6892-1:2009 [26]. The machine registered the applied force and the displacement of the piston in the upper part of the machine. To retrieve the elongation of the T-stub connections, an extensometer was connected to the web as closely to the flanges as possible.

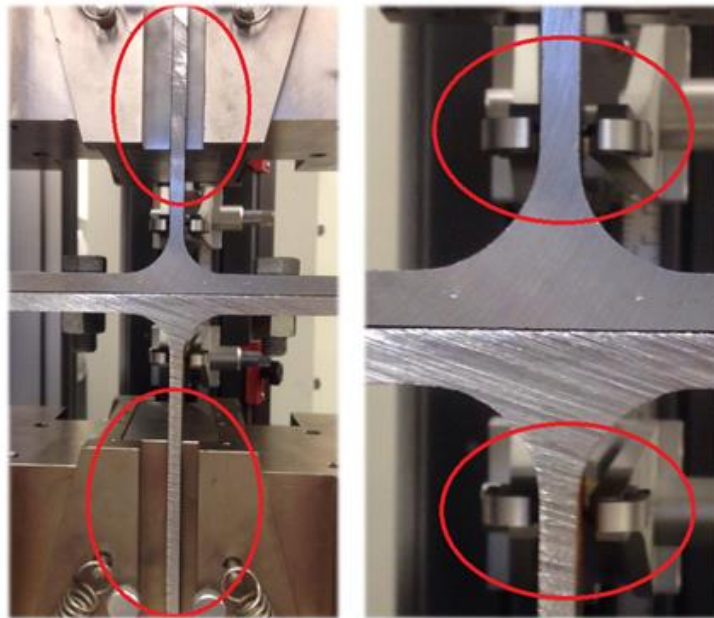


Figure 5.7: Clamping of the webs (left) and extensometer (right)

5.3 Test results

For each test the force-displacement curves were plotted, where the displacement was retrieved from the extensometer. All tests were driven until failure, which appeared in most cases in the bolt, but for one case in one of the aluminium – steel connections, thread stripping occurred.

For comparison with the finite element analysis and the Eurocode, the given values for maximum force in Table 5.1 and Table 5.2 are used as the tensile strength.

5.3.1 Steel – steel connection

The failure mode of the connection and the registered results are presented in Table 5.1. With a difference of 3 mm from the biggest and smallest extension registered among the different specimens, the failure for each one occur at a surprisingly similar maximum force. Failure occurred in the bolt for all the specimens.

Table 5.1: Test results

Test specimen	Max force (kN)	Extension at max force (mm)	Force at break (kN)	Extension at break (mm)	Failure at
1	177.4	29.65	160.0	33.34	Bolt
2	177.9	32.49	165.9	34.14	Bolt
3	178.5	31.51	140.2	39.15	Bolt

In Figure 5.8: the force – displacement curve for the three specimens are presented.

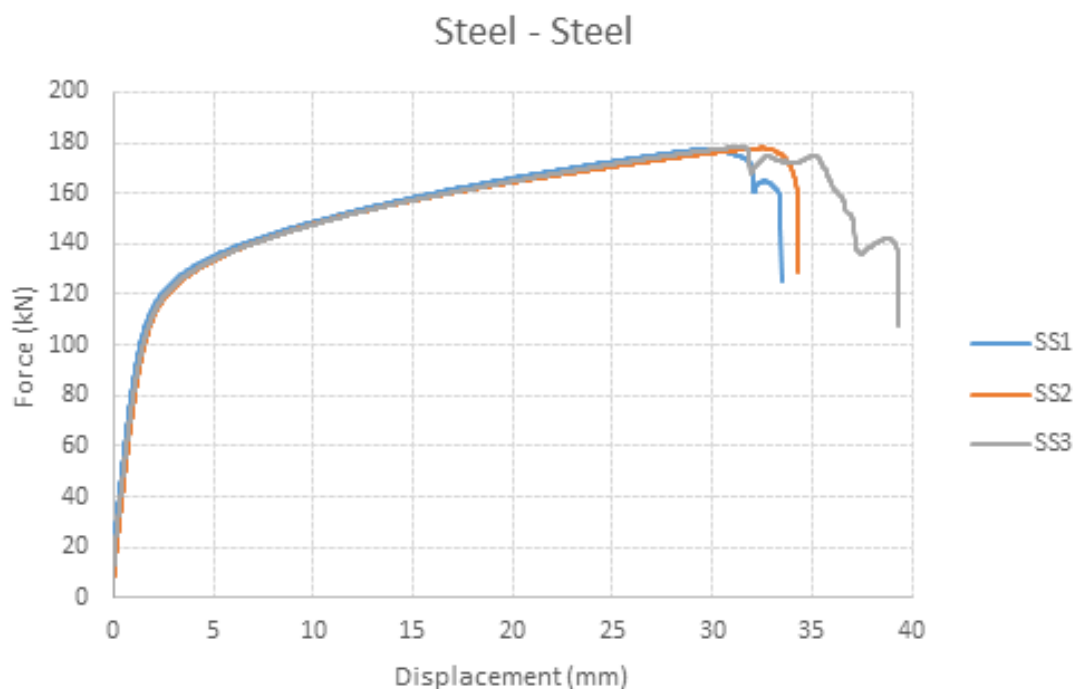


Figure 5.8: Force – displacement curves for steel – steel connection

Figure 5.9 of the specimen 1 (SS1), the plastic deformation is clearly shown, with a total displacement at the centre of flanges were measured to be 33.34 mm. The right bolt and flanges were bent but remained in contact with the ends, which demonstrate the contribution of prying action.

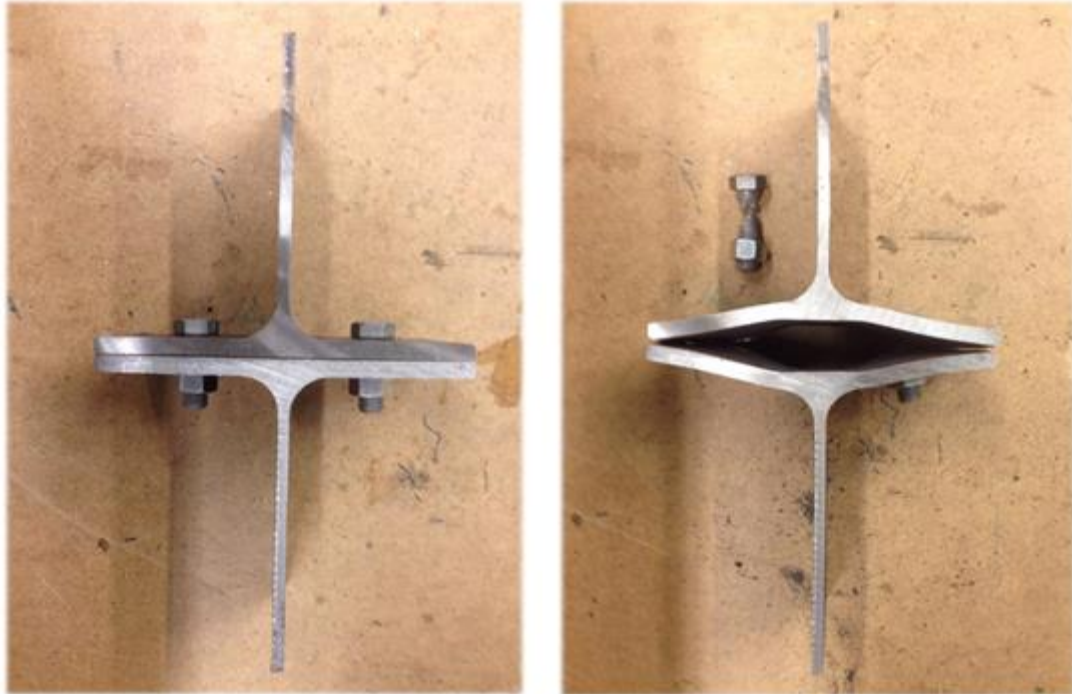


Figure 5.9: Specimen 1 (SS1) before and after test

5.3.2 Aluminium – steel Connection

The failure mode of the connection and the registered results are presented in Table 5.2. The maximum forces among the three specimens do not differ much, despite the failure due to thread stripping in specimen 1. Figure 5.12 shows the failure of the bolt and failure in the nut (thread stripping). The difference between the biggest and smallest extension registered is approximately 2.4 mm. The difference is small as for the steel – steel connection, which verify a credible test.

Table 5.2: Test results

Test specimen	Max force (kN)	Extension at max force (mm)	Force at break (kN)	Extension at break (mm)	Failure at
1	181.5	18.27	151.3	24.77	Nut
2	184.1	18.36	172.5	23.43	Bolt
3	181.9	20.69	137.9	26.99	Bolt

In Figure 5.10 the force – displacement curve for the three specimens are presented.

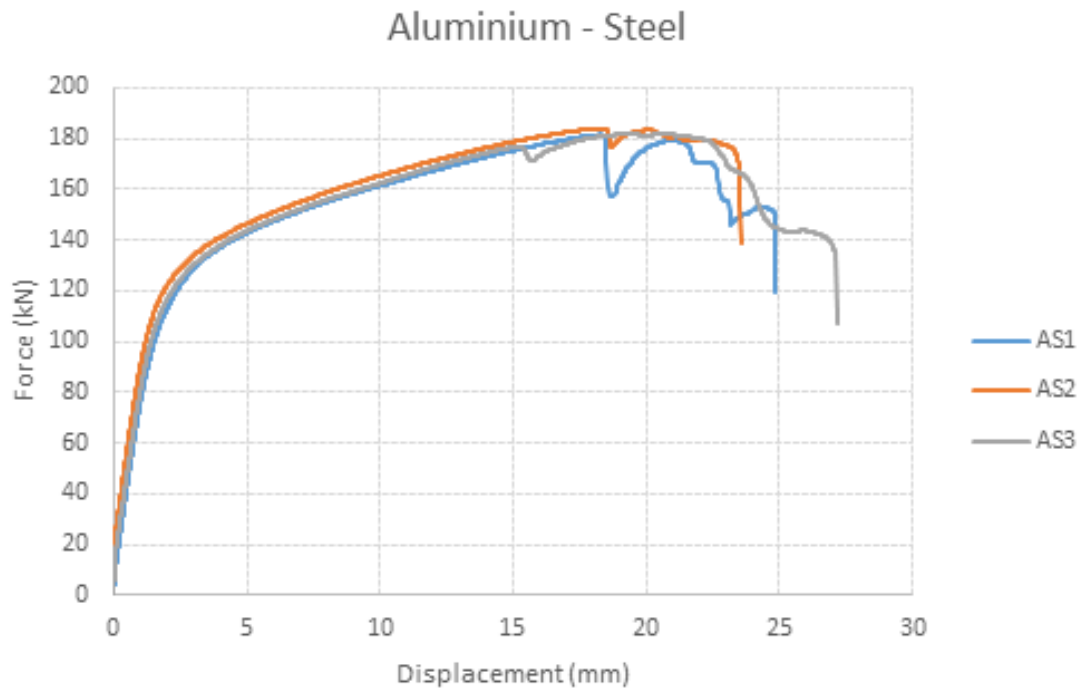


Figure 5.10: Force – displacement curves for aluminium – steel connection

For specimen 1, Figure 5.11, the plastic deformation of the steel flange (bottom) is clearly shown, while the aluminium flange (top) has an almost unclear plastic deformation. The total displacement at the centre of flanges was measured to be 27.77 mm. According to Eurocode 3, the amount of bending stiffness in the aluminium flange is larger compared to the steel flange (Chapter 6.3), so the outcome of the test was as expected. The higher value of stiffness contributed from the aluminium T-stub, resulted to a higher maximum force of 4-5 kN compared to the steel – steel connection.

The failure occurred in the nut due to thread stripping but did not have a significant effect on the maximum force and extension compared to the other two specimens.

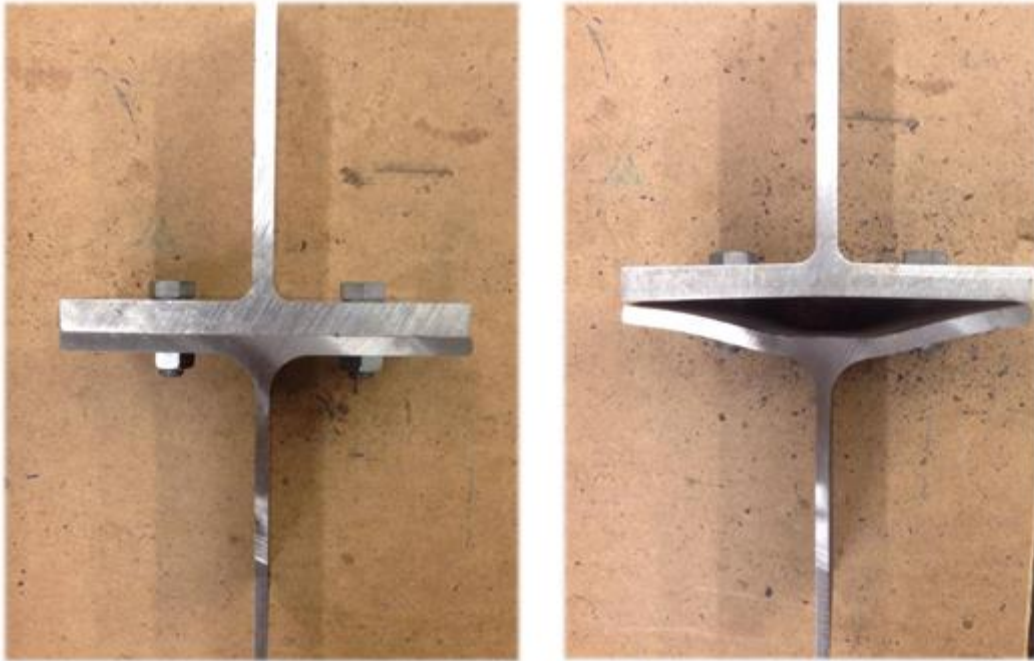


Figure 5.11: Specimen 1 (AS1) before and after test



Figure 5.12: Failure at nut (left) and failure at bolt (right)

6 CAPACITY OF THE BOLTED CONNECTION: THEORETICAL INVESTIGATION

In this chapter theoretical approach for the capacity will be conducted on the T-stubs considered in Chapter 4. All the calculations are based on the rules given in the Eurocode 3, Part 1-8 [1] described in Chapter 3. It has also been calculated the stiffness's of the different bolted connections

In order to achieve the best basis for comparing the load capacity calculations with the results of the finite element analysis and the laboratory experiments, the partial safety factors are set equal to 1.0. Since the factor is used as a safety for achieving failure, the best assessment of the regulations is without the partial safety factor. The dimensioning capacities (with the use of partial safety factor) are meant to have a lower value than the actual capacity. The material data of the flanges that are used was gathered from the results of the tensile test from Chapter 7.1.3. The material data used for the bolts is calculated (ref. Appendix E) in accordance with the standard NS-EN ISO 898-1 [27].

Only calculated results of capacity and stiffness are presented in this chapter, while the full calculations are attached in the Appendices.

6.1 Effective length - l_{eff}

As mentioned in Chapter 3, a T-stub has three possible failure modes and is it desired, with customised dimensions, that the connection gets a ductile behaviour with bolt failure (failure mode 2). One way of governing the way the connection reacts at ultimate state with the chosen geometry, is to vary the effective length (l_{eff}) of the T-stub.

Table 6.1: Dimensions of a T-stub flange

Distance between the bolts		$w = 110 \text{ mm}$	
Distance between the bolt and the edge of web	Steel flange	$m_s = \frac{w - t_{w,s}}{2} - 0.8r = 37.35 \text{ mm}$	
	Aluminium flange	$m_a = \frac{w - t_{w,a}}{2} - 0.8r = 35.6 \text{ mm}$	
Distance from bolt to edge of flange, smallest of		$e_1 = \frac{b-w}{2} = 45 \text{ mm}$	$\rightarrow e_{min} = 45 \text{ mm}$
		$e_{2s} = 1.25m_s = 47 \text{ mm}$	
		$e_{2a} = 1.25m_a = 45 \text{ mm}$	

The effective length can be determined by knowing the distances m (smallest among m_s and m_a) and e_{min} . According to Eurocode 3 the effective length shall be determined using one of three tables given in the standard. In this case, the table for the effective lengths for an unstiffened column flange given in Chapter 3.4 Table 3.3 is used. The effective length is determined in the table below. The lengths are in millimetre.

Table 6.2: Calculations of effective length

Effective length, $l_{eff,cp}$ – Circular patterns		Effective length, $l_{eff,nc}$ – Non-circular patterns		Length, L
$2\pi m$	$\pi m + 2e_{min}$	$4m + 1.25e_{min}$	$2m + 0.625e_{min} + e_{min}$	-
224	202	199	144	110

The smallest of all calculated effective lengths is the length of the T-stub, L.

$$L = l_{eff} = 110 \text{ mm} \quad 6.1$$

6.2 Design resistance

The tension resistance of the T-stub flange is determined from Table 3.4, given in Chapter 3.4. Detailed review of the calculations of the design resistance is in Appendix C.

6.2.1 Bolts

The design tension resistance of one single bolt,

$$F_{t,Rd} = \frac{0.9f_{ub}A_{s,bolt}}{\gamma_{M2}} = 126.6 \text{ kN} \quad 6.2$$

gives the T-stub flange design resistance at failure mode 3 by

$$F_{T,3,Rd} = \sum F_{t,Rd} = 253.2 \text{ kN} \quad 6.3$$

6.2.2 Steel T-stub

To calculate the capacity of the connection of failure mode 1 and 2, the plastic moment capacity for steel must be known.

The plastic moment for steel flange is

$$M_{pl,Rd,s} = \frac{0.25l_{eff}t_{f,s}^2f_{y,s}}{\gamma_{M0}} = 1017 \text{ kNmm} \quad 6.4$$

Design resistance at failure mode 1

$$F_{T,1,Rd,s} = \frac{4M_{pl,Rd,s}}{m_s} = 108.9 \text{ kN} \quad 6.5$$

Design resistance at failure mode 2

$$F_{T,2,Rd,s} = \frac{2M_{pl,Rd,s} + e_{min} \sum F_{t,Rd}}{m_s + e_{min}} = 163.1 \text{ kN} \quad 6.6$$

According to the Standard NS-EN 1993-1-8 [1] the smallest value of among the design resistances be the dominant failure mode. In this case failure mode 2 has the smallest value, $F_{T,1,Rd,s} = 108.9 \text{ kN}$, bolt failure with yielding of the flange.

6.2.3 Aluminium T-stub

To calculate the capacity of the connection of failure mode 1 and 2, the plastic moment capacity for aluminium must be known.

$$M_{pl,Rd,a} = \frac{0.25l_{eff}t_{f,a}^2f_{y,a}}{\gamma_{M0}} = 2198 \text{ kNmm} \quad 6.7$$

Design resistance at failure mode 1

$$F_{T,1,Rd,a} = \frac{4M_{pl,Rd,a}}{m_a} = 246.9 \text{ kN} \quad 6.8$$

Design resistance at failure mode 2

$$F_{T,2,Rd,a} = \frac{2M_{pl,Rd,a} + e_{min} \sum F_{t,Rd}}{m_a + e_{min}} = 195.9 \text{ kN} \quad 6.9$$

The dominant failure mode for the aluminium T-stub, is failure mode 2 with a design resistance of $F_{T,2,Rd,a} = 195.9 \text{ kN}$, bolt failure with yielding of the flange.

The design loads for each T-stub are listed in Table 6.3

Table 6.3: Design loads of T-stubs

T-stub	Tension load capacity (kN)		
	Failure mode 1	Failure mode 2	Failure mode 3
Steel	108.9	163.1	253.2
Aluminium	246.9	195.9	253.2

Since both connections contains a steel T-stub as the weakest part, failure mode 1 is dimensioning according to the Eurocode with a design load of 108.9 kN.

6.3 Stiffness

When connecting two different materials by bolts, the different components have different Young's modulus, affecting the stiffness and the behaviour of the connection when subjected to tension. For steel flange and bolt $E_{steel} = 205 \text{ GPa}$ (ref. Chapter 7.1.3.1), and for aluminium $E_{alu} = 70 \text{ GPa}$. The thickness of the aluminium flange is 16 mm, so the total thickness of the flanges in a steel aluminium connection is thicker than on the steel against steel connection. A detailed review of the calculations of stiffness is in Appendix D.

Steel

The grip length, L_b , is the sum of the thickness of the flange plus the half of height for both the bolt head and nut. Grip length for the bolt in connection with two T-stubs, half the thickness of the bolt head and nut must be divided by 2 to ensure that not two sets of bolt heads and nuts are involved in the connection.

$$L_{b,s} = t_{f,s} + \frac{\frac{t_{head}}{2} + \frac{t_{nut}}{2}}{2} = 16.20 \text{ mm} \quad 6.10$$

The stiffness coefficient of the bolts in the steel T-stub are

$$k_{c,10,s} = \frac{1.6 \cdot A_s}{L_{b,s}} = 15.51 \text{ mm} \quad 6.11$$

The stiffness coefficient in the steel flange is

$$k_{c,5,s} = \frac{0.9 \cdot l_{eff} \cdot t_{f,s}^3}{m^3} = 1.90 \text{ mm} \quad 6.12$$

The total stiffness coefficient of the steel T-stub with the two bolts is

$$k_{c,tot,s} = \frac{1}{2} \frac{1}{\left(\frac{1}{k_{c,5,s}}\right) + \left(\frac{1}{k_{c,10,s}}\right)} = 0.85 \text{ mm} \quad 6.13$$

Multiplying the stiffness coefficient with the Young's modulus to find the elastic initial stiffness

$$K_{el,s} = k_{c,tot,s} \cdot E_s = 173.49 \frac{kN}{mm} \quad 6.14$$

Aluminium

The grip length of the bolt in an aluminium - steel connection for one of the flanges is

$$L_{b,a} = t_{f,a} + \frac{\frac{t_{head}}{2} + \frac{t_{nut}}{2}}{2} = 22.20 \text{ mm} \quad 6.15$$

The stiffness coefficient of the bolts in the aluminium T-stub are

$$k_{c,10,a} = \frac{1.6 \cdot A_s}{L_{b,a}} = 11.32 \text{ mm} \quad 6.16$$

The stiffness coefficient in the aluminium flange is

$$k_{c,5,a} = \frac{0.9 \cdot l_{eff} \cdot t_{f.a}^3}{m^3} = 8.99 \text{ mm} \quad 6.17$$

The total stiffness coefficient of the aluminum T-stub with the two bolts is

$$k_{c,tot.a} = \frac{1}{2} \frac{1}{\left(\frac{1}{k_{c,5,a}}\right) + \left(\frac{1}{k_{c,10,a}}\right)} = 2.51 \text{ mm} \quad 6.18$$

Multiplying the stiffness coefficient with the Young's modulus to find the elastic initial stiffness

$$K_{el.a} = k_{c,tot.a} \cdot E_a = 175.31 \frac{kN}{mm} \quad 6.19$$

Steel – steel connection

The stiffness of the assembled steel – steel connection is

$$K_{el.s-s} = \frac{1}{2} (K_{el.s} + K_{el.s}) = 173.50 \frac{kN}{mm} \quad 6.20$$

Aluminium – steel connection

The stiffness of the assembled aluminum – steel connection is

$$K_{el.a-s} = \frac{1}{2} (K_{el.a} + K_{el.s}) = 174.41 \frac{kN}{mm} \quad 6.21$$

Table 6.4 summarises the stiffness coefficients and the total elastic stiffness among the two configurations. The total elastic stiffness among the configurations is approximately the same, despite the differences in the total stiffness. By having thicker aluminium flange than steel flange compensates for the difference in Young's modulus in order to maintain similar elastic stiffness for both configurations.

Table 6.4: Summary of total elastic stiffness and stiffness coefficients

T-Stub	Coefficient [mm]		
	Bolts (in tension)	Flange (in bending)	Total
Steel	15.51	1.90	0.85
Aluminum	11.32	8.99	2.51
Connection	Total Elastic stiffness [kN/mm]		
Steel - steel	173.50		
Aluminium - steel	174.41		

Bending stiffness coefficients of the flanges differs with the coefficient $k_{c,10,s} = 1.9$ and $k_{c,10,a} = 8.99$. When multiplying the coefficient with the Young's modulus for the different materials, the bending stiffness for the flanges is obtained.

$$K_{10,s} = k_{c,10,s} \cdot E_s = 389.5 \frac{kN}{mm} \quad 6.22$$

$$K_{10,a} = k_{c,10,a} \cdot E_a = 629.3 \frac{kN}{mm} \quad 6.23$$

$$Ratio = \frac{K_{10,a}}{K_{10,s}} = 1.62 \quad 6.24$$

The ratio of the bending stiffness in the flanges is 1.62, explains the deformations occurred in the tests of the aluminium – steel connection.

7 CAPACITY OF THE BOLTED CONNECTION: NUMERICAL INVESTIGATION

Finite element models of the T-stub connections presented in Chapter 4 have been created using the finite element program Abaqus version 6.13. The load conditions and the geometry in the finite element analysis were the same as in the laboratory tests.

A fine mesh must be applied to represent the geometry of the threads. This implies that the system will become computationally ineffective. To reduce the computational time required by the full system, the threads on the bolt and nut have been ignored in the element analysis. By ignoring threads on the bolt, the diameter of the bolt has been investigated, in Chapter 7.2, to represent the tensile stress area of the bolt properly.

7.1 Calibration of the material parameters

In finite element analysis, the material parameters are crucial in the model for obtaining the right behaviour and capacity of the bolted connection. Different materials have different yield strength and ductility, and it is important that they are defined correctly. The elastic material data for all the components are obtained from NS-EN 1993-1-1 [11] (Table 4.1). The plastic material data for the different components is reviewed in the upcoming subsections.

7.1.1 True stress and true strain

If one wishes to simulate a structure from laboratory tests in numerical analysis, the materials must be calibrated with the same material parameters gathered from tensile tests. True stress and true strain, defining the plasticity behaviour of the materials, should be required as an input parameter for Abaqus. From tensile tests, the force – displacement curve is used to calculate engineering stress and engineering strain. In a numerical analysis, these must be converted to true stress and true strain. With the use of true stress and true strain, one considers that the area changes when the stress changes instead of using the initial area. The assumption is constant volume.

When considering a tensile specimen loaded with a force F , and the specimen initial area is A_0 , the engineering stress is

$$\sigma_{eng} = \frac{F}{A_0} \quad 7.1$$

When the load exceeds such that the behaviour of the material becomes non-linear, the initial area, A_0 , reduces to the area A . The corresponding true stress becomes

$$\sigma_{true} = \frac{F}{A} = \sigma_{eng} \frac{A_0}{A} \quad 7.2$$

When the specimen extends, the engineering strain can be measured from the extension from $L - L_0$, where L_0 is the initial length. The engineering strain is then

$$\varepsilon_{eng} = \frac{L - L_0}{L_0} \quad 7.3$$

The relationship between true and engineering stress are given by assuming both plastic and elastic incompressible deformation. By additionally consider Hooke's law, the relation between plastic and elastic deformation is

$$L_0 A_0 = L A \quad 7.4$$

Inserting Equation 7.4 in the Equation 7.2 is then

$$\sigma_{true} = \sigma_{eng} \frac{L}{L_0} = \sigma_{eng} (1 + \varepsilon_{eng}) \quad 7.5$$

The strain which defines the plastic behaviour is not the plastic strain, but the total true strain in the material. The total true strain must be decomposed to a plastic true strain and an elastic true strain. The plastic true strain is then

$$\varepsilon_{pl.true} = \varepsilon_{true} - \varepsilon_{el.true} = \ln(1 + \varepsilon_{eng}) - \frac{\sigma_{true}}{E} \quad 7.6$$

where $\varepsilon_{pl.true}$ is true plastic strain, ε_{true} is total true strain, $\varepsilon_{el.true}$ is true elastic strain, σ_{true} is true stress and E is the Young's modulus of the material.

7.1.2 Bolts

The bolts used in the element analysis is M16 bolts of quality 8.8, which means that the tensile strength is 800 MPa and the yield strength is 640 MPa. For calculating the material parameters of the bolt, the equations in the previous chapter were used. According to the standard [27], a bolt of grade 8.8 has a minimum of 12% elongation after fracture. Material data for the bolts are given in Table 7.1. For detailed calculations, see Appendix E.

Table 7.1: Material data for 8.8 bolt

Quality	Engineering stress σ_{eng} (MPa)	Engineering strain ε_{eng}	True stress σ_{true} (MPa)	True strain ε_{true}
8.8	640	0.003048	641.95	0
	800	0.12	896	0.1091

The material is assumed to behave elastically until it has reached yield stress of 641.95 MPa, and plastically until an ultimate stress of 896 MPa. The material data is shown graphically in Figure 7.1.

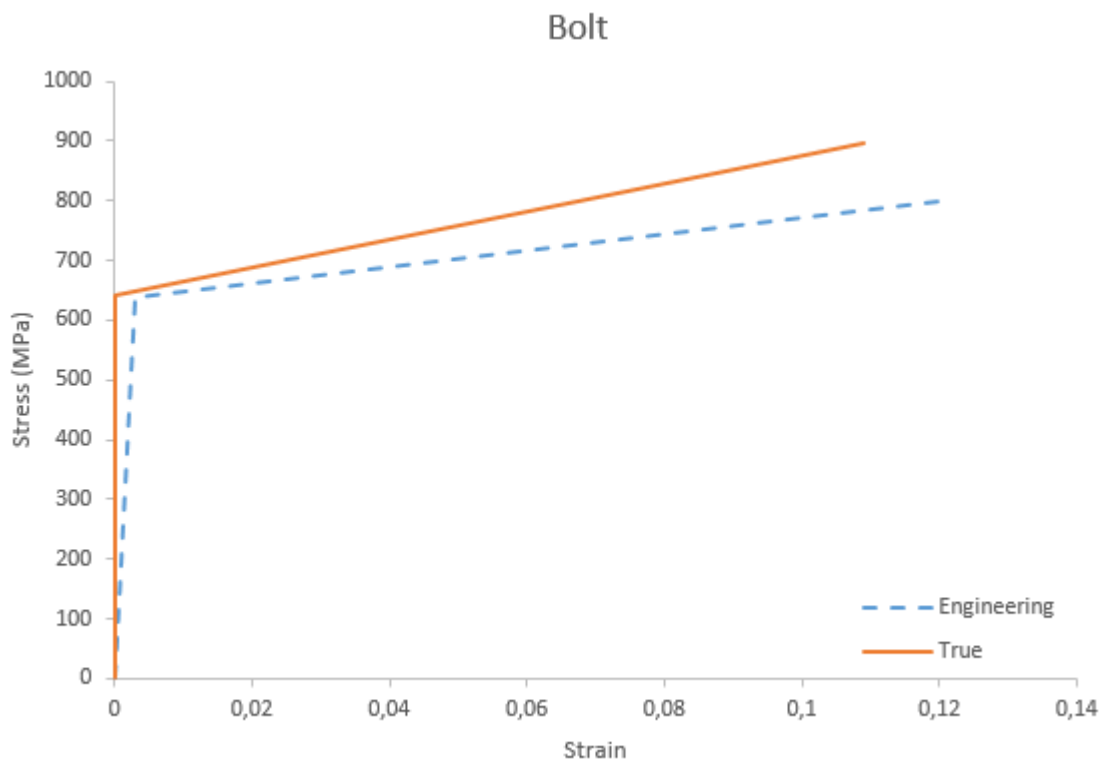


Figure 7.1: Material data for bolt

7.1.3 Tensile tests

It was carried out tensile tests from both materials, S355 (steel) and 6082 (aluminium), to obtain material data used in the numerical analysis in Abaqus, and in the theoretical approach. From the tensile tests, force-displacement curves were obtained. Knowing the force - displacement the engineering stress and strain were calculated. In numerical analysis, the engineering stress and strain must be converted to true stress and strain. These data can be used until diffuse necking occur, i.e. the area in the necking area deform faster than the material is able to harden.

The dimensions of the tensile specimen are according to NS-EN ISO 6892-1:2016 [26], shown in Figure 7.2. The specimen for 6082 was a section cut of the aluminium flange of 16 mm thickness, and the specimen for s355 was a section cut of the steel flange of 10 mm thickness.

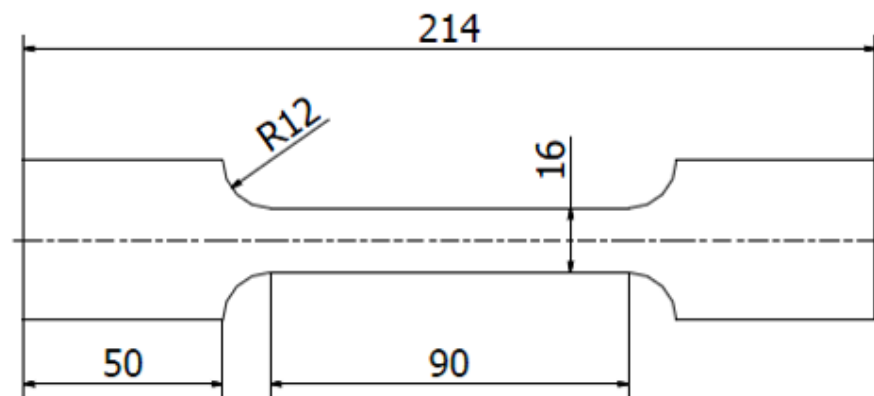


Figure 7.2: Geometry of specimen



Figure 7.3: Specimens before and after tensile test

For each material, it was conducted three tensile tests. The bottom of the specimen was fully constraint on the bottom grip, and the top was moving at a speed which gave a strain rate of 0.00025 s^{-1} before yielding and 0.0067 s^{-1} after yielding.

7.1.3.1 Steel - S355

Figure 7.4 shows the stress – strain diagram for both engineering- and true strain from the tensile tests of steel with 10 mm thickness. The average yield strength, f_y , among the three tests is 369.5 MPa, which is somewhat higher than the expected 355 MPa. The tensile strength, f_u , of the steel was 559.9 MPa. Average Young's modulus among the three tests was 205 GPa.

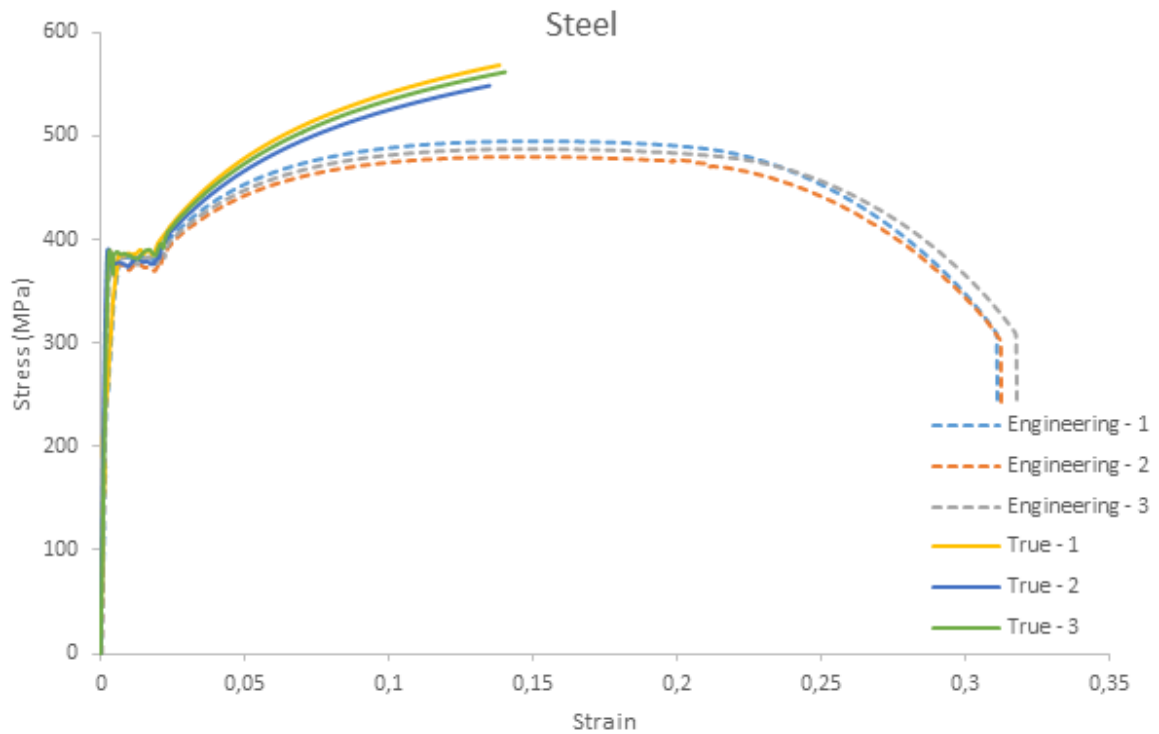


Figure 7.4: Stress – strain of steel

7.1.3.2 Aluminium - 6082

Figure 7.5 shows the stress – strain diagram for both engineering- and true strain from the tensile test of aluminium with 16 mm thickness. The average yield strength, f_y , among the three tests is 312.2 MPa, which is a lot higher than the expected 260 MPa. The tensile strength, f_u , of the steel was 374.8 MPa. Average Young's modulus among the three tests was the expected 70 GPa.

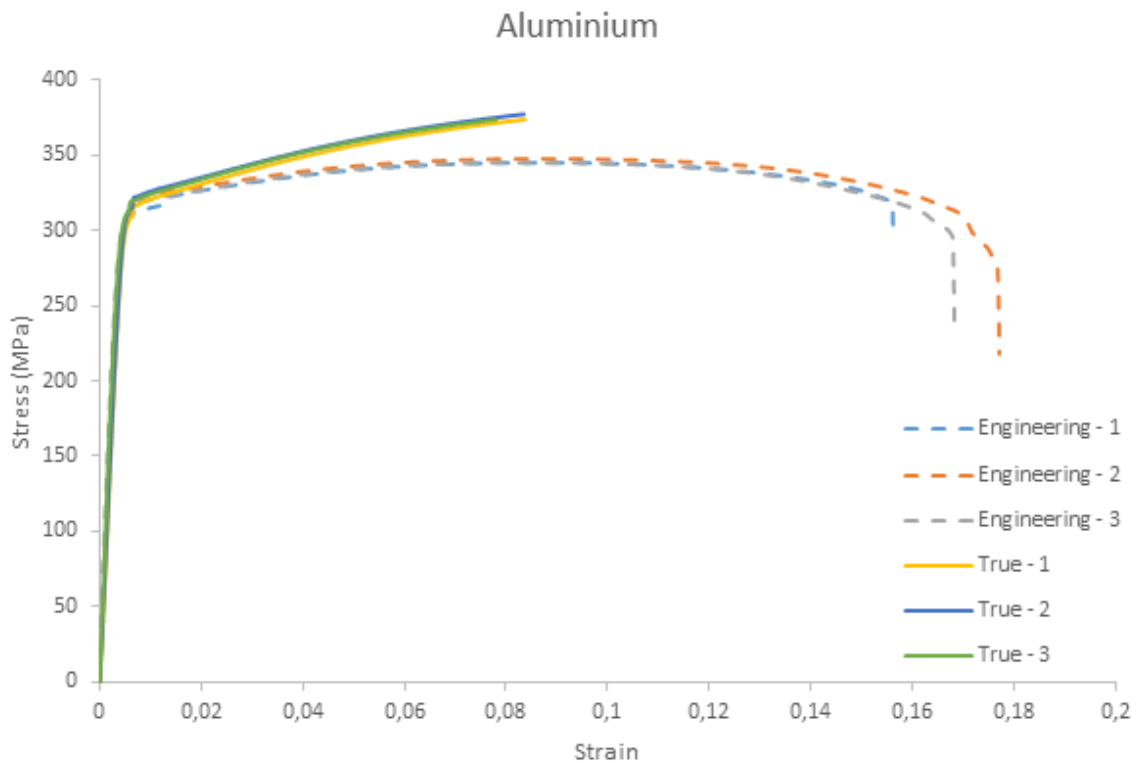


Figure 7.5: Stress – strain of aluminium

7.2 Initial Model

The models analysed were assembled of subcomponents which were modelled separately. The complete model consisted of bolt and profiles both in steel, or profiles of steel and aluminium. Figure 7.6 shows the subcomponents used in the analysing. Each model is made to recreate the laboratory work as accurately as possible. Both models have the same boundary conditions, interactions, loadings and mesh. When applying the tension load, preload force on the bolt was ignored. According to Eurocode 3, the preload force does not have an effect on the capacity of the bolts. On the connections subjected to thermal load, the preload force was applied.

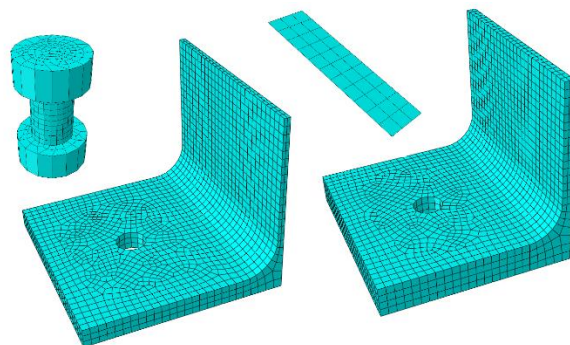


Figure 7.6: Subcomponents used in the analyse

7.2.1 Simplified bolt

As mentioned, a simplified element model of the bolt without threads has been used. Because the threads on the bolts have been ignored, the bolt and nut were modelled as one part. This simplification will ignore the possibility of failure due to thread stripping, but they should be able to recreate the physical response up to failure due to tensile load, where this is the case.

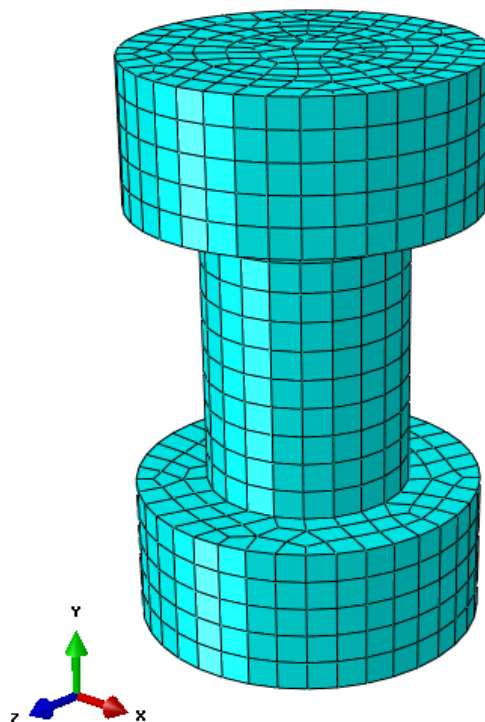


Figure 7.7: Simple bolt model

As mentioned at the beginning of Chapter 5, the ideal diameter to properly represent the tensile stress area of the bolt must be investigated. To find the ideal diameter of a simplified bolt, a study from a previous master thesis has been performed on an M16 bolt of quality 8.8 without threads in element analysis compared to two fully threaded bolts in a DIC analysis [28]. The grip length was set to 118 mm.

Three different diameters of the simplified bolt were considered:

- The nominal diameter of the bolts, 16.00 mm
- The pitch diameter of bolt thread, 15.35 mm
- The diameter of the tensile stress area defined in NS-EN ISO 898-1 [27] , 14.14 mm

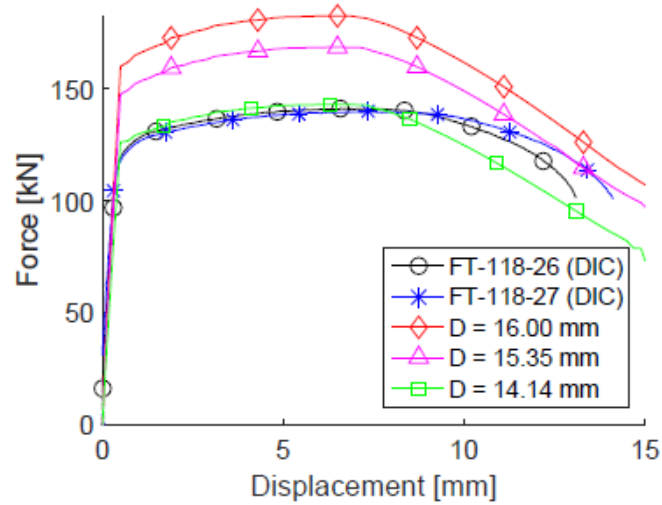


Figure 7.8: Force-displacement curve for simplified M16 bolt [28]

The force- displacement curves of the three different diameters compared with the results from the DIC analysis, confirms the diameter defined in NS- EN ISO 898-1 of 14.14 mm to be the best-suited diameter to recreate the load level of the threaded M16 bolt.

7.3 Element characteristics

In the model, it is used three-dimensional hexahedral elements with eight nodes at each corner of a shown in Figure 7.9. Each node has three degrees of freedom. Every element is linear, and the reduced integration would reduce the computational time by only consider the linearly varying part of the incremental displacement. The definition of the volume element used is C3D8R [29].

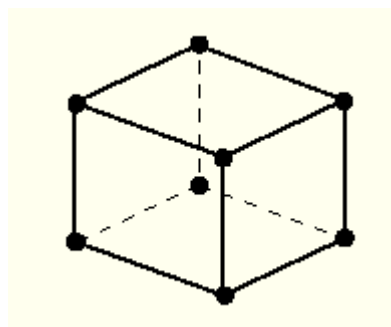


Figure 7.9: Hexahedral element, C3D8R

The initial model consists of different element sizes. The element sizes at the flange of the profile and the middle section of the bolt had finer mesh compared to the shank,

nut and rest of the non-critical part of the model. The parts that are not prioritised for further investigation has coarser mesh applied for limiting the computational time.

7.4 Step- and increment size

Throughout the analysis, Abaqus adjust the size of the increments, but it is up to the user to decide the limitations of the increments. The model consists of an initial step where the initial conditions and properties are added, and following steps there the loads and boundary conditions is applied. Both models for tension and thermal loading had an initial increments size of 0.01.

For the tension model, the total time was set to 1, which means that the displacement in the first increment is 1 percent of the total displacement.

For the thermal model, the total time was split into two steps, where step 1 was preload of the bolt and step 2 was increasing the ambient temperature. Step 1 had a total time of 1 and step 2 had a total time of 6. In order to get a better overview of the heating process compared to the preload, the total time was longer for step 2.

Each increment was limited by the minimum size of $1e10^{-5}$ and maximum size of 0.01. Total allowed increments was 200. If the analysis required either more increments or increment size beyond the limitations, the analysis would be cancelled. The limitations were set to prevent the analysis to run for long period of time without significant progress.

7.5 Boundary conditions

The bolted connection consists of two symmetrical parts, so regarding reducing the computational time, only one-half of the connection was modelled. In Abaqus, it is possible to add symmetry characteristics as boundary conditions, which makes it possible only to model the part of the connection that is necessary. As illustrated in Figure 7.10 X- and Z symmetry is used along Y-direction of the model. On the bottom, the web is constrained to a rigid plate. The rigid plate is fixed to prevent the connection from moving or rotating in all direction.

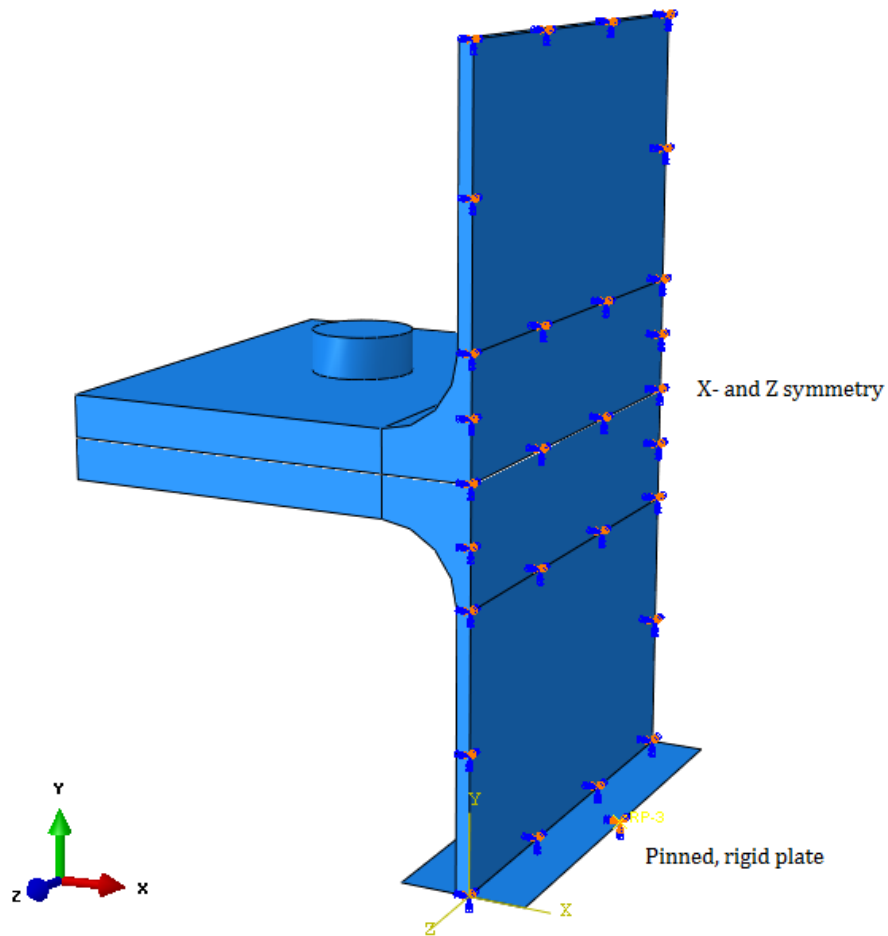


Figure 7.10: Boundary conditions

7.6 Interactions

In the model, there are two types of interaction, “surface-to-surface contact” as shown in Figure 7.11, and “general contact” with “All* with self”. According to the Abaqus manual [29], general contact is the easiest way to define contact for the model covering all the outer element surfaces. “surface-to-surface” reduces numerical problems when interacting surfaces with different element sizes.

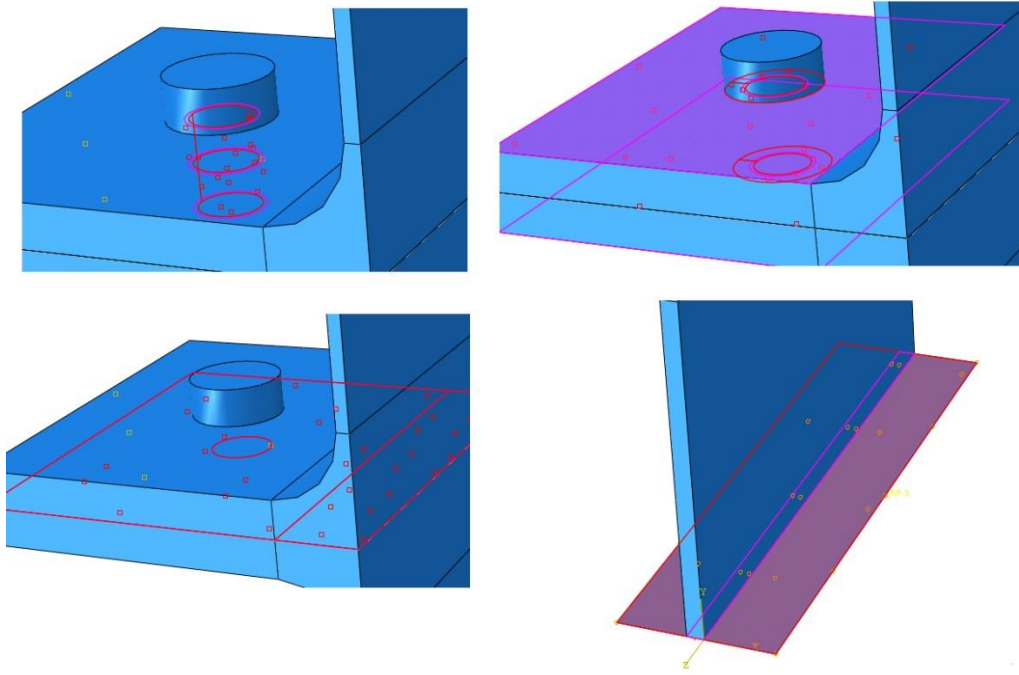


Figure 7.11: Interactions

7.7 Load

Tension load was applied by adding displacement in Y-direction on the top web as a boundary condition. The remaining degrees of freedom was set to be zero. Each node on the top web registered a displacement, giving the data for the total displacement by summing all the data from each node.

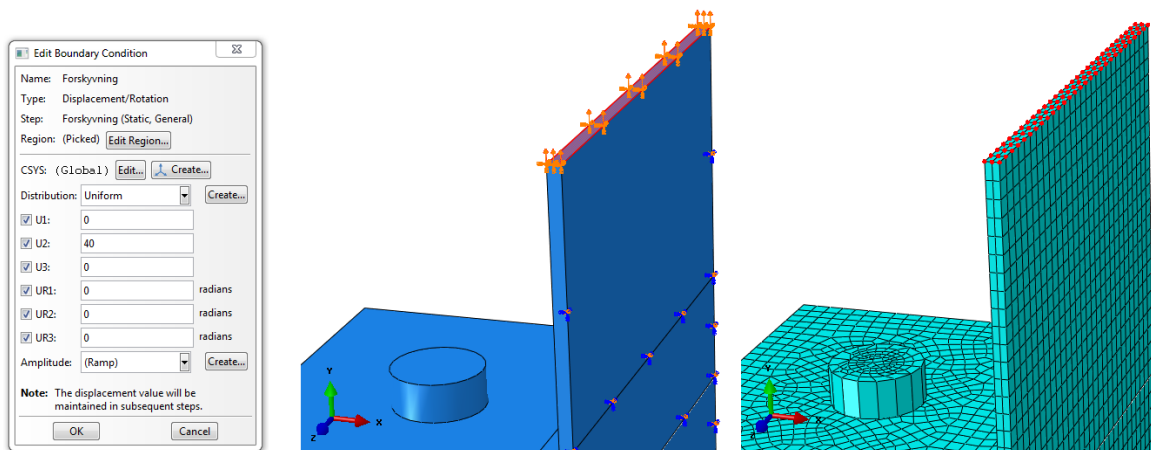


Figure 7.12: Load application and nodes on top web

The model with the thermal load the temperature was initial set to be $-20\text{ }^{\circ}\text{C}$, and at step one, the bolt was preloaded with a force of 89300 N . Then the ambient temperature was set to be $200\text{ }^{\circ}\text{C}$, and the whole connection was uniformly heated until it reached the desired temperature.



Figure 7.13: Initial conditions, step 1 and step 2

7.8 Results

In order to achieve the best possible results compared to the result from the laboratory tests, the reference points must be at the same location. In the element analysis model, the reference point 1 for displacement is shown in Figure 7.14, which is approximately the same location as the extensometer in the laboratory.

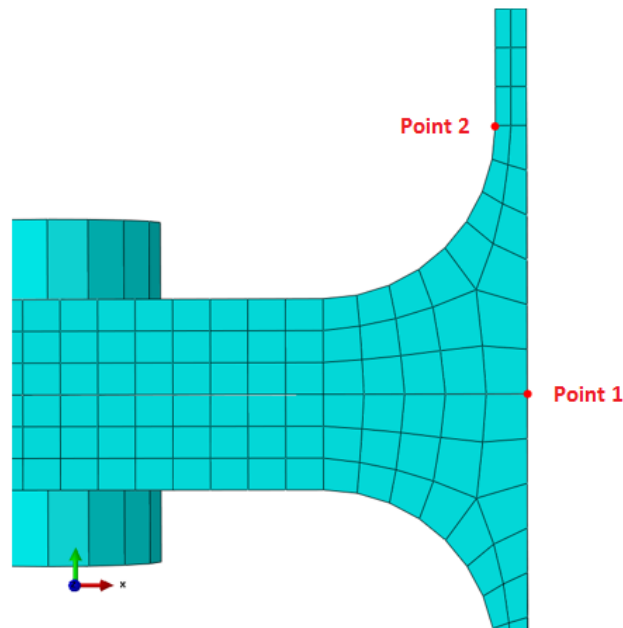


Figure 7.14: Reference points for measuring displacement in steel – steel connection

To ensure that measurements from reference point 1 instead of reference point 2 (which is preferred) have no or small effects on the results, a comparison was made. Figure 7.15 shows the force - displacement curve for the two different reference points. The plot confirms that the position of the extensometer and the reference point in the model represent an accurate measurement of the displacement of the model.

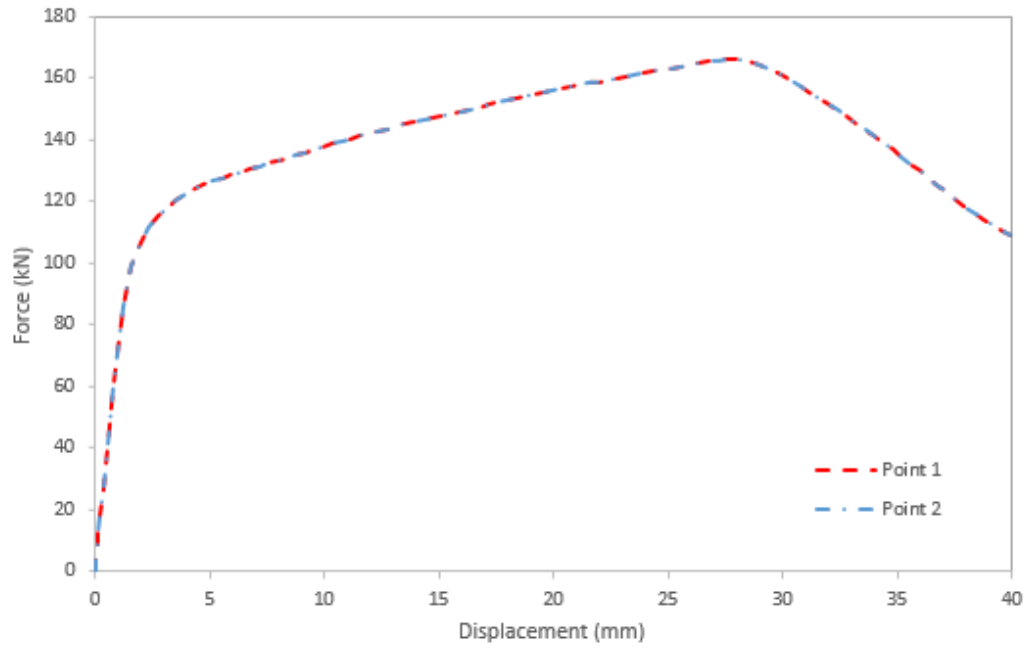


Figure 7.15: Force - displacement curves at two different reference points

7.8.1 Tension load

For both configuration the force - displacement curves were plotted. The connections were stretched around 10 mm further after failure. The failure appeared to be in the bolt as expected. Due to the symmetry of the model, the force was multiplied by two in order to get the correct results. Figure 7.16 illustrates the use of symmetry in the steel - steel connection and the deformation at maximum force.

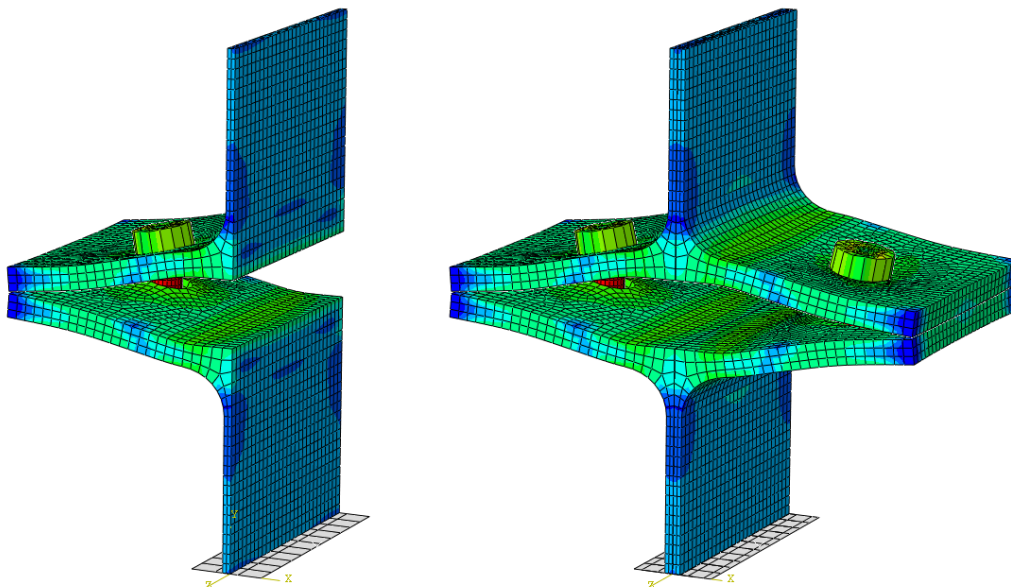


Figure 7.16: Original model (left) mirrored in YZ-plane (right)

7.8.1.1 Steel – steel connection

Figure 7.17 shows the force – displacement curve, based on the reference point shown in Figure 7.14. The maximum force is 166.3 kN at a displacement of 27.56 mm.

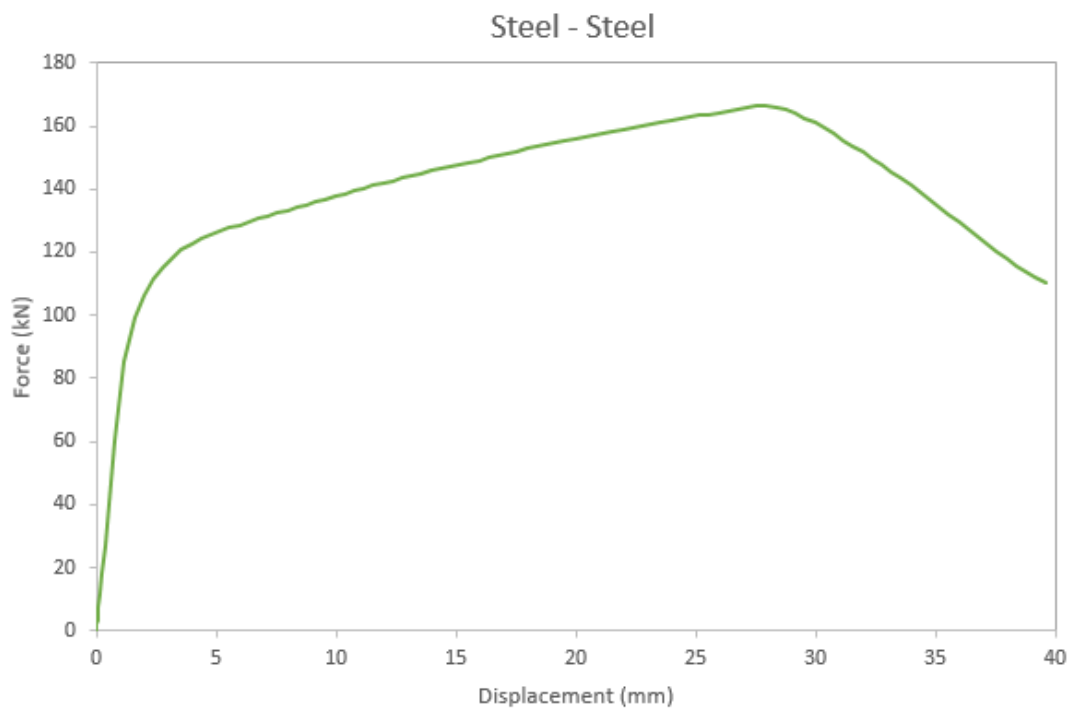


Figure 7.17: Force – displacement curves for steel – steel connection

Figure 7.18 shows the connection cut in the Z-plane at a load of 166.3 kN. The colour indicates the von Mises tension in MPa on the model. The deformations resemble the deformations from the laboratory, i.e. the flanges are slightly bent at the position of the bolts in addition to contact between on the edges. As the figure clearly shows, the finite element achieves model failure mode 2 as in the laboratory tests.

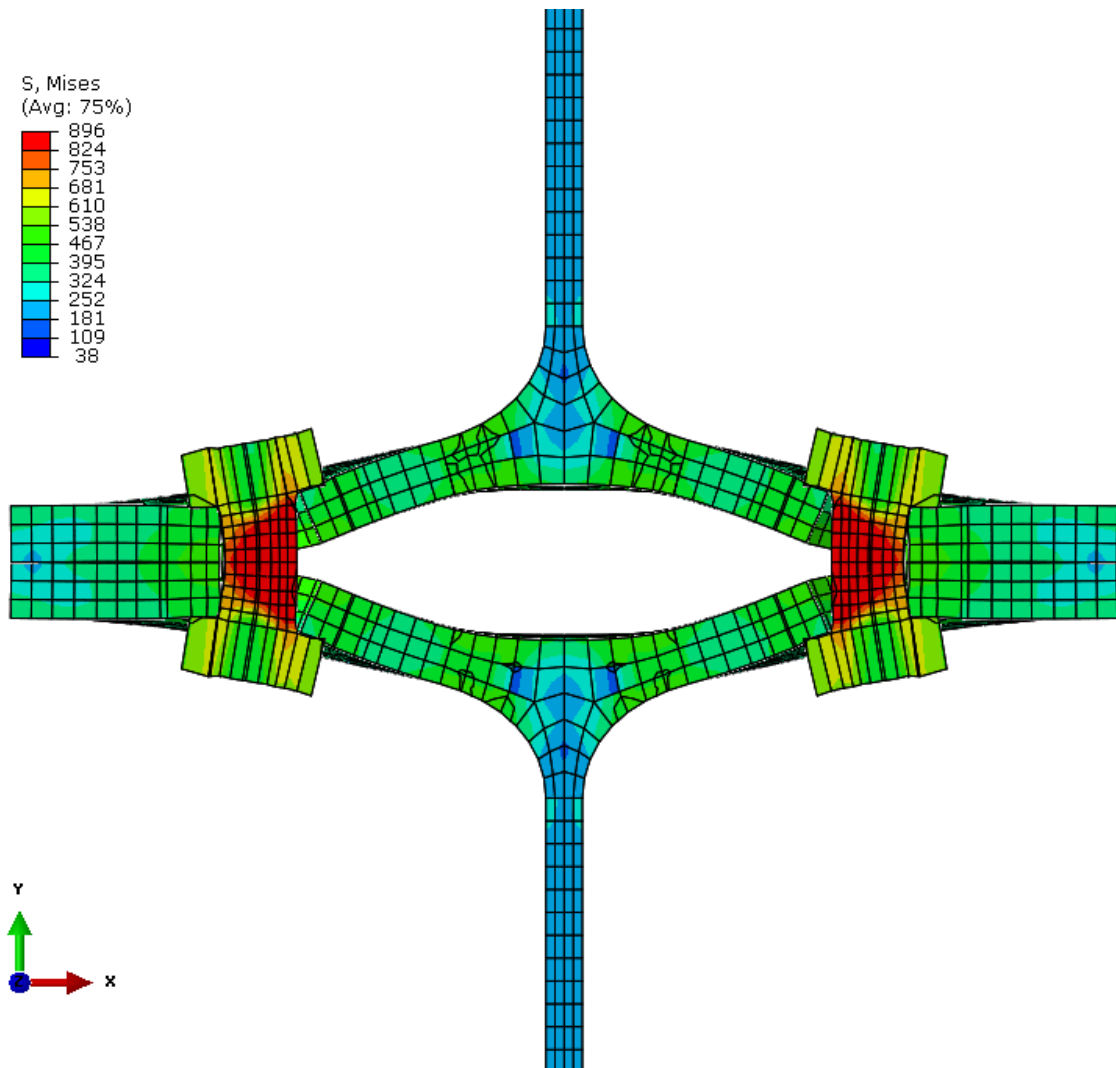


Figure 7.18: Steel – steel connection at 166.3 kN

7.8.1.2 Aluminium – steel connection

Figure 7.19: shows the force – displacement curve, based on the reference point shown in Figure 7.14. The maximum force is 171.9 kN at a displacement of 17.42 mm.

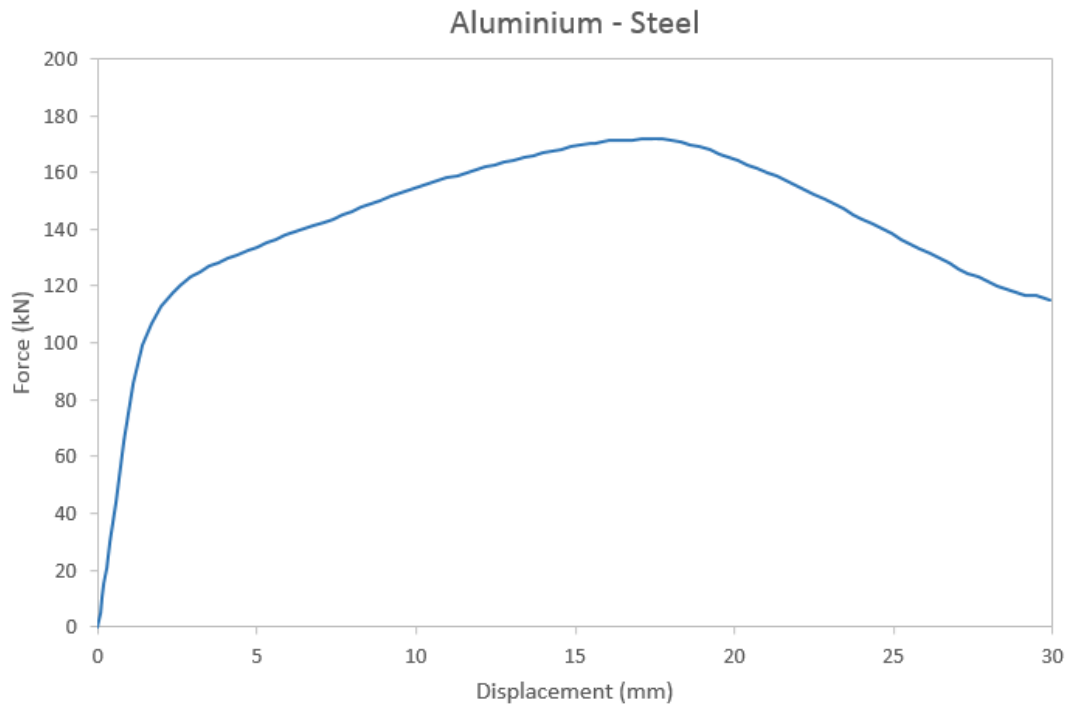


Figure 7.19: Force – displacement curves for aluminium – steel connection

Figure 7.20 shows the connection cut in the Z-plane at a load of 171.9 kN. The deformations for this connection also resembles the deformations from the laboratory. The aluminium flange is very stiff compared to the steel flange and hardly deform at all. The steel flange deforms the same way as the flanges in the steel – steel connection. The stiff aluminium flange contradicts the deformation to a greater extent, which reduces the total deformation until failure. As the figure shows, the finite element model achieves failure mode 2.

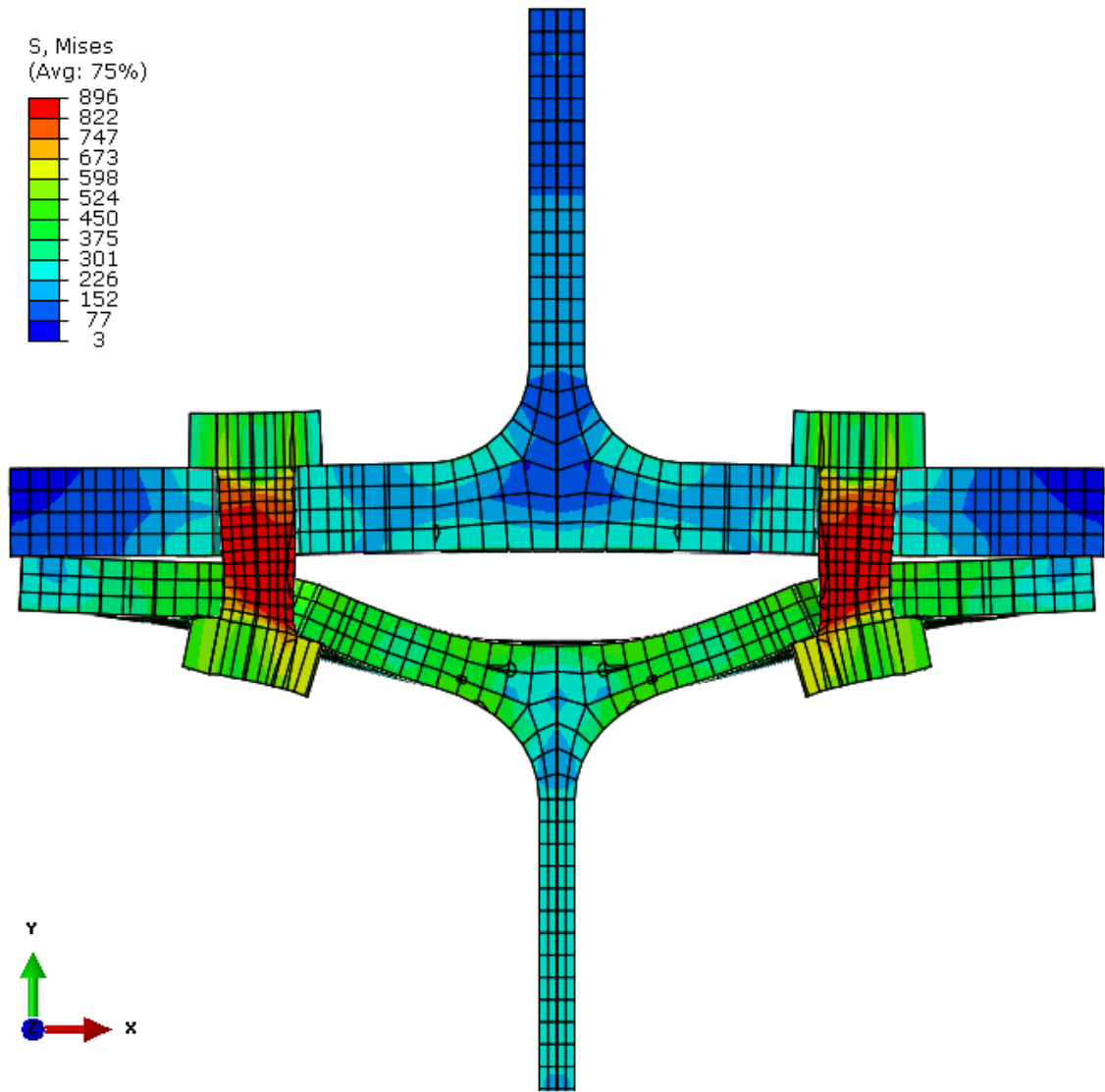


Figure 7.20: Aluminium – steel connection at 171.9 kN

7.8.2 Thermal load

For both configuration the preload stress - temperature curves were plotted. In order to get more efficient analyse time, the model was simplified, as shown in Figure 7.21. The bolt dimensions were the same, but the T-stubs were simplified to just the two flanges. For both configurations, the flanges had the same thickness (10 mm) to get a better comparison among them. According to Equations 2.20 and 2.21, the expansion is affected by the thickness of the flanges and the length of the bolt. In the analysis, the final temperature was set to be 200 °C in order to get a complete picture of the behaviour of the connection. 200 °C is beyond what to expect regarding bolted connection in offshore structures.

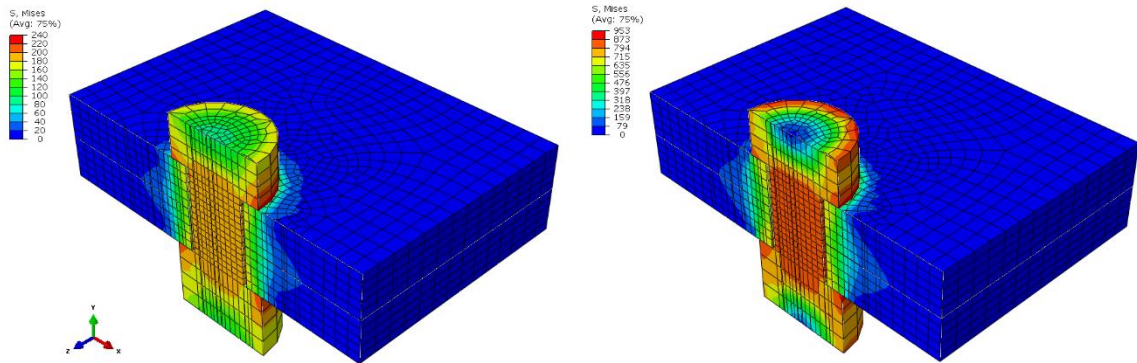


Figure 7.21: Simplified preloaded connection before and after thermal load

7.8.2.1 Steel – steel connection

Figure 7.22 shows the percent of preload stress as the temperature rises from initial -20 °C to final 200 °C. The registered stresses are the average stress along the grip of the bolt and flanges. At 100 percent the bolt is preloaded with 89300 N giving the initial preload stresses on both the bolt and flanges. As the bolt is preloaded and the temperature starts to rise, the preload stress in the connection reduces. At 200 °C, the percent of preload stress in the connection reduces by 0.47 %.

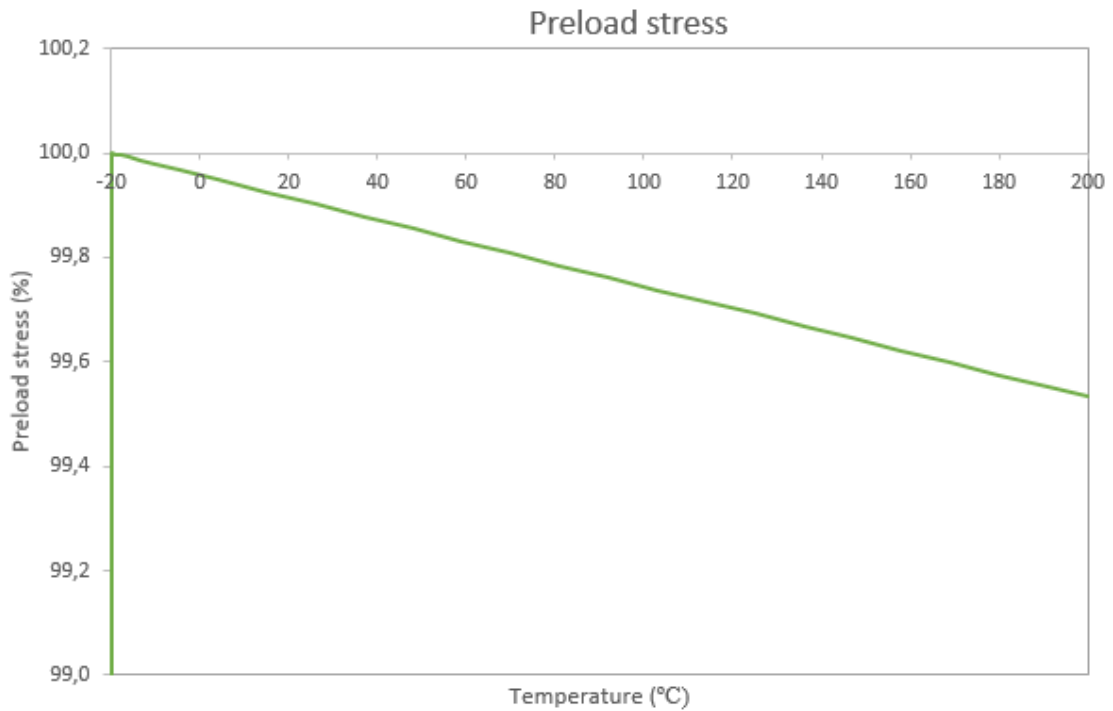


Figure 7.22: Percent preload stress – Temperature

In Figure 7.23 the rate of expansion is shown for the flanges and bolt during thermal load. During preload, both the bolt grip length and the thickness of the flanges decreases to 19.96 mm. Due to thermal load, the grip length of the bolt increases equally as the sum of the thickness of the flanges, with 0.049 mm. After preload, the total increase is then 0.245 %. As expected, both the flanges expand equally.

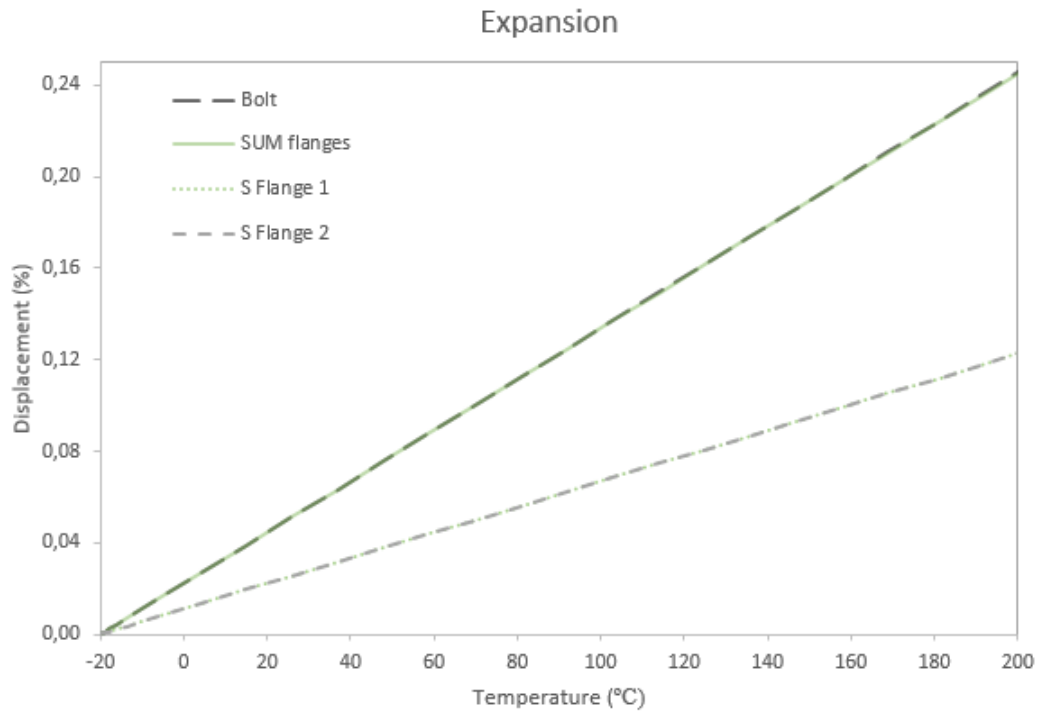


Figure 7.23: Expansion in Y-direction

The Von Mises stress of the bolt and flanges during heating is illustrated in Figure 7.24 and Figure 7.25. It is clearly illustrated that the stress decreases in both the bolt and the flanges during heating.

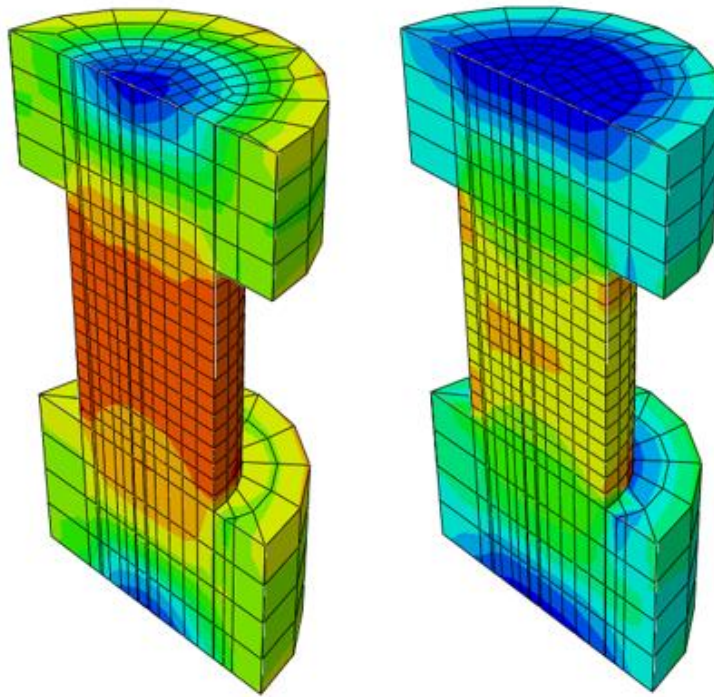


Figure 7.24: Preloaded bolt before and after thermal load

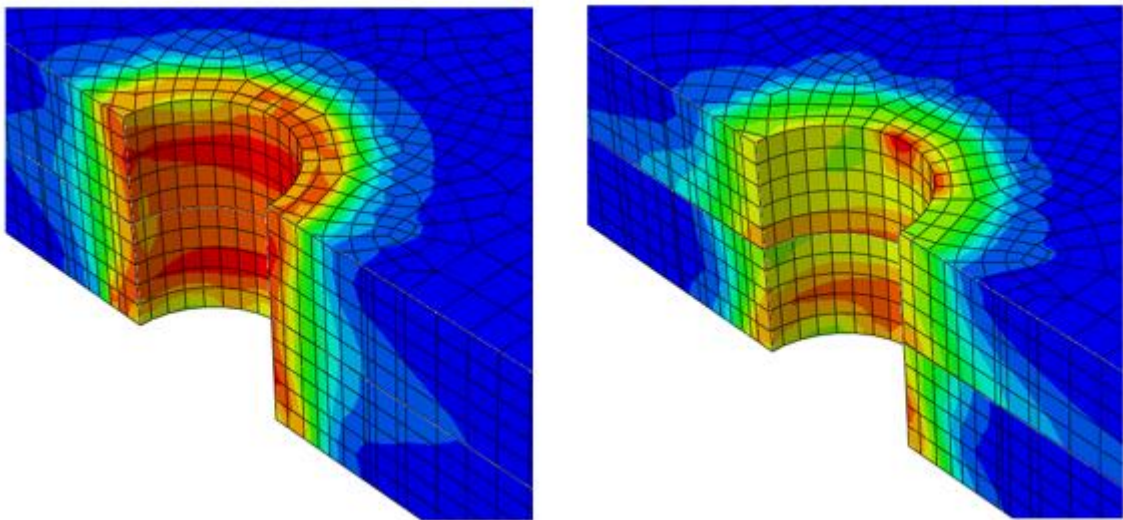


Figure 7.25: Preloaded bolt on flanges before and after thermal load

7.8.2.2 Aluminium – steel connection

Figure 7.26 shows the percent of preload stress as the temperature rises from initial -20 °C to final 200 °C. Similar as in the steel – steel connection, the registered stresses are along the grip length, and the bolt is preloaded with 89300 N. As the bolt is preloaded and the temperature starts to rise, the preload stress in the connection increases. At 200 °C, the percent of preload stress on the connection increased by 4.16 %.

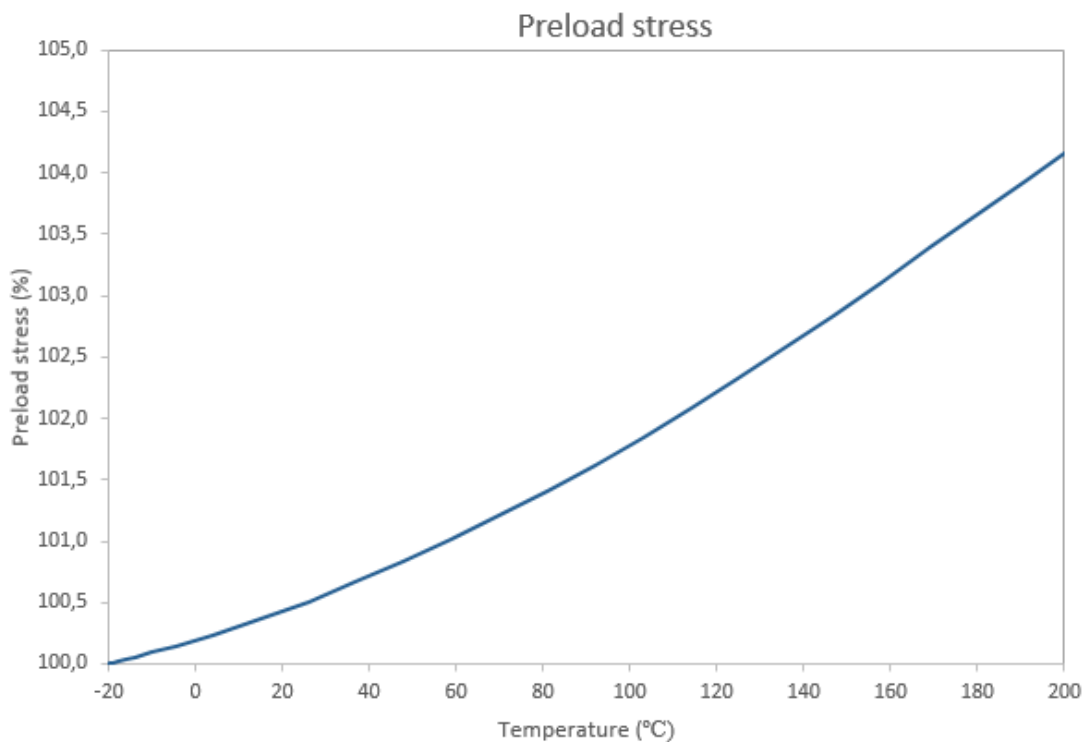


Figure 7.26: Percent preload stress – Temperature

The expansion of the bolt versus the flange may change at a different rate, due to different stiffness. In Figure 7.27, the rate of expansion is shown for the flanges and bolt during thermal load. During preload, both the bolt grip length and the thickness of the flanges decreases to 19.93 mm. Due to thermal load, the bolt increases its grip length with 0.073 mm and the sum of the flanges increases its thickness with 0.071 mm. After preload, the total increase of the bolt grip length is 0.365%, and of the flanges, the thickness is 0.357%. As expected, the aluminium flange expands more than the steel flange, approximately by 27%.

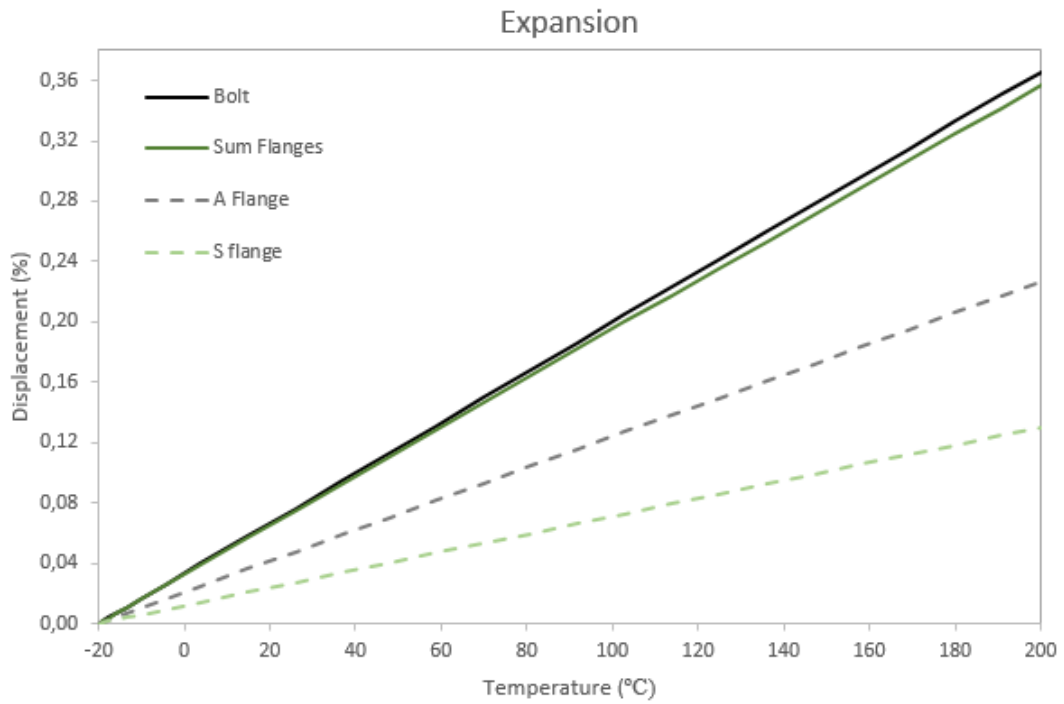


Figure 7.27: Expansion in Y-direction

The Von Mises stress of the bolt and flanges during heating is illustrated in Figure 7.28 and Figure 7.29. It is clearly illustrated that the stress increases in both the bolt and the flanges during heating.

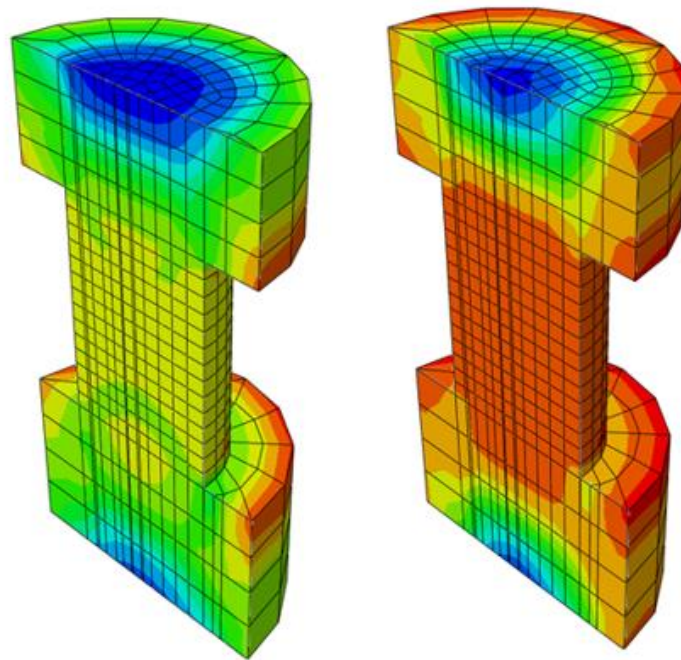


Figure 7.28: Preloaded bolt before and after thermal load

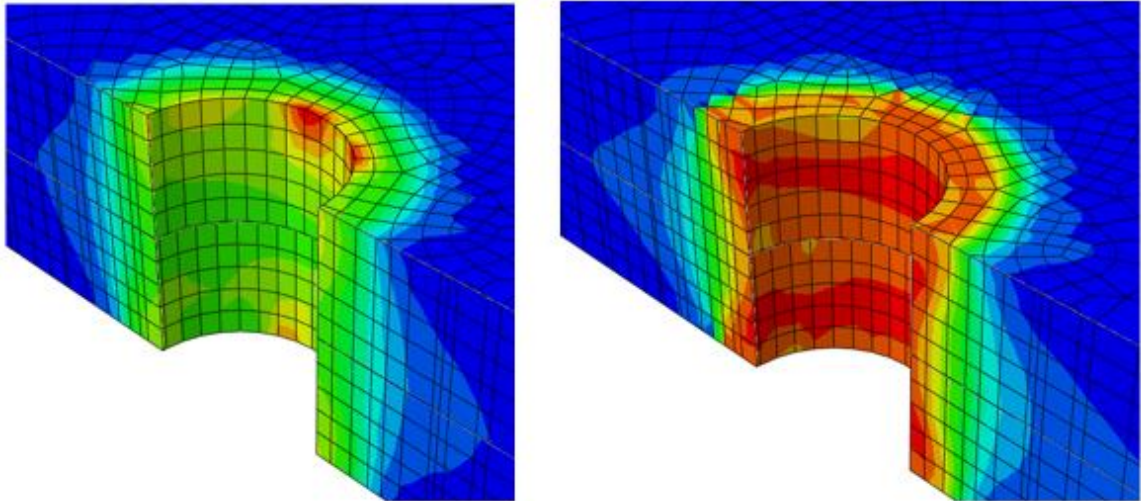


Figure 7.29: Preloaded bolt on flanges before and after thermal load

8 DISCUSSION OF RESULTS

8.1 Tension capacity

Figure 8.1 shows the similarity of the steel – steel connection after failure between the tensile test and the FE model visually. The distance from the centre of the flanges at failure is 27.56 mm in the FE model and 29.65 mm from SS1 (lowest force at failure among the tests). The FE model is a good approximation of the plasticization observed from the tensile test.

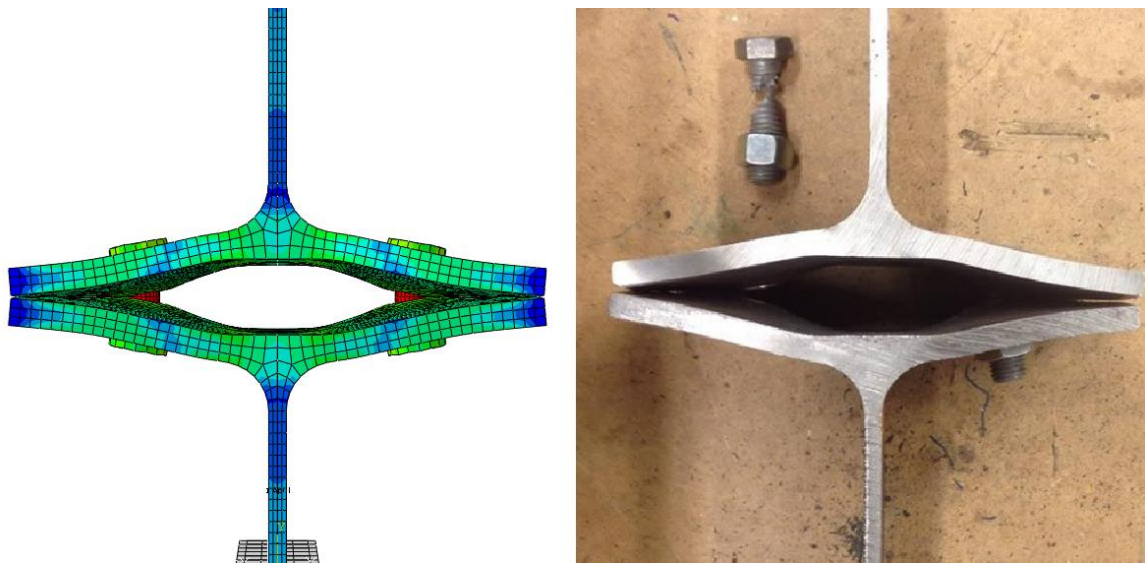


Figure 8.1: Comparison of the deformation from SS1

In Figure 8.2 representative force – displacement curves from the tensile tests, FE model and the design load according to Eurocode 3 are plotted together. The FE model is somewhat conservative considering it is yielding earlier than the tensile tests. During the plastic zone, the curve from the FE model lies evenly and parallel below the specimens until it reaches its maximum force of 166.3 kN, which is a lower maximum force than registered in the tensile tests.

The tensile tests for each sample performed in the laboratory had approximately the same values for displacement until the bolt began to yield and eventually break. Every single test exhibited the desired failure mode, and they roughly had the same force at failure (Table 5.1). As expected, all registered maximum forces were higher than the corresponding design load. According to the Eurocode, failure mode 1 occurred with a force of 109.9 kN. If one consider failure mode 2, the design load is 163.1 kN which corresponds well to the results from the FE model.

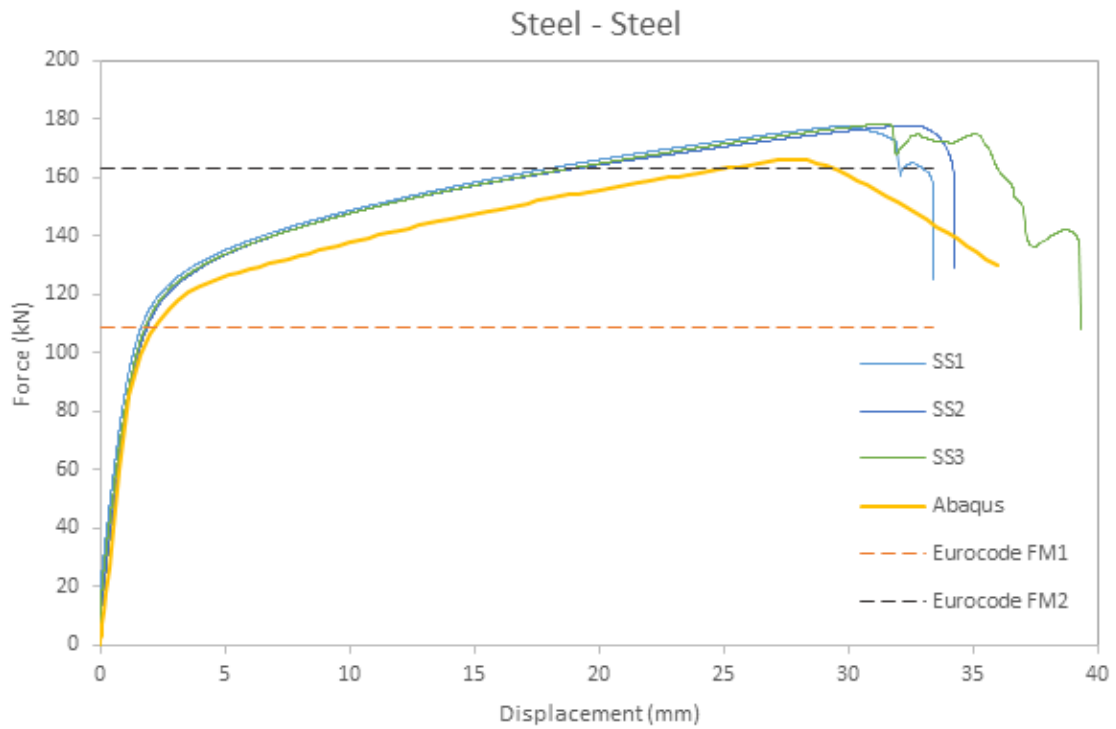


Figure 8.2: Comparison of capacity for steel - steel connection

Figure 8.3 shows the similarity of the aluminium - steel connection after failure between the tensile test and the FE model visually. The distance from the centre of the flanges at failure is 17.42 mm in the FE model and 18.36 mm from AS1 (lowest force at failure among the tests). On the contrary of the steel - steel connection where the failure occurred at the centre of the bolt, the failure occurred just above the nut inside the steel flange. The reason for the changed fracture position of the bolt is clearly shown in the figure below. The bolt is to a much greater extent bent during plasticization of the steel flange.

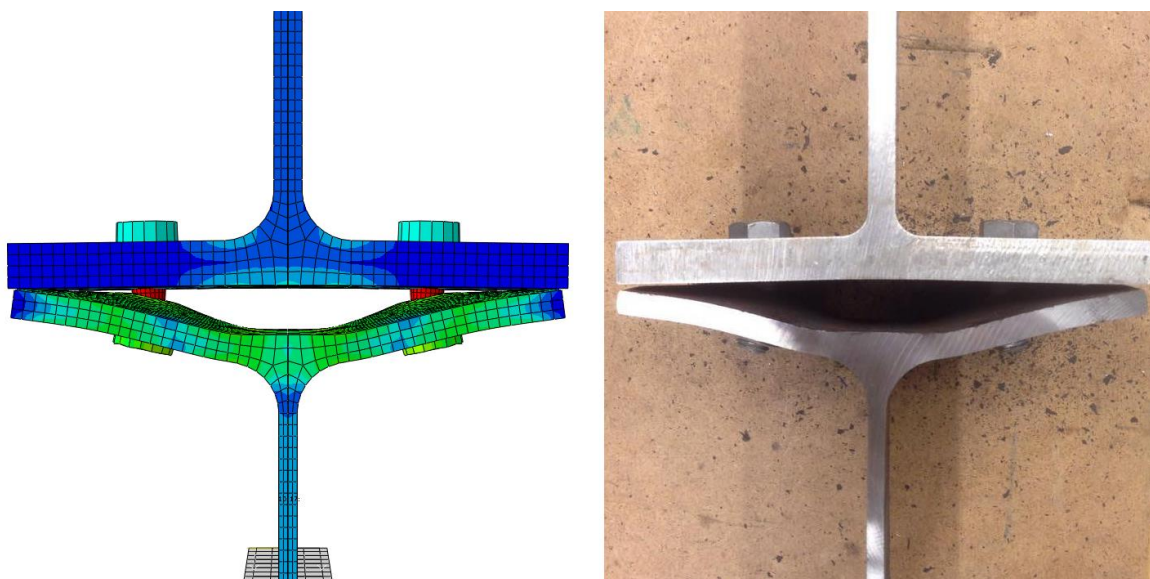


Figure 8.3: Comparison of the deformation from AS1

In Figure 8.4 representative force – displacement curves from the tensile tests, FE model and the design load according to Eurocode 3 are plotted together. The same tendencies of displacement of the tensile tests were observed in this as in the previous configuration. The FE model is somewhat conservative in the plastic zone and with its maximum force of 171.9 kN. As expected, all registered maximum forces were higher than the corresponding design load. According to the Eurocode, failure mode 1 occurred with a force of 108.9 kN as in the steel – steel connection. If one consider failure mode 2, the design load is 163.1 kN which corresponds not as good as in the steel – steel connection but still well compared to the actual design load in this case.

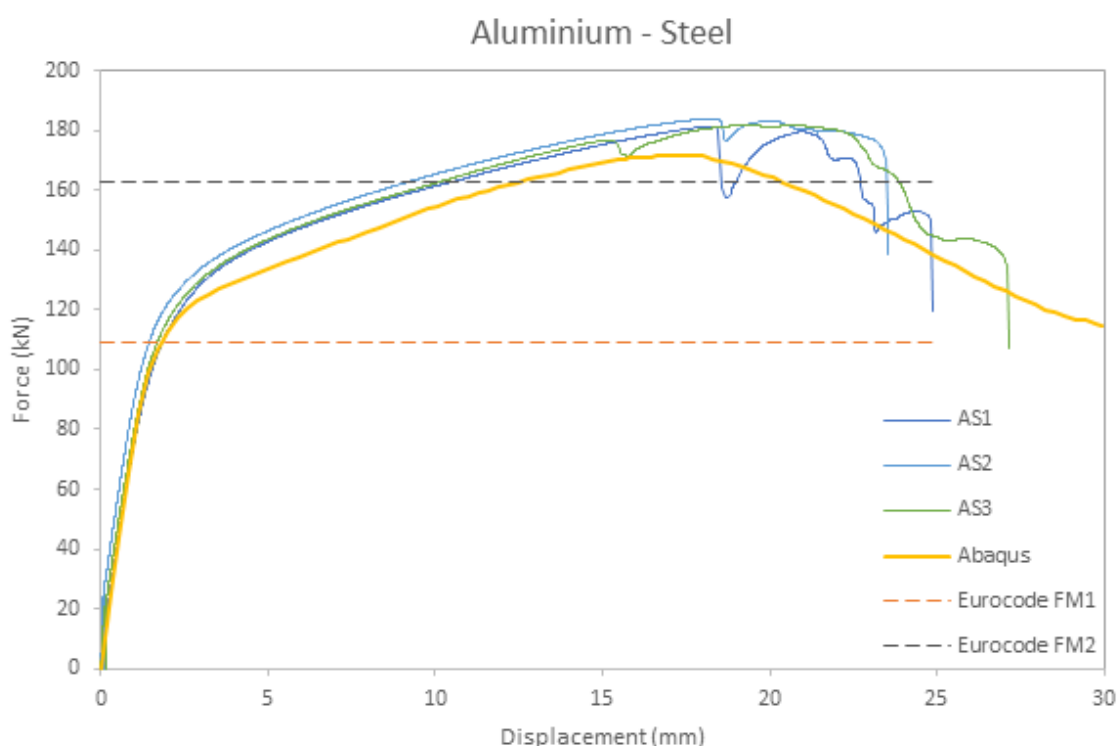


Figure 8.4: Comparison of capacity for aluminium – steel connection

In Table 8.1 the maximum force and the corresponding displacement at max failure for the Eurocode, FE model and the tensile test are given. The percentage of deviation between the given capacities are also given and is calculated as follows:

$$p = \frac{Lab - FE\ model / Eurocode}{Lab} \cdot 100\% \quad 8.1$$

Table 8.1: Comparison of tension capacities

Configuration	Laboratory		FEM		Eurocode	
	Max force [N]	Disp. at max force [mm]	Max force [N]	Disp. at max force [mm]	Failure mode 1 [N]	Failure mode 2 [N]
SS1	177422	29.65	166323	27.56	108900	163100
SS2	177881	32.49	166323	27.56	108900	163100
SS3	178518	31.51	166323	27.56	108900	163100
AS1	181489	18.27	171971	17.42	108900	163100
AS2	184085	18.36	171971	17.42	108900	163100
AS3	181910	20.69	171971	17.42	108900	163100

Configuration	Deviation in %	Deviation in %		Max force/Disp. max force	
	Lab vs FEM	Lab vs Eurocode		Lab vs FEM	
		Failure mode 1	Failure mode 2		
SS1	6.26	38.62	8.07	1.009	AVG SS
SS2	6.50	38.78	8.31	1.102	<u>1.059</u>
SS3	6.83	39.00	8.64	1.065	
AS1	5.24	40.00	10.13	0.994	AVG AS
AS2	6.58	40.84	11.40	0.985	<u>1.034</u>
AS3	5.46	40.14	10.34	1.123	

The largest deviation from the results of the Laboratory tests is the Eurocode, and it is very conservative compared to the deviation with the FE model, which is much more comparative to reality.

For both configurations, the FE model had less force after yielding throughout the whole plastic zone. Despite the lower value of force, the ratio of maximum force generated compared to the displacement at failure was similar to the laboratory tests. The simplified bolt geometry in the model might have an influence on the behaviour. Smooth shank will not cause stress concentrations in the roots of the threads as in the fully threaded bolts used in the laboratory. The compensation to minimise the diameter of the shank in the model, described in Chapter 7.2.1, should not have an effect on the yielding of the flanges. The simplified bolt, however, did probably have an impact on the lower value of maximum force of the bolts giving the reduced design load of the connection in the FE model compared to the tensile tests.

Despite the differences from the Eurocode and the reality, the Eurocode is quite consistent when looking at the percent deviation between the configurations. With a difference of ~38.8% in the steel – steel connection and ~40.3% in the aluminium – steel connection, it confirms to consistent results even though it differs conservatively. Based on the deviations from the Eurocode, it may be more accurate to assume that failure mode 2 is more an estimate of the yield strength of the connection rather than failure mode 1. The average deviation of failure mode 2 and

the tests was $\sim 8.3\%$ in the steel – steel connection and $\sim 10.6\%$ in the aluminium – steel connection.

8.2 Stiffness

A comparison among the initial elastic stiffness for both configurations among the laboratory tests, the FE model and the Eurocode is adapted in order to get a better overview of how the stiffness corresponds.

Figure 8.5 shows the first 2.5 mm of displacement in the Force – Displacement curve for the steel – steel connection. Up to approximately 1.1 mm, the initial elastic stiffness is illustrated. The FE model and the laboratory test are well matched. The Eurocode, on the other hand, is overestimating the initial stiffness and has a significant deviation from both the FE model and laboratory tests. The deviation between the Eurocode and the laboratory tests is 58.5%, and the deviation between the FE model and the laboratory tests is 1.95%.

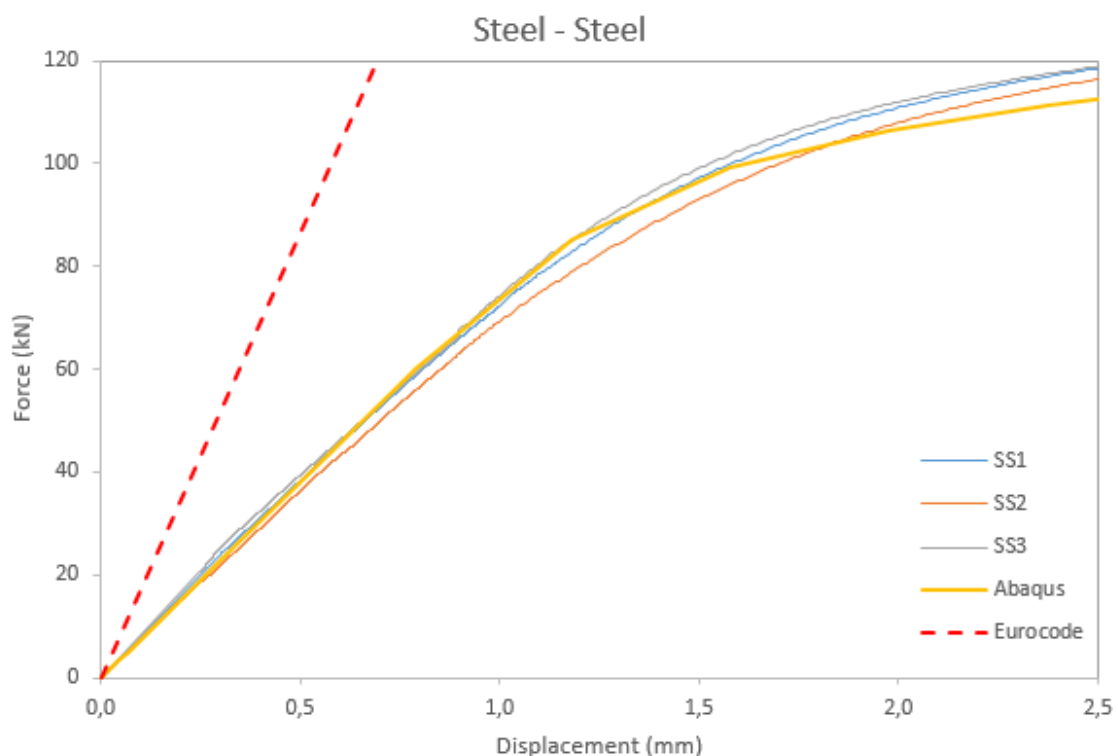


Figure 8.5: Comparison of stiffness for steel – steel connection

Figure 8.6 shows the first 2.5 mm of displacement in the Force – Displacement curve for the aluminium – steel connection. Up to approximately 1 mm, the initial elastic stiffness is illustrated. As well as the previous connection, the FE model and the laboratory test are well matched. The Eurocode, on the other hand, is still overestimating the initial stiffness and has a significant deviation from the both the

FE model and laboratory tests. The deviation between the Eurocode and the laboratory tests is 58.3%, and the deviation between the FE model and the laboratory tests is 5.8%.

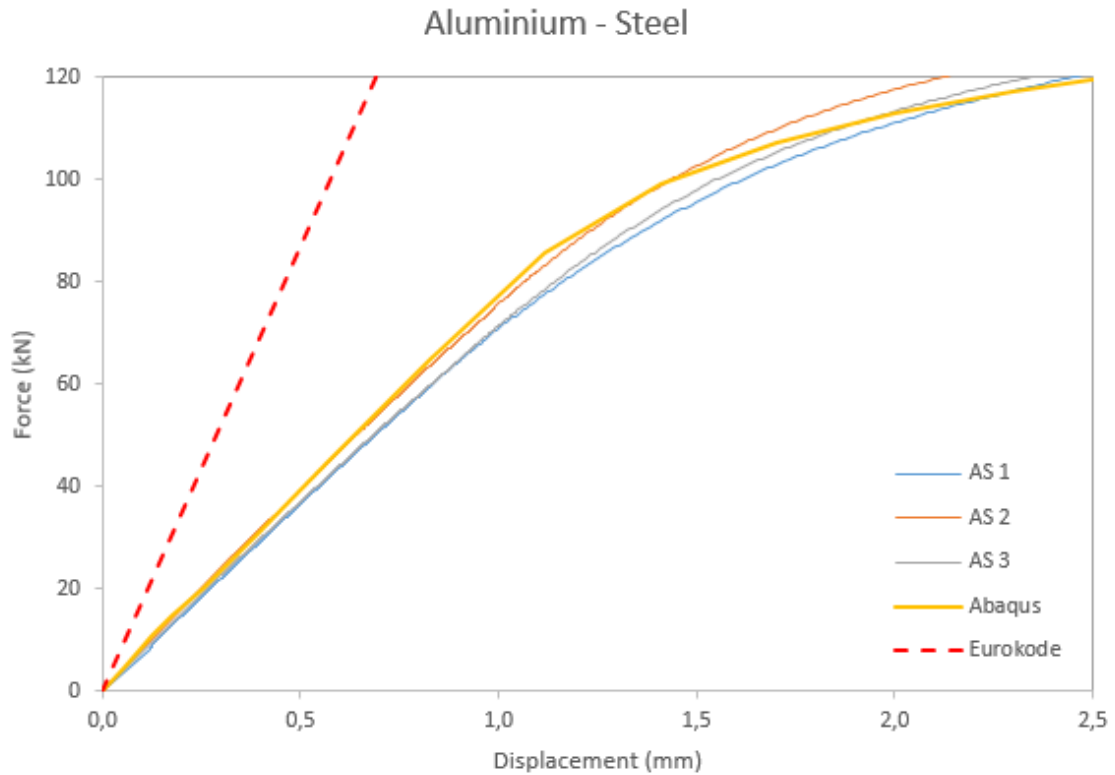


Figure 8.6: Comparison of stiffness for aluminium - steel connection

Table 8.2 summarizes the initial stiffness for the different configurations.

Table 8.2: Summary of stiffness's

	K_{Lab1} (kN/mm)	K_{Lab2} (kN/mm)	K_{Lab3} (kN/mm)	$K_{Lab.Avg}$ (kN/mm)	K_{FE} (kN/mm)	K_{Eur} (kN/mm)
Steel - Steel	72.2	69.4	74.3	71.9	73.4	173.5
Aluminium - Steel	70.9	75.7	71.5	72.7	77.2	174.4

The stiffness in the table above was used to calculate the total average deviation from the laboratory tests ($K_{Lab.Avg}$) with the FE model (K_{FE}) and the Eurocode (K_{Eur}). The deviation from the Eurocode stands out with its overestimated values of 58.8% and 58.3% as mentioned. This indicates that the stiffness calculated from the Eurocode is hard to recreate in reality. Minor inaccuracies in the assembly of the T-stubs can explain the deviations between the Eurocode and the laboratory tests. For example,

the Eurocode assume the flanges are flat and creates full contact between each other. Nor does the Eurocode take into account that some material is removed due to the bolt hole. Based on that, the stiffness will probably be overestimated. It is reasonable to assume that a big bolt hole in the flange will provide decreased stiffness behaviour on the contrary of a small bolt hole. The transition from theory to practice also provides limitations, for example that the static systems used are two-dimensional representations of three-dimensional effects.

The minor inaccuracies in the assembly can also explain the deviation between the FE model and the laboratory tests. In Abaqus, every component is modelled perfect, regarding dimensions, contact, material properties, etc., but in reality, it differs from this.

8.3 Thermal load

The percent preload stress for both configurations is plotted in Figure 8.7. As expected, the preload stress for the aluminium – steel configurations increased after preload, considering the higher value of thermal expansion factor in the aluminium flange compared to the bolt. The preload stress increased, as mentioned earlier to 104.16% at 200 °C. At 50 °C, giving a temperature difference of 70 °C, is a more realistic temperature change a bolted connection may be exposed for. At 50 °C the preload stress increased to 100.87%, equivalent to a preload force of 90077 N.

In connection with two steel flanges, the preload stress slightly decreased. At 200 °C the preload stress reduced to 99.53% and at 50 °C it reduced to 99.85%. A preload stress reduced to 99.85 % is equivalent to a preload force of 89166.1 N.

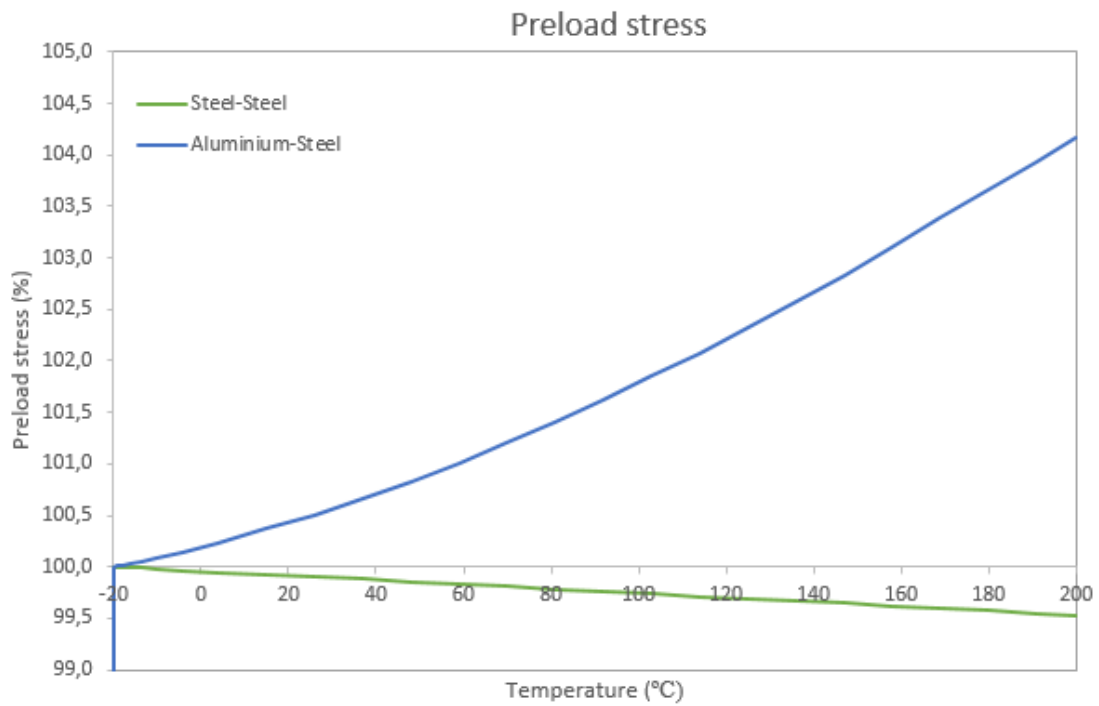


Figure 8.7: Preload stress of both configurations

Shown in Figure 8.8, the bolt expanded 0.36% in the aluminium – steel connection and 0.25% in the steel – steel connection. Despite the same thermal expansion factor of the bolt in both configurations, the bolt expanded more in connection with an aluminium flange. Due to the higher rate of expansion in the aluminium contributed in stretching the bolt, which increased the preload force. The steel flange in both configurations expanded relative the same, $\sim 0.13\%$, compared to the increase of 0.22% in the aluminium flange.

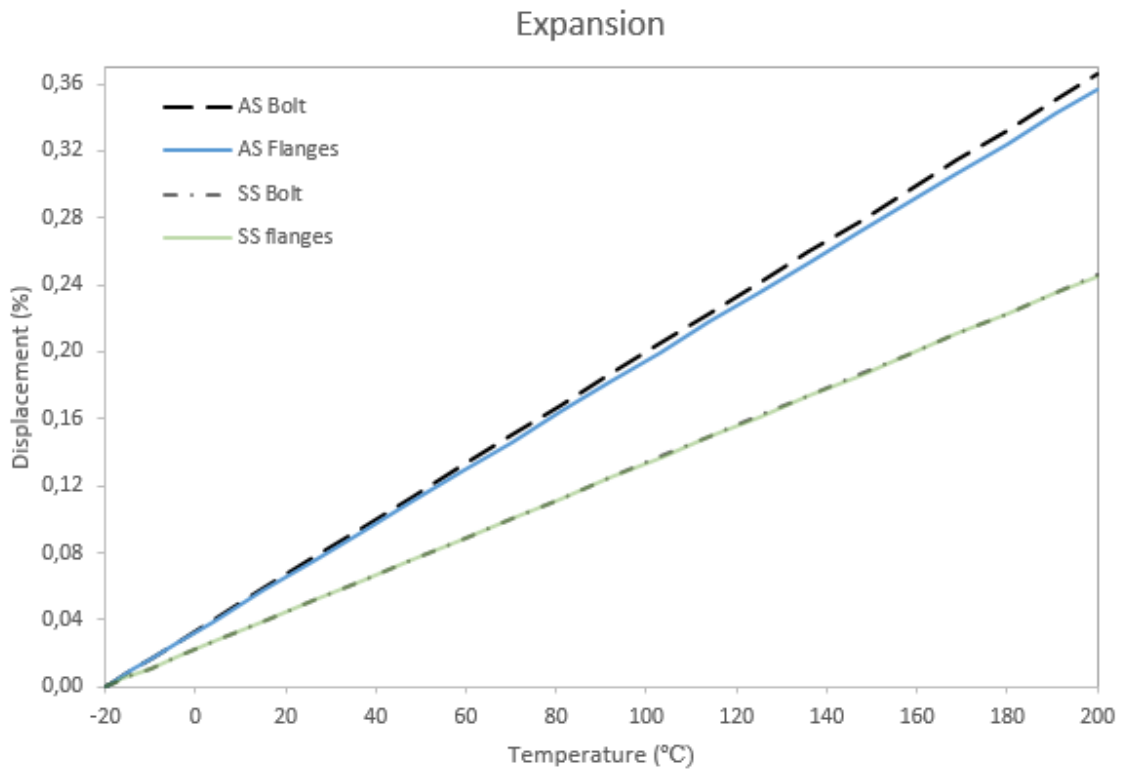


Figure 8.8: Expansion of bolt and flanges of both configurations.

Neither the increase in preload stress in the aluminium – steel connection and the decrease in the steel – steel connection are not, with these particular dimensions, remarkable regarding a problematic effect, as described in Chapter 2.3. As described in Chapter 2.4.2, tightening tools should have an accuracy of $\pm 4\%$, giving a vary preload of ± 7144 N. Due to the compensation for the inaccuracy of the tightening tools, the variation of the preload force due to thermal load is not of great significance. With an increase to 90077 N, there is not a chance of a failure in the bolt, and a decrease to 89166.1 N the connection still maintains a clamping force establishing the frictional force.

The reaction to the connection is as expected considering the increase of preload stress in a connection assembled with an aluminium flange and the approximately equal preload stress in a connection assembled by parts of the same material. An aluminium flange with a thickness of 10 mm, as in this case, has a smaller potential to increases its thickness compared to a thicker flange which is used in bolted connections on a helideck. For a connection with a thicker flange, the preload stress will probably be more significant.

9 CONCLUSION

In this thesis, laboratory tests have been carried out to establish tensile test data for T-stub connections. One of the connections is with two T-stubs of steel, and the other connection is with T-stubs of both aluminium and steel. The aim of the task was to investigate the actual behaviour of the connection subjected to thermal load and maximum tensile load. It was also investigated how well the T-stub connections could be estimated by finite element modelling and the equations given in the Eurocode, NS-EN 1993-1-8 [1].

The Eurocode proved to be very conservative, as it turned out to be a significant percentage deviations from the dimensioning force gathered from the Eurocode and the results from the tensile tests. According to the Eurocode, failure mode 1 was dimensioning, describing failure in the flange. The bolted connections real failure mode was failure mode 2, which is failure at the bolt simultaneous with yielding of the flange. Comparisons made of failure mode 2 from the Eurocode with the laboratory attempts, gave an average percentage error of 8.34% in the steel – steel connection and 10.62% in the aluminium – steel connection. Although the failure mode 2 proved to be a much better approach regarding bolt failure, several attempts should be made on different geometries to determine that the failure mode 2 is a better estimate.

In comparison with the laboratory tests and the numerical analysis, it was shown that all the force – displacement curves from the FE model were below, in the plastic zone, each tensile test from the laboratory. Unlike the results from the Eurocode, failure mode 2 was obtained for both configurations. The average percentage deviation of preload stress in the tensile tests was 6.53 % in the steel – steel connection and 5.76 % in the aluminium – steel connection. The FE model is somewhat conservative but still a good approximation to what has been observed in the laboratory.

In the elastic area, the Eurocode greatly overestimates the stiffness of the connections. The stiffness of both configurations was overwhelmingly similar. The deviations of the stiffness from the tensile tests and the Eurocode of both connections were 58.5 % in the steel – steel connection and 58.3 % in the aluminium – steel connection. The stiffness of the FE model was quite similar to the steel – steel connection with an average deviation of only 1.95 %. The deviation in the aluminium - steel connection was slightly larger with its 5.8%. Despite similar stiffness, the connections in the FE – model started to yield earlier for both configurations, as shown in Figure 8.5 and Figure 8.6. The steel – steel connection from the FE model began to yield at a displacement of ~ 1.1 mm compared to ~ 1.5 mm as in the tensile tests.

In both connections subjected to thermal load with a temperature variation of 220 °C after preload, the outcome was as expected. In the steel – steel connection where it was similar thermal expansion factor for all the components, the preload stress remained almost equal during the entire heating. In the aluminium – steel connection,

the bolt expanded more. In addition to the thermal expansion, the aluminium flange expanded at a higher rate than the bolt, giving an increase in the elongation in the bolt. The different rate of expansion in the aluminium flange compared to the bolt and steel flange caused the increase of the preload stress in the bolt. In the range of -20 to 50 °C where bolted connections can be exposed in real life situations, there is no significant danger of a weakened bolt connection or a bolt/flange breakage due to increased preload stress.

9.1 Further work

Bolted connections including washers would be interesting to investigate, considering the outcome of having a longer grip length of the bolts.

The experimental work in this thesis was limited in terms of number of tests and configurations. More tests would give a better estimate for failure mode 2 from the Eurocode as the dimensioning failure mode in a T-stub connection.

In the FE model, it should be investigated how the preload of the bolts in the T-stub connection affects the results of the tensile strength. Besides, the change of position of the bolt may be interesting to see how it could affect the stiffness.

In this thesis, the lack of resources and time became the reason for not carrying out laboratory tests of the connection exposed to thermal load. It may be of great interest to study it against the results from the FE model.

BIBLIOGRAPHY

- [1] *Eurocode 3: Design of steel structures. Part 1-8: Design of joints*, 1993-1-8:2005+NA:2009, NS-EN, 2009.
- [2] Norconsult, "Hvorfor ryker så mange bolter?," Konstruksjonsdagen 2016, [Online]. Available: <http://www.ptil.no/getfile.php/PDF/07%20-%20Hvorfor%20ryker%20s%C3%A5%20mange%20bolter.pdf>. [Accessed 11 10 2016].
- [3] Statoil, "Hendelse på Gudrun helikopterdekk," Konstruksjonsdagen 2016, [Online]. Available: <http://www.ptil.no/getfile.php/PDF/06%20-%20Hendelsene%20p%C3%A5%20Gudrun-helikopterdekk.pdf>. [Accessed 11 10 2016].
- [4] Statoil, "Kvalitetssvikt ved design og oppfølging av bærende struktur på Gudrun helikopterdekk," 2015.
- [5] J. H. Bickford, *Introduction to the design and Behaviour of Bolted Joints*, 4th edition, CRC Press, 2008.
- [6] F. E. & D. Support, "Fastenal," 2009. [Online]. Available: <https://www.fastenal.com/content/feds/pdf/Article%20-%20Bolted%20Joint%20Design.pdf>. [Accessed 12 01 2017].
- [7] G. L. Kulak, J. W. Fisher and J. H. Struik, *Guide to Design Criteria for Bolted and Riveted Joints*, 2nd edition, American Institute of Steel Construction.
- [8] R. G. Budynas and J. K. Nisbett, *Shigley's Mechanical Engineering Design*, eighth edition, Mc Graw Hill.
- [9] Y. I. J. Toyoda and S. Nagata, "Interface Pressure Distribution in a Bolt-Flange Assembly," ASME paper no. 77-WA/DE-11, 1977.
- [10] Å. Ø. Waløen, *Maskindeler 2*, Tapir.
- [11] *Eurokode 3: Prosjektering av stålkonstruksjoner, Del 1-1: Allmenne regler og regler for bygnigner*, NS-EN 1993-1-1:2005+NA:2008, 2008.
- [12] A. G. R. Reyes, "Uniaxial behaviour, Univeristy Lecture," 2006.
- [13] P. K. Larsen, *Dimensjonering av stålkonstruksjoner*, 2nd edition, Tapir Akademisk, 2010.
- [14] Boltight, "Boltight," [Online]. Available: <http://www.boltight.com/resources/Data-Sheets/DS-90-High-Temperature-Stress-Relaxation.pdf>. [Accessed 13 03 2017].
- [15] *Eurokode 9: Prosjektering av aluminiumskonstruksjoner, Del 1-1: Almenne regler*, NS-EN 1999-1-1:2007/NA:2009, 2009.
- [16] *Assembly tools for screw and nuts. Hand torque tools. Requirements and test methods for design conformance testing, quality conformance and procedure*, BS EN ISO 6789, 2003.
- [17] *Execution of steel structures and aluminium structures - Part 2: Technical requirements for steel structures*, NS-EN 1090-2:2008+A1:2011, 2011.
- [18] *Joints in Steel Constructions - Joints to Eurocode 3 (P398)*, SCI and BCSA, 2013.
- [19] P. E. Thoresen, *Kompendium 2 i statikk*, Oslo: HiOA, 2015.
- [20] H. Ersland, "End plate joint for hollow sections," NTNU, Trondheim, 2011.
- [21] T. Draycott and P. Bullman, *Structural Elements Design manual*, Elsevier Ltd, 2009, p. 26.
- [22] K. Weynand, J.-. P. Jaspart and M. Steenhuis, "The stiffness model of revised Annex J of Eurocode 3," in *Proceedings of the Third International Workshop on Connections in Steel Structures*, Trento, 1995, pp. 441-452.
- [23] *Eurokode 3: Prosjektering av stålkonstruksjoner, Del 1-1: Allmenne regler og regler for bygnigner*, NS-EN 1993-1-1:2005+A1:2014+NA:2015, 2015.
- [24] K. A. Iden, M. Reistad, O. J. Aarnes, R. Gangstø, G. Noer and N. E. Hughes, "Kunnskap om vind, bølger, temperatur, isutbredelse, siktforhold mv. - "Barentshavet SØ"," Norwegian Meteorological Institute, 2012.
- [25] Hertel, "Structural Baiss of Design HELIDECK," 2014.

- [26] *Metallic materials - Tensile testing - Part 1: Method of test at room temperature*, NS-EN ISO 6892-1:2016, 2016.
- [27] *Mechanical properties of fasteners made of carbon steel and alloy steel, Part 1: Bolts, screws and studs with specified property classes, Coarse thread and fine pitch thread*, NS-EN ISO 898-1:2013, 2013.
- [28] E. S. Skavhaug and S. I. Østhus, "Tension-loaded bolted connections in steel structures," Norwegian University of Science and Technology, Trondheim, 2015.
- [29] Simula, "Abaqus 6.10, Analysis User*s Manual Volume IV: Elements," Simula, 2010.

APPENDICES

Appendix A

Prying force

Vertical displacements due to external load (Δ_1) and unit load (Δ_2) used when determining the prying force in an equivalent T-stub.

$$\Delta_1 = \int_0^L \frac{M_1 M_2}{EI} dx = \int_0^{1.25m} 0.5Fx(-x) \frac{1}{EI} dx + \int_{1.25m}^{2.25m} 0.5Fx(-1.25m) \frac{1}{EI} dx$$

$$\Delta_1 = \int_0^{1.25m} -0.5Fx^2 \frac{1}{EI} dx + \int_{1.25m}^{2.25m} -\frac{5}{8} Fxm \frac{1}{EI} dx$$

$$\Delta_1 = \frac{1}{EI} \left\{ \left[-\frac{1}{6} Fx^3 \right]_0^{1.25m} + \left[-\frac{5}{16} Fmx^2 \right]_{1.25m}^{2.25m} \right\}$$

$$\Delta_1 = \frac{1}{EI} \left\{ \left(-\frac{1}{6} 1.25^3 Fm^3 \right) + \left(\left(-\frac{5}{16} 2.25^2 Fm^3 \right) - \left(-\frac{5}{16} 1.25^2 Fm^3 \right) \right) \right\} = -\frac{545Fm^3}{384EI}$$

$$\Delta_2 = \int_0^L \frac{M_1 M_2}{EI} dx = \int_0^{1.25m} (-x)(-x) \frac{1}{EI} dx + \int_{1.25m}^{2.25m} (-1.25m)(-1.25m) \frac{1}{EI} dx$$

$$\Delta_2 = \int_0^{1.25m} x^2 \frac{1}{EI} dx + \int_{1.25m}^{2.25m} (-1.25m)^2 \frac{1}{EI} dx$$

$$\Delta_2 = \frac{1}{EI} \left\{ \left[\frac{1}{3} x^3 \right]_0^{1.25m} + \left[\frac{25}{16} m^2 x \right]_{1.25m}^{2.25m} \right\}$$

$$\Delta_2 = \frac{1}{EI} \left\{ \left(\frac{1}{3} 1.25^3 m^3 \right) + \left(\left(\frac{25}{16} 2.25 m^3 \right) - \left(\frac{25}{16} 1.25 m^3 \right) \right) \right\} = \frac{425m^3}{192EI}$$

Appendix B

Effective length

Calculations of the effective lengths of a T-stub connection in accordance with NS-EN 1993-1-8

Thickness of web, steel: $t_{w_s} = 6.5 \text{ mm}$

Thickness of web, aluminium: $t_{w_a} = 10 \text{ mm}$

Thickness of flange, steel: $t_{f_s} = 10 \text{ mm}$

Thickness of flange, aluminium: $t_{f_a} = 16 \text{ mm}$

Width of T-stub connections: $b = 200 \text{ mm}$

Length of T-stub connections: $L = 110 \text{ mm}$

Radius: $r = 18 \text{ mm}$

Distance between the bolts: $w = 110 \text{ mm}$

Distance between the bolt and the edge of web:

Steel flange

$$m_s = \frac{w - t_{w_s}}{2} - 0.8r = \frac{110 - 6.5}{2} - 0.8 \cdot 18 = 37.35 \text{ mm}$$

Aluminium flange

$$m_a = \frac{w - t_{w_a}}{2} - 0.8r = \frac{110 - 10}{2} - 0.8 \cdot 18 = 35.6 \text{ mm}$$

Distance from bolt to edge, smallest of

$$e_1 = \frac{b-w}{2} = \frac{200-110}{2} = 45 \text{ mm}$$

$$e_{2s} = 1.25m_s = 1.25 \cdot 37.35 = 47 \text{ mm}$$

$$e_{2a} = 1.25m_a = 1.25 \cdot 35.6 = 45 \text{ mm}$$

$$e_{\min} = \min(e_1, e_{2s}, e_{2a}) = 45 \text{ mm}$$

l_{eff} is the smallest of (where m is the smallest of m_s and m_a):

Circular pattern ($l_{eff,cp}$):

$$2\pi m = 2\pi \cdot 35.6 = 223.7 \text{ mm}$$

$$\pi m + 2e_{min} = \pi \cdot 35.6 + 2 \cdot 45 = 201.8 \text{ mm}$$

Non-circular pattern ($l_{eff,nc}$):

$$4m + 1.25e_{min} = 4 \cdot 35.6 + 1.25 \cdot 45 = 198.7 \text{ mm}$$

$$2m + 1.25e_{min} = 2 \cdot 35.6 + 0.625 \cdot 45 + 45 = 144.3 \text{ mm}$$

Length: $L = 110 \text{ mm}$

Effective length: $l_{eff} = \min(l_{eff,cp}, l_{eff,nc}, L) = 110 \text{ mm}$

Appendix C

Capacity

Calculations of the design resistance loads.

Bolt tension capacity

$$F_{t,Rd} = \frac{0.9f_{ub}A_{s,bolt}}{\gamma_{M2}} = \frac{0.9 \cdot 896 \cdot 157}{1} = 126.6 \text{ kN}$$

Steel T-stub

Plastic moment: $M_{pl,Rd,s} = \frac{0.25l_{eff}t_f^2f_{y,s}}{\gamma_{M0}} = \frac{0.25 \cdot 110 \cdot 10^2 \cdot 369.9}{1} = 1017 \text{ kNm}$

Failure mode 1: $F_{T,1,Rd,s} = \frac{4M_{pl,Rd,s}}{m_s} = \frac{4 \cdot 1017}{37.35} = 108.9 \text{ kN}$

Failure mode 2: $F_{T,2,Rd,s} = \frac{2M_{pl,Rd,s} + e_{min} \sum F_{t,Rd}}{m_s + e_{min}} = \frac{2 \cdot 1017 + (2 \cdot 45 \cdot 126.6)}{37.35 + 45} = 163.1 \text{ kN}$

Aluminium T-stub

Plastic moment:
$$M_{pl,Rd,a} = \frac{0.25 l_{eff} t_{f,a}^2 f_{y,a}}{\gamma_{M0}} = \frac{0.25 \cdot 110 \cdot 16^2 \cdot 312.2}{1} = 2198 \text{ kNmm}$$

Failure mode 1:
$$F_{T,1,Rd,a} = \frac{4M_{pl,Rd,a}}{m_a} = \frac{4 \cdot 2198}{35.6} = 246.9 \text{ kN}$$

Failure mode 2:
$$F_{T,2,Rd,a} = \frac{2M_{pl,Rd,a} + e_{min} \sum F_{t,Rd}}{m_a + e_{min}} = \frac{2 \cdot 2198 + (2 \cdot 45 \cdot 126.6)}{35.6 + 45} = 195.9 \text{ kN}$$

Appendix D

Stiffness

Calculations of the stiffness of the bolted connections

Bolt in steel flange

Elongation length:

$$L_{b,s} = 10 + \frac{5 + 7.4}{2} = 16.2 \text{ mm}$$

Stiffness coefficient:

$$k_{c,10,s} = \frac{1.6 \cdot A_s}{L_{b,s}} = \frac{1.6 \cdot 157}{16.2} = 15.51 \text{ mm}$$

Stiffness coefficient of steel flange in bending

$$k_{c,5,s} = \frac{0.9 \cdot l_{eff} \cdot t_{f,s}^3}{m_s} = \frac{0.9 \cdot 110 \cdot 10^3}{37.35} = 1.9 \text{ mm}$$

Stiffness coefficient of steel flange with bolt

$$k_{tot,s} = \frac{1}{2} \cdot \frac{1}{\frac{1}{k_{c,10,s}} + \frac{1}{k_{c,5,s}}} = \frac{1}{2} \cdot \frac{1}{\frac{1}{15.51} + \frac{1}{1.9}} = 0.846 \text{ mm}$$

Stiffness of steel T-Stub

$$K_{el,s} = k_{tot,s} \cdot E = 0.846 \cdot 205000 = 175\,316 \frac{N}{mm}$$

Bolt in aluminium flange

Elongation length:

$$L_{b,a} = 16 + \frac{5 + 7.4}{2} = 22.2 \text{ mm}$$

Stiffness coefficient:

$$k_{c,10,a} = \frac{1.6 \cdot A_s}{L_{b,a}} = \frac{1.6 \cdot 157}{22.2} = 11.32 \text{ mm}$$

Stiffness coefficient of aluminium flange in bending

$$k_{c,5,a} = \frac{0.9 \cdot l_{eff} \cdot t_{f,a}^3}{m_a} = \frac{0.9 \cdot 110 \cdot 16^3}{35.6} = 8.9 \text{ mm}$$

Stiffness coefficient of aluminium flange with bolt

$$k_{tot,a} = \frac{1}{2} \cdot \frac{1}{\frac{1}{k_{c,10,a}} + \frac{1}{k_{c,5,a}}} = \frac{1}{2} \cdot \frac{1}{\frac{1}{11.32} + \frac{1}{8.9}} = 2.505 \text{ mm}$$

Stiffness of aluminium T-stub

$$K_{el,a} = k_{tot,a} \cdot E_a = 2.505 \cdot 70000 = 173\,495 \frac{N}{mm}$$

Appendix E

Material data

Calculations of the material data of the bolt

Yield stress: $f_y = 640 \text{ MPa}$

Ultimate stress: $f_u = 800 \text{ MPa}$

Young's modulus: $E = 210000 \text{ MPa}$

Elongation: $\delta = 0.12$

Engineering elastic strain:

$$\varepsilon_{eng.el} = \frac{f_y}{E} = \frac{640}{210000} = 0.003048$$

True elastic strain:

$$\varepsilon_{true.el} = \ln(1 + \varepsilon_{eng.el}) - \varepsilon_{eng.el} = \ln(1 + 0.003048) - 0.003048 \approx 0$$

Engineering plastic strain:

$$\varepsilon_{eng.pl} = 0.12$$

True yield stress:

$$\sigma_{true} = f_y \cdot (1 + \varepsilon_{eng.el}) = 641.95 \text{ MPa}$$

True ultimate stress (plastic):

$$\sigma_{true.pl} = f_u \cdot (1 + \varepsilon_{eng.pl}) = 896 \text{ MPa}$$

True plastic strain (plastic):

$$\varepsilon_{true.pl} = \ln(1 + \varepsilon_{eng.pl}) - \frac{\sigma_{true.pl}}{E} = 0.1091$$

Appendix F

F.1 Tensile tests: Steel – steel

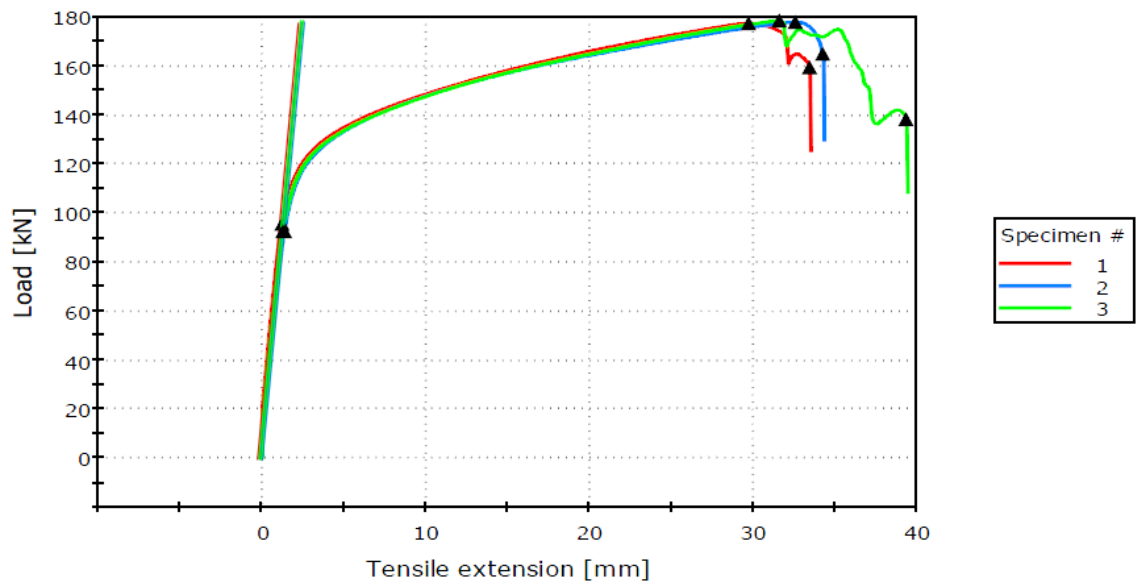


03 April 2017

Instron Applications Laboratory

This template is suitable for creating test procedures that comply with ISO 6892-1: 2009. Test rates and control are set according to "Method A" recommended ranges. Template is intended for specimens that produce a clearly-defined linear elastic region and homogeneous deformation. Default calculated results include Rp 0.2, Fm and Rm.

Specimen 1 to 3



	Specimen label	Load at Offset yield 0.2% [N]	Extension at Offset yield 0.2% [mm]	Fm [N]
1	ISO 6892-1 Specimen	95870	3.052	177400
2	ISO 6892-1 Specimen	92820	3.768	177900
3	ISO 6892-1 Specimen	92860	3.033	178500

F.2 Tensile tests: Aluminium – steel

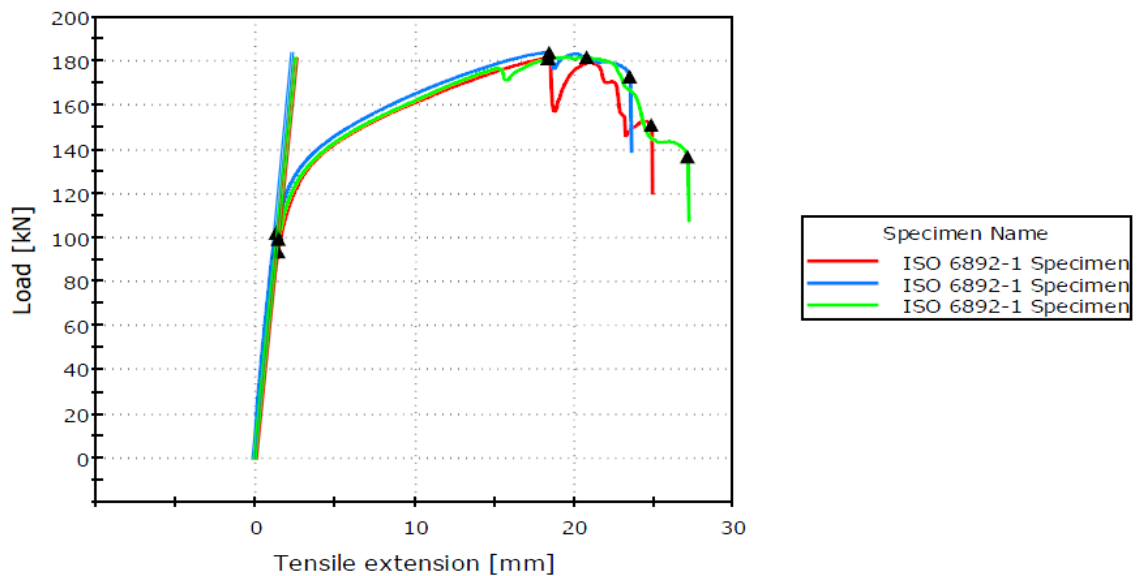


04 April 2017

Instron Applications Laboratory

This template is suitable for creating test procedures that comply with ISO 6892-1: 2009. Test rates and control are set according to "Method A" recommended ranges. Template is intended for specimens that produce a clearly-defined linear elastic region and homogeneous deformation. Default calculated results include R_p 0.2, F_m and R_m .

Load vs. Extension



	Specimen label	Load at Offset yield 0.2% [N]	Extension at Offset yield 0.2% [mm]	F_m [N]
1	ISO 6892-1 Specimen	93980	3.094	181500
2	ISO 6892-1 Specimen	102400	3.069	184100
3	ISO 6892-1 Specimen	99650	3.297	181900